

Direct reaction and r-process nucleosynthesis

Nobu Imai

今井伸明

CNS, University of Tokyo

Contents

- 1st lecture
 - Brief introduction of r -process
 - Waiting point approximation
 - Two mechanism of the neutron capture reaction
- 2nd lecture
 - Direct radiative capture reaction channel
 - DWBA
 - Inverse kinematics
- 3rd lecture
 - Compound reaction channel
 - Surrogate reaction
 - Recent highlights at OEDO/RIBF

Origin of the elements in the Universe

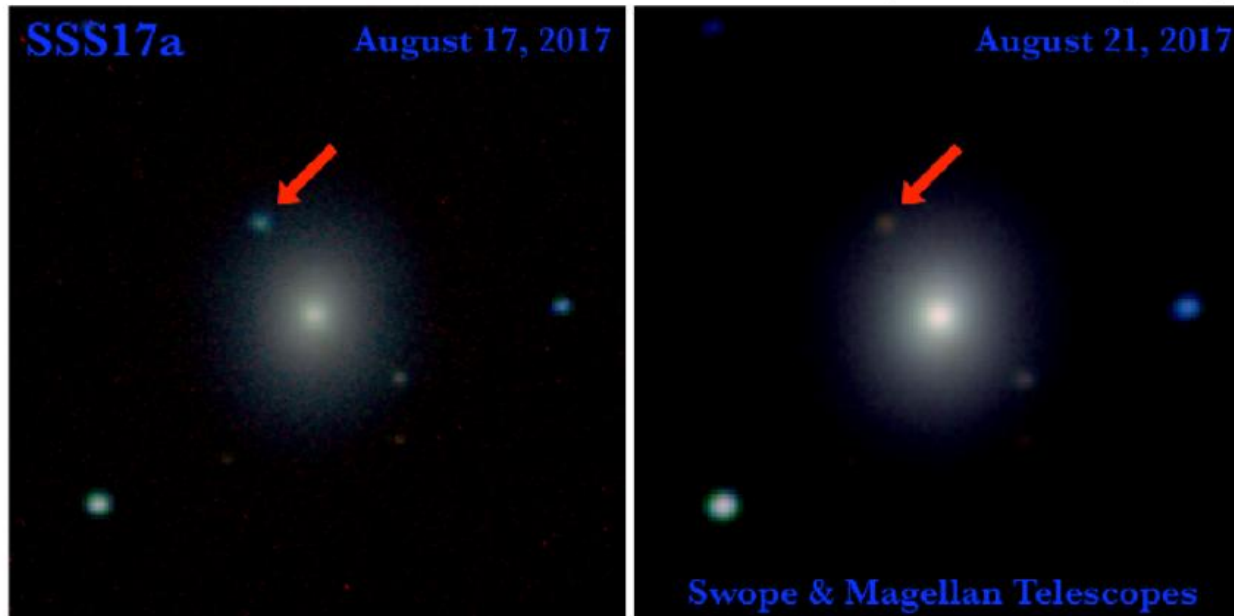
- Where do we come from?
- How are the heavier elements synthesized?

Third of 11 unanswered questions in 2002

<https://www.discovermagazine.com/the-sciences/the-11-greatest-unanswered-questions-of-physics>



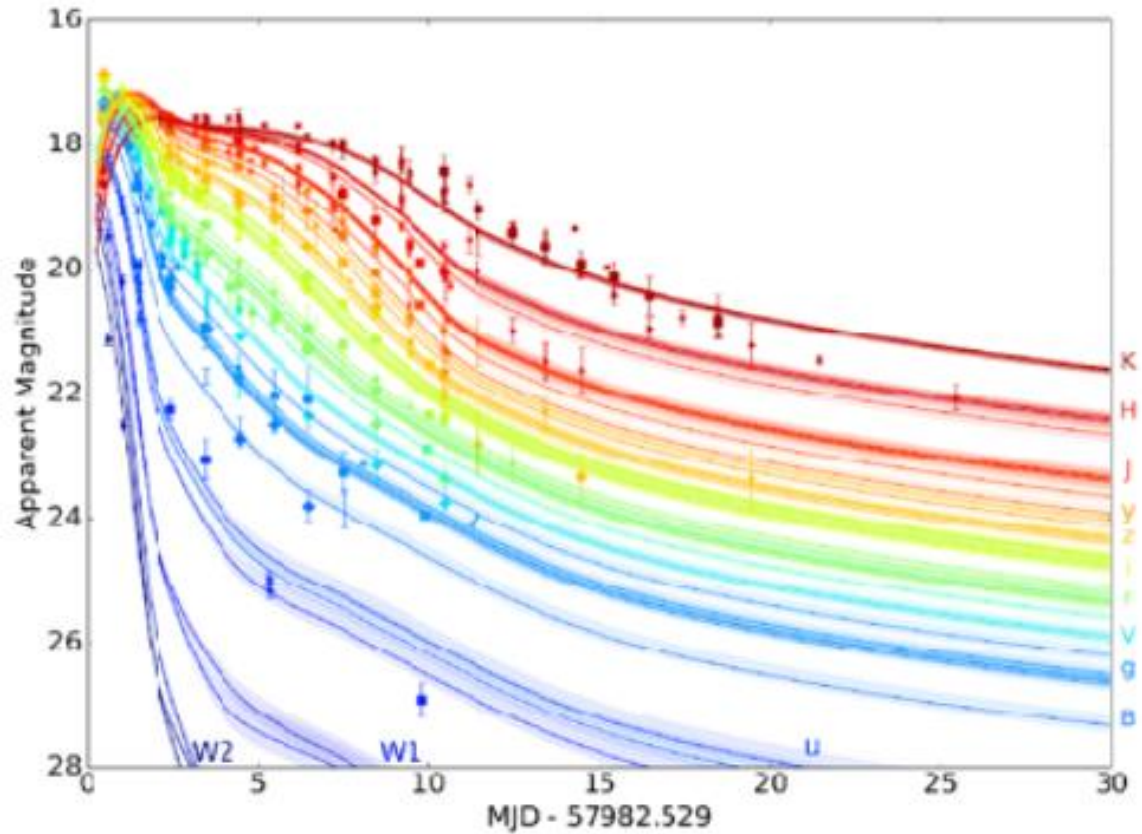
Neutron-star Merger



Discovery of the gravitational wave on 2017.8.17

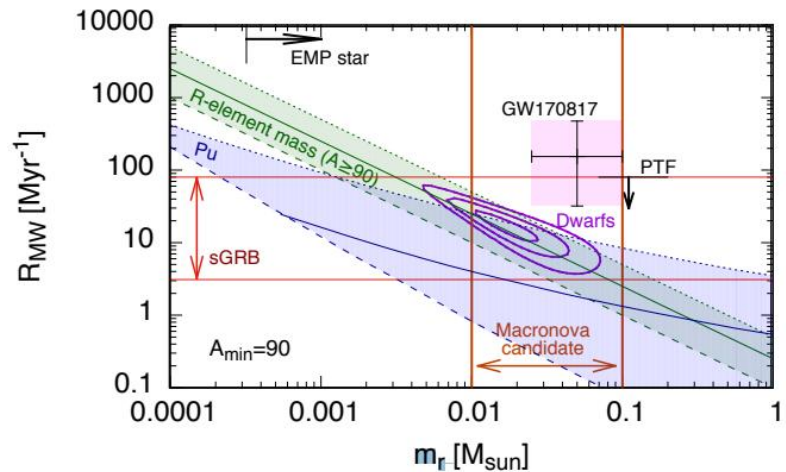
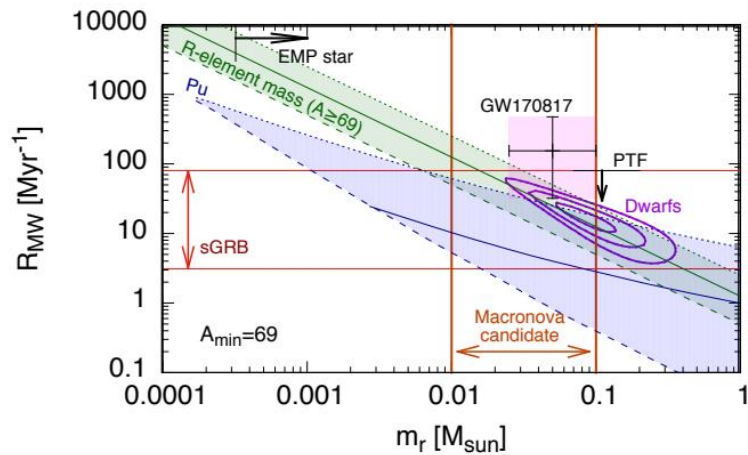
M.R. Drout et al., Science 358, 1750 (2017)

Time-evolution of the light-curve



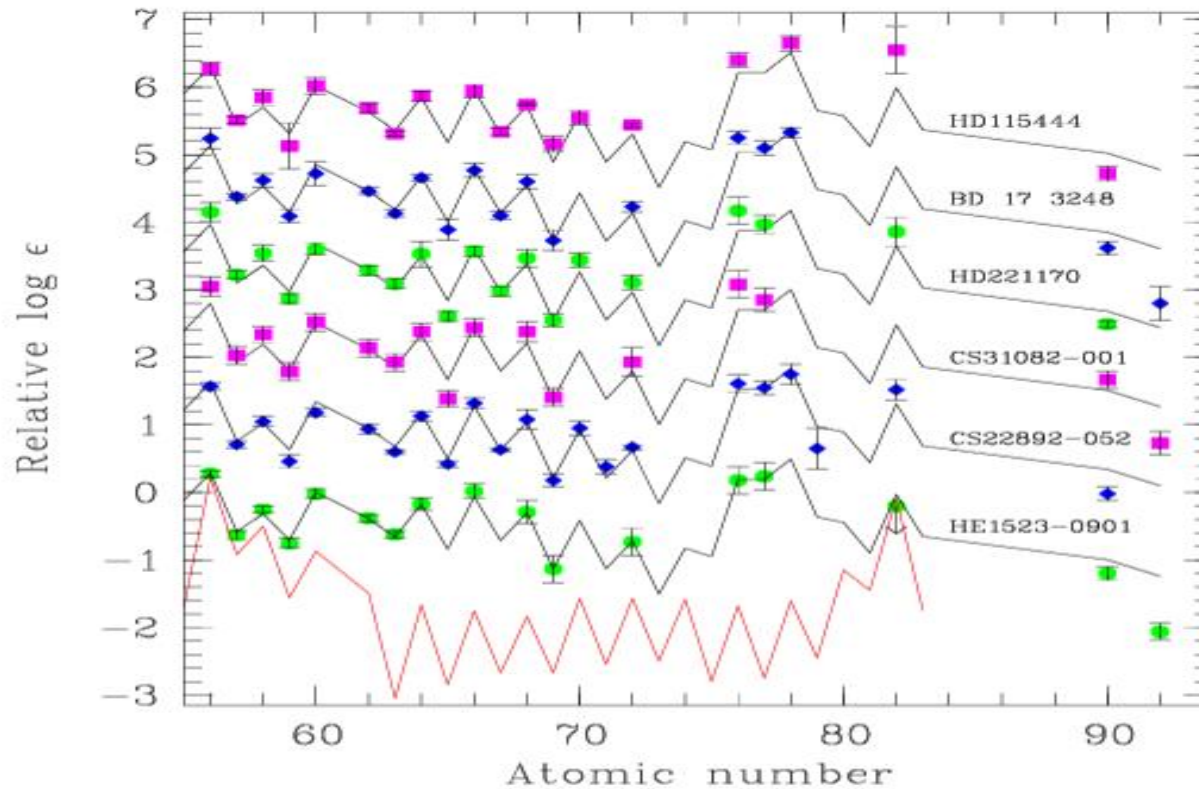
V.A. Villar et al., ApJL 851 L21 (2017)

NS merger is enough ?



K. Hotokezak et al., [arXiv:1801.01141](https://arxiv.org/abs/1801.01141)

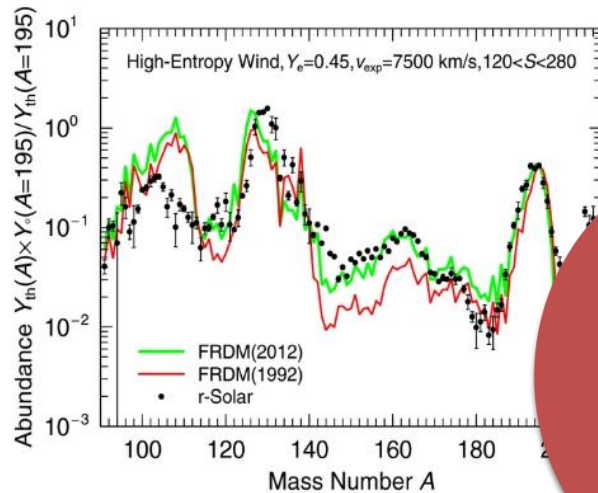
Universality of r -process abundance



A. Frebl (2008)

Center for Nuclear Study
Univ. of Tokyo

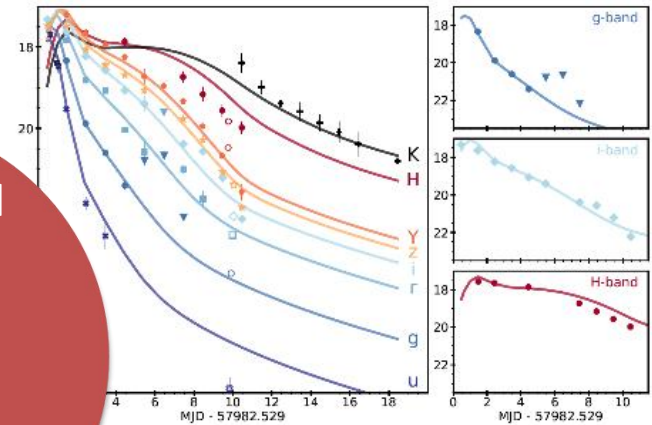
Study of *r*-process nucleosynthesis



r-process abundance peak

Astronomical observation

Multi-messenger astronomy,
Meteorite



Origin of the element
In the universe

Simulation

3D-hydrodynamical model

Nuclear Physics Param.

decay, mass,

EOS,
neutroncapture

Nuclear Physics Param. for nucleosynthesis

2016



Review

The impact of individual nuclear properties on r -process nucleosynthesis

M.R. Mumpower^{a,*}, R. Surman^{a,*}, G.C. McLaughlin^b, A. Aprahamian^a

^a Department of Physics, University of Notre Dame, Notre Dame, IN 46556, USA

^b Department of Physics, North Carolina State University, Raleigh, NC 27695, USA

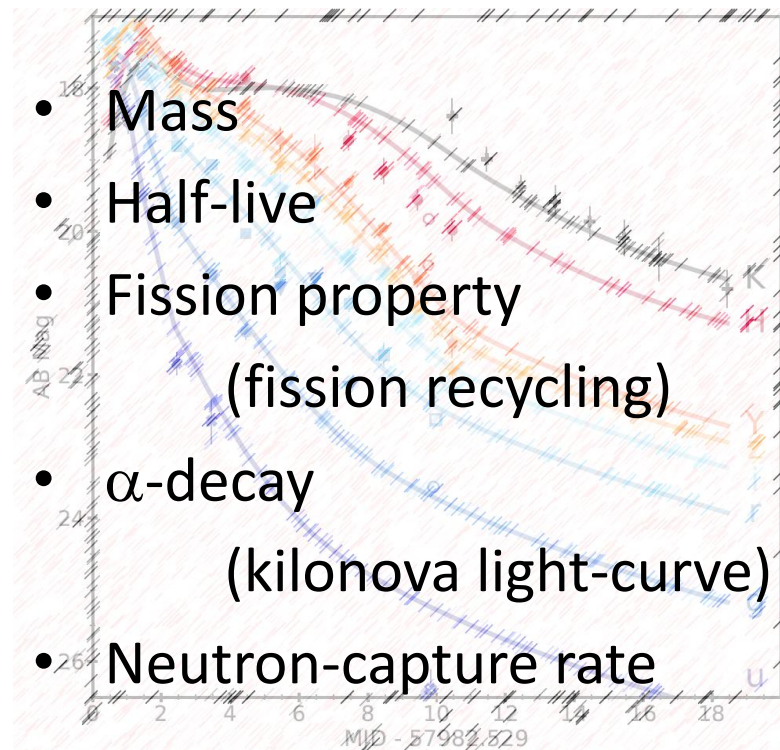


2021

REVIEWS OF MODERN PHYSICS, VOLUME 93, JANUARY–MARCH 2021

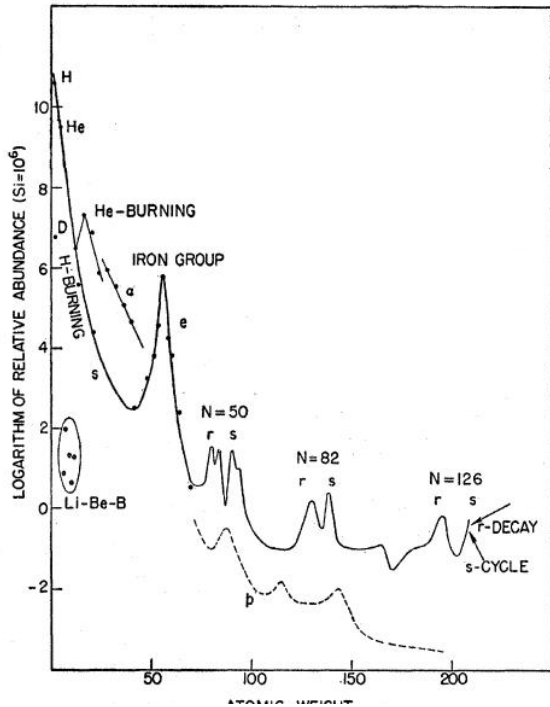
Origin of the heaviest elements: The rapid neutron-capture process

J. J. Cowen et al.,



- Mass (r-process path)
- Half-live (speed)
- Neutron-capture rate (abundance pattern)

2 processes for heavier elements



The Nobel Prize in Physics 1983

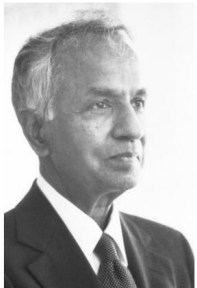


Photo from the Nobel Foundation archive.
Subramanyan Chandrasekhar



Photo from the Nobel Foundation archive.
William Alfred Fowler

REVIEWS OF MODERN PHYSICS

VOLUME 29, NUMBER 4

OCTOBER, 1957

Synthesis of the Elements in Stars*

E. MARGARET BURBIDGE, G. R. BURBIDGE, WILLIAM A. FOWLER, AND F. HOYLE

*Kellogg Radiation Laboratory, California Institute of Technology, and
Mount Wilson and Palomar Observatories, Carnegie Institution of Washington,
California Institute of Technology, Pasadena, California*

“It is the stars, The stars above us, govern our conditions”;
(*King Lear*, Act IV, Scene 3)

but perhaps

“The fault, dear Brutus, is not in our stars, But in ourselves,”
(*Julius Caesar*, Act I, Scene 2)

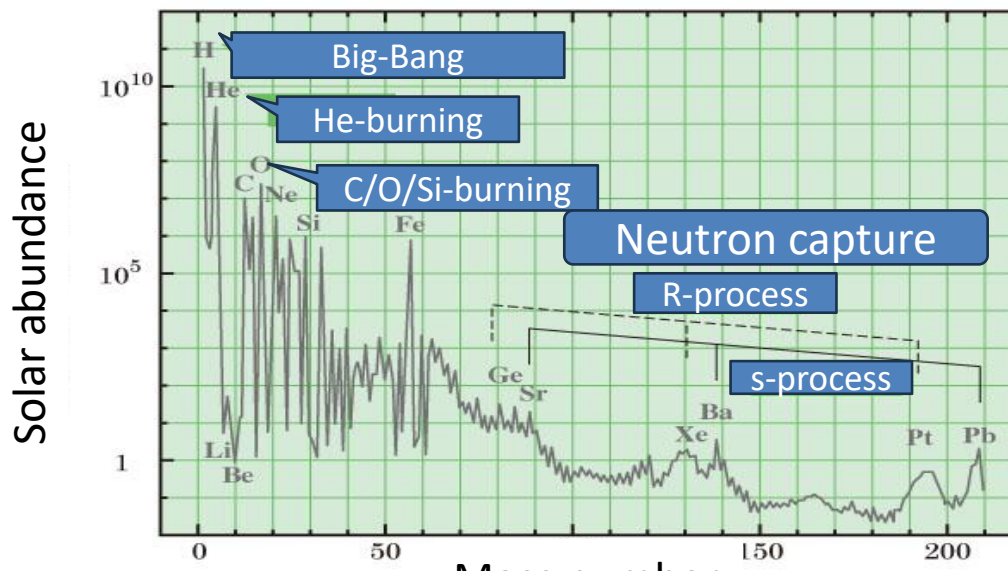
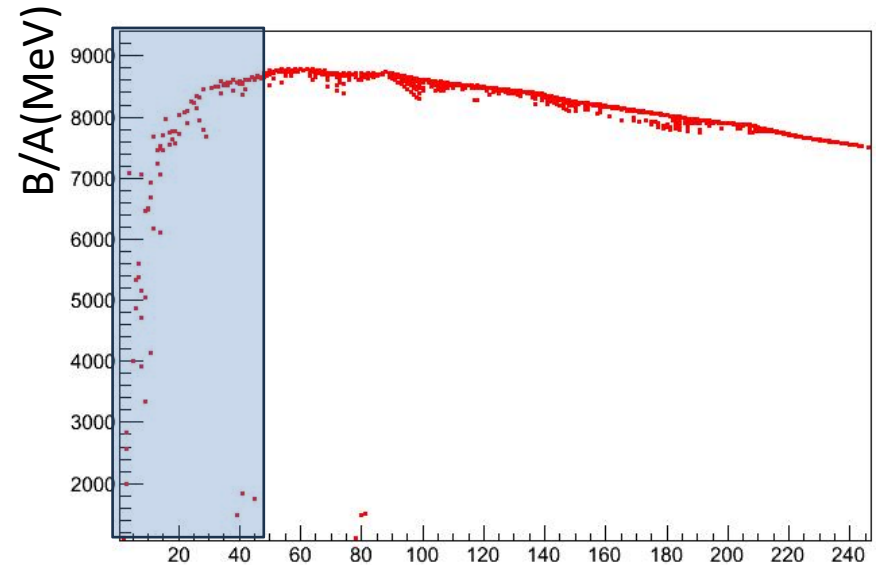
TABLE OF CONTENTS

<https://journals.aps.org/rmp/abstract/10.1103/RevModPhys.29.547>

Solar abundance

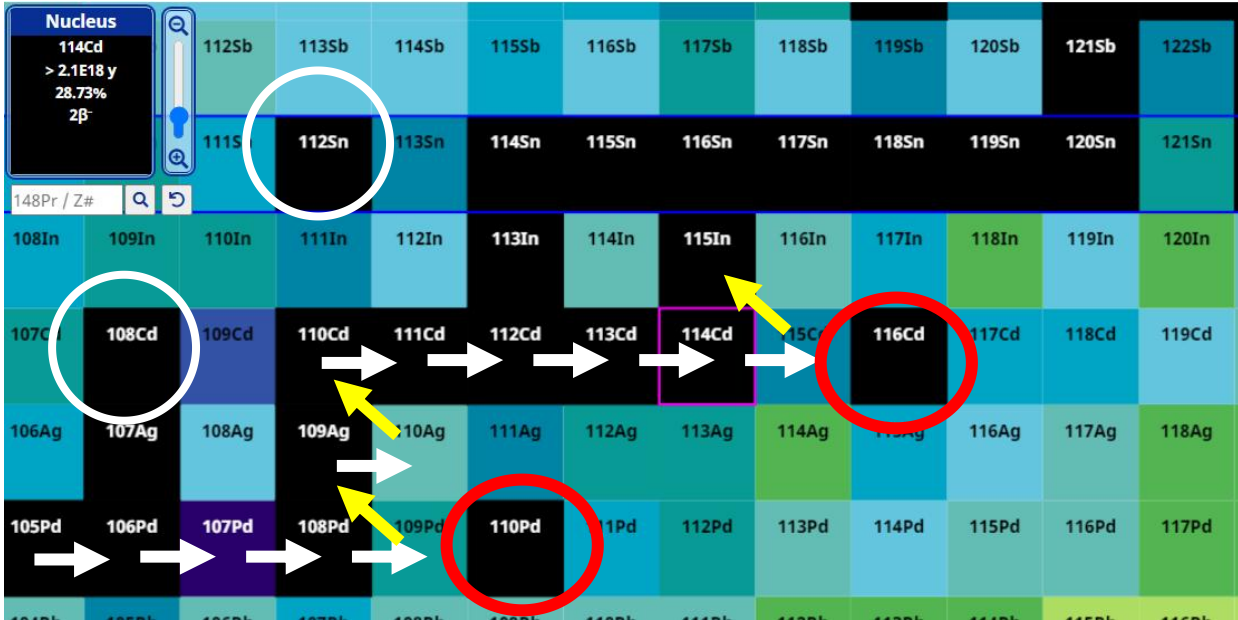
- Hydrogen burning
- Helium burning
- α process

- s -process
- r -process

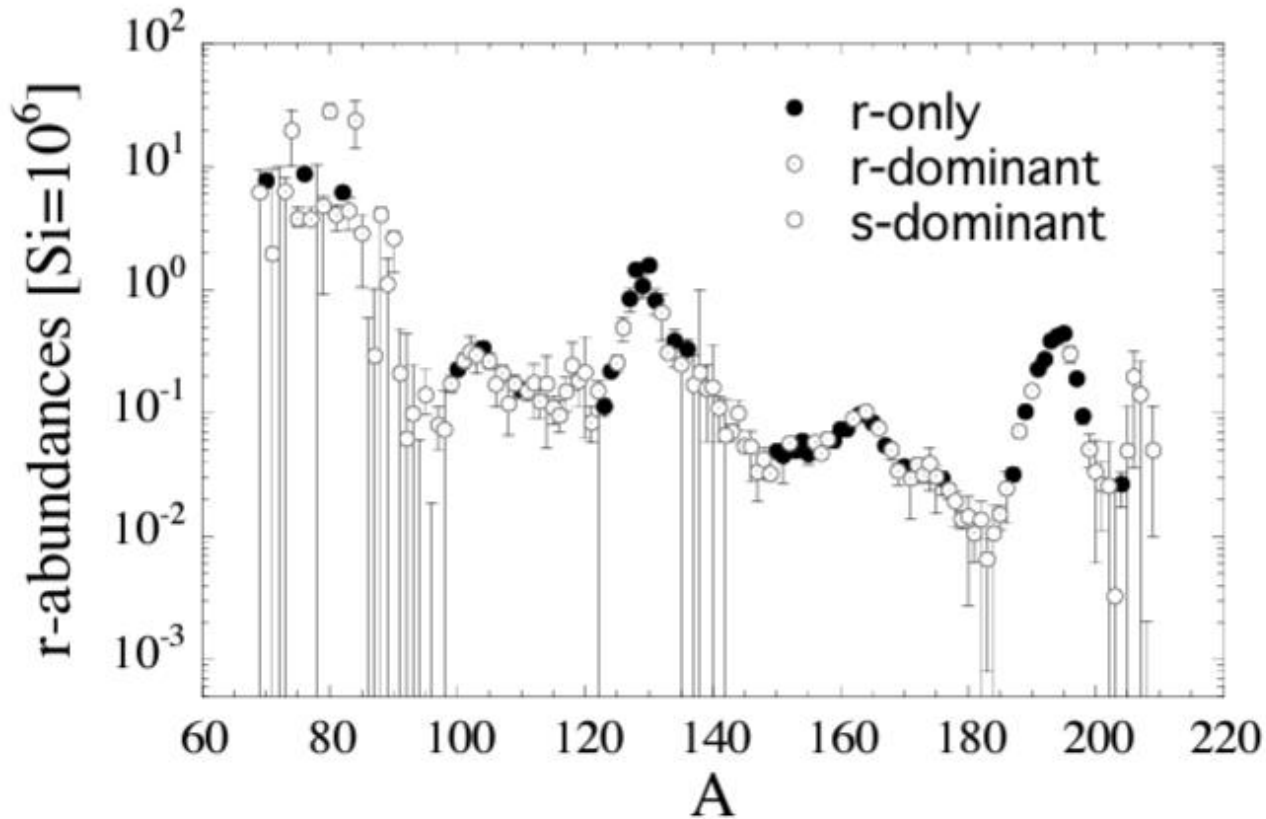


A

- $$N_n \sim 10^{11} \text{m}^{-3}, \tau_{(n,\gamma)} \sim 10^5 \text{ year}$$

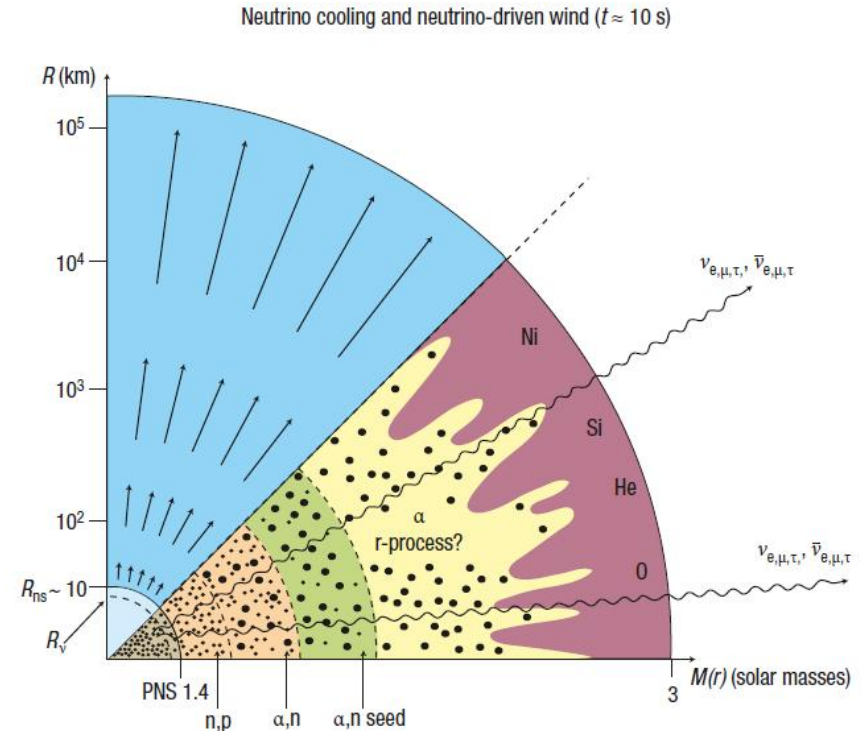
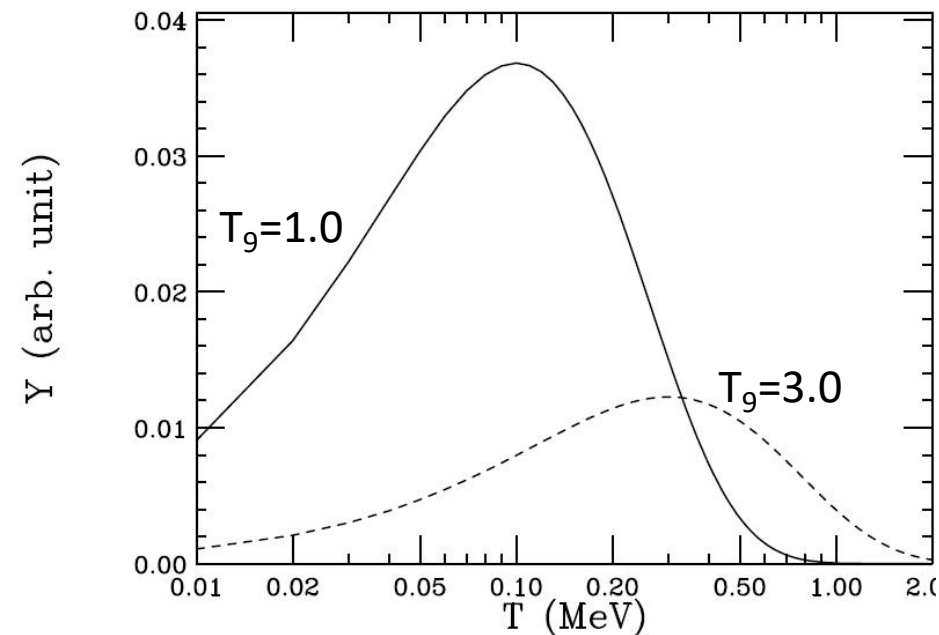


r-process abundance



$$rprocess = total - sprocess$$

Temperature in r-process

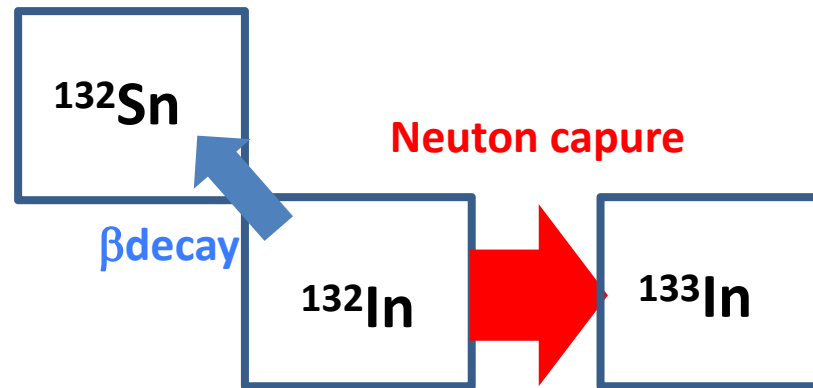


n-capture @ $1 < T_9 < 3$

S. Woosley and T. Janka,
Nature Physics 172, 147 (2005)

Elementary process of r-process

β decay and neutron-capture



$$\beta \text{ rate } \omega_{\beta} = 1/t = 2.47 [\text{s}^{-1}]$$

$$\begin{aligned} \omega_n &= N_n \langle \sigma \rangle^{\text{max}} v \\ &= 10^{20} \times 0.1 \text{ mb} \times 4.4 \times 10^8 [\text{cm/s}] \\ &= 4.38 [\text{s}^{-1}] \\ & (T^9 = 1 \sim 0.1 \text{ MeV}) \end{aligned}$$

Cross section would constrain the neutron density/temperature.

β Decay and neutron capture

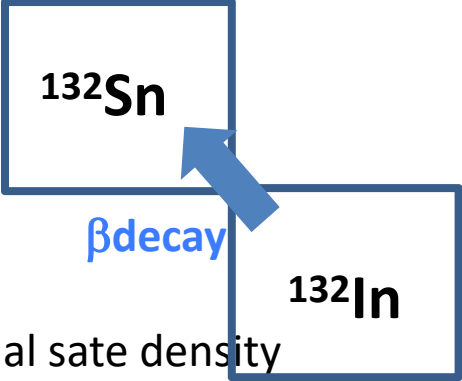
- β decay

$$- \beta^-, (Z, A) \rightarrow (Z + 1, A) + e^- + \bar{\nu}$$

$$\frac{1}{\tau} = \frac{2\pi}{\hbar} \left| \langle \phi_f | O | \phi_i \rangle \right|^2 \rho_f$$

Outgoing channel
 Entrance channel
 Interaction (G.T., Fermi, etc...)

Final state density

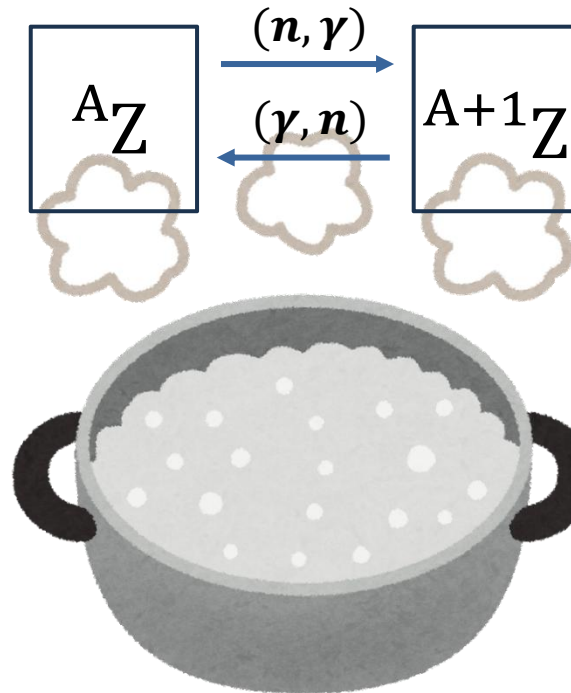


- (Direct radiative) neutron capture reaction

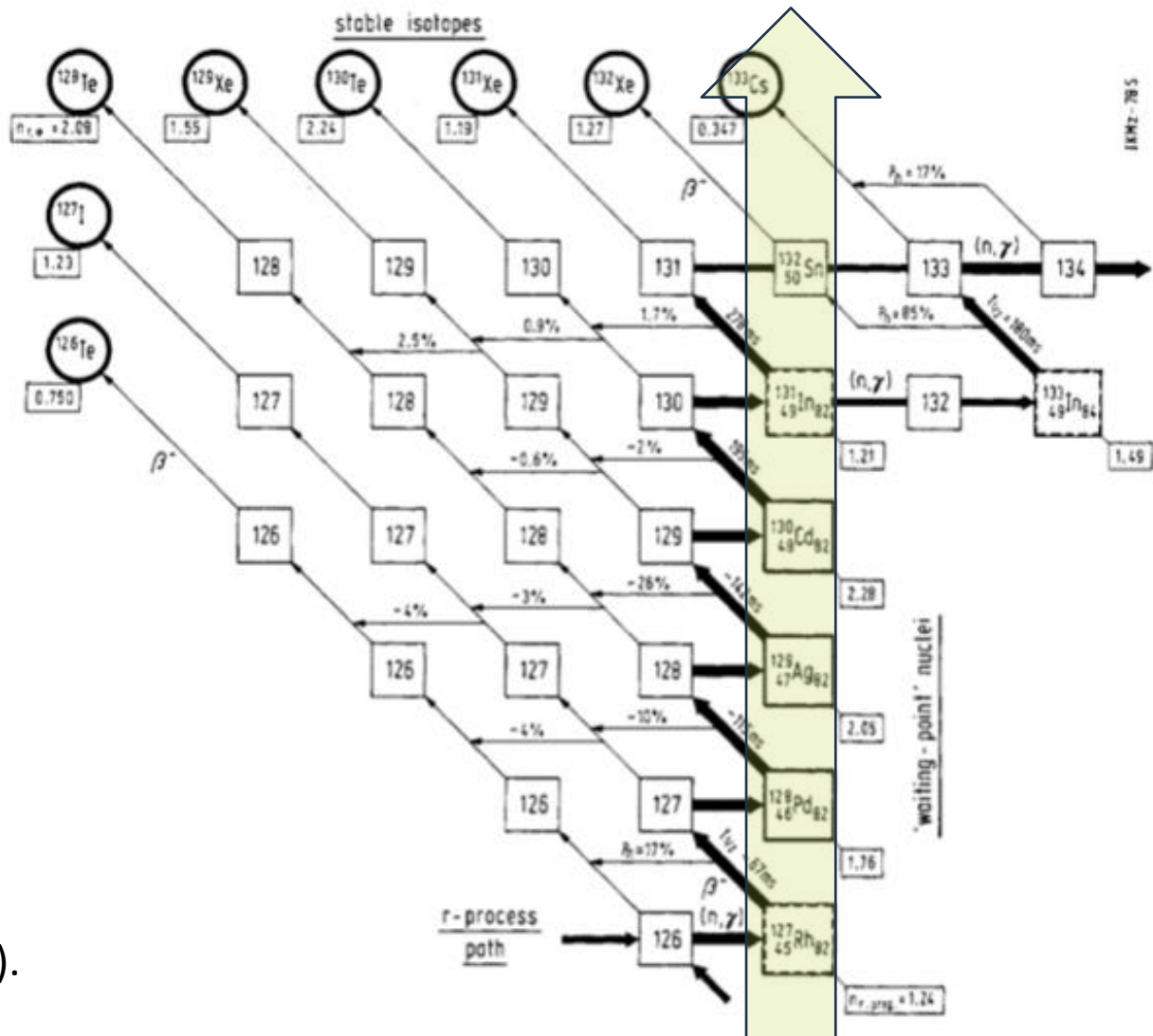
$$\sigma_{n\gamma} = \frac{16\pi}{9\hbar} \left(\frac{\varepsilon_\gamma}{\hbar c} \right)^3 \bar{e}^2 \left| \langle \varphi_f | \hat{T}^{E1} | \Psi_i \rangle \right|^2$$

Photodisintegration

r-process happens in a hot bath



At the nucleus which has the magic number, the neutron capture rate drops, giving rise to the local equilibrium.



K.L. Kratz, et al.,
JPG 14, S331 (1988).

Waiting-point approximation

- Neutron capture rate

$$- r_{n,\gamma}(A, Z) = \langle \sigma_{n,\gamma} v \rangle n_n N(A, Z)$$

- Photodisintegration ; detailed balance

$$- r_{\gamma,n}(A+1, Z) = \frac{G(A, Z) G_n}{G(A+1, Z)} \left(\frac{A}{A+1} \right)^{3/2} \left(\frac{2\pi k T m_u}{h^2} \right)^{3/2} \langle \sigma_{n,\gamma} v \rangle N(A+1, Z) e^{-\frac{S_n}{kT}}$$

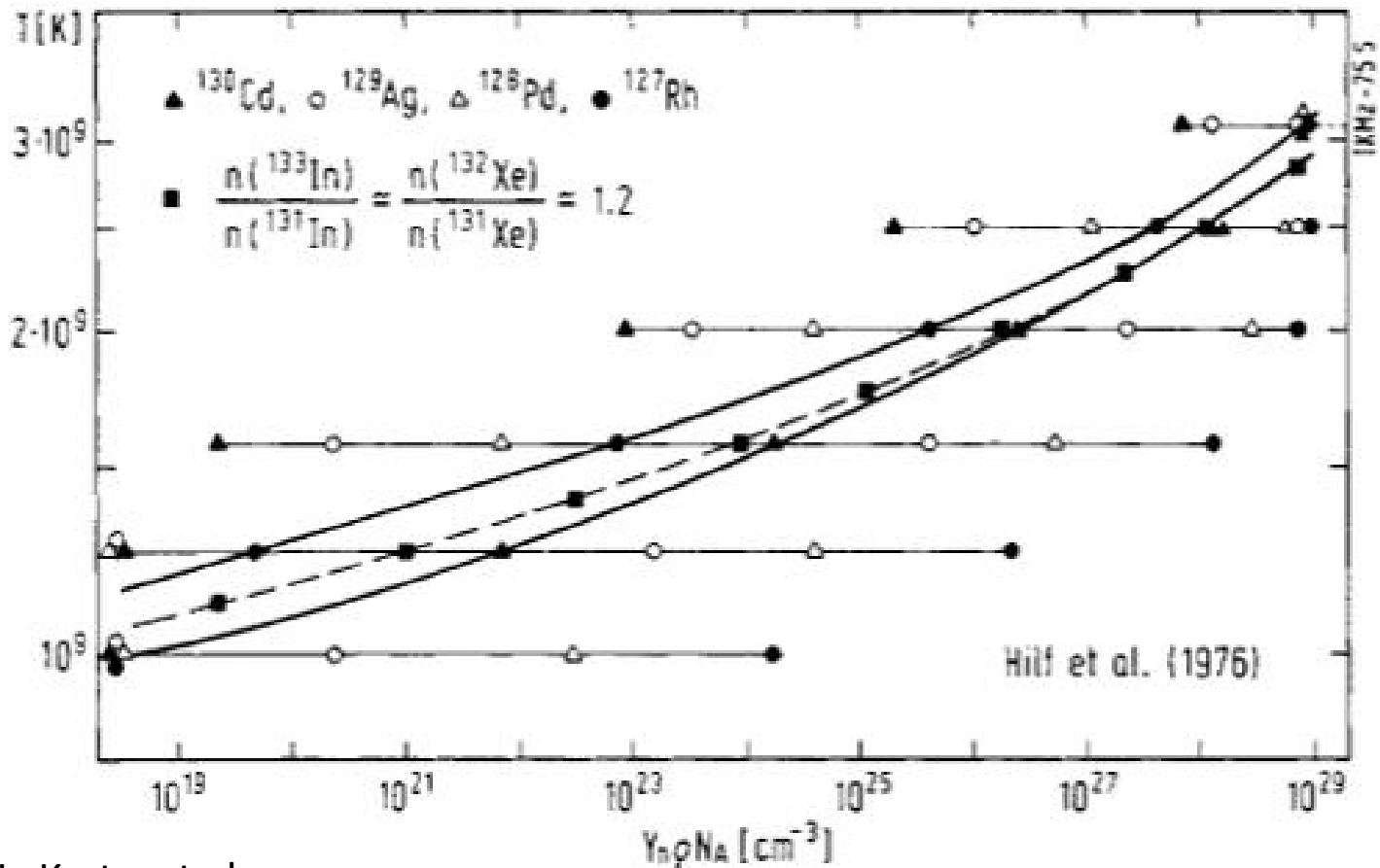
- G : partition function

- $(\gamma, n) \leftrightarrow (n, \gamma)$ equilibrium

$$\Rightarrow r_{n,\gamma}(A, Z) = r_{\gamma,n}(A+1, Z)$$

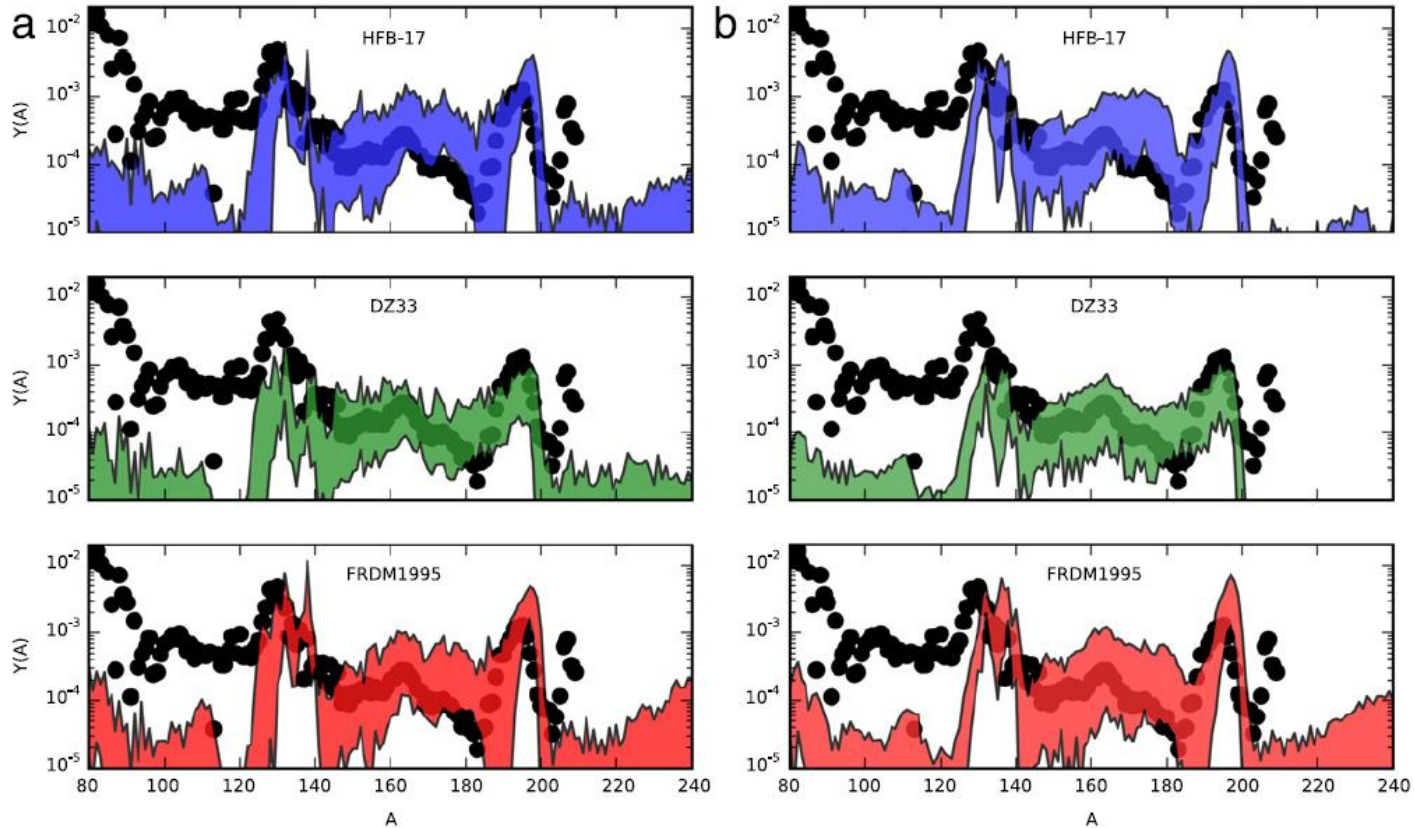
$$- \frac{N(A+1, Z)}{N(A, Z)} = n_n \frac{G(A+1, Z) G_n}{G(A, Z)} \left(\frac{A+1}{A} \right)^{3/2} \left(\frac{2\pi \hbar^2}{m k T} \right)^{3/2} \exp[S_n(Z, A)/kT]$$

T-N_n for second peak



K.L. Kratz, et al.,
JPG 14, S331 (1988).

Influence to the final abundance

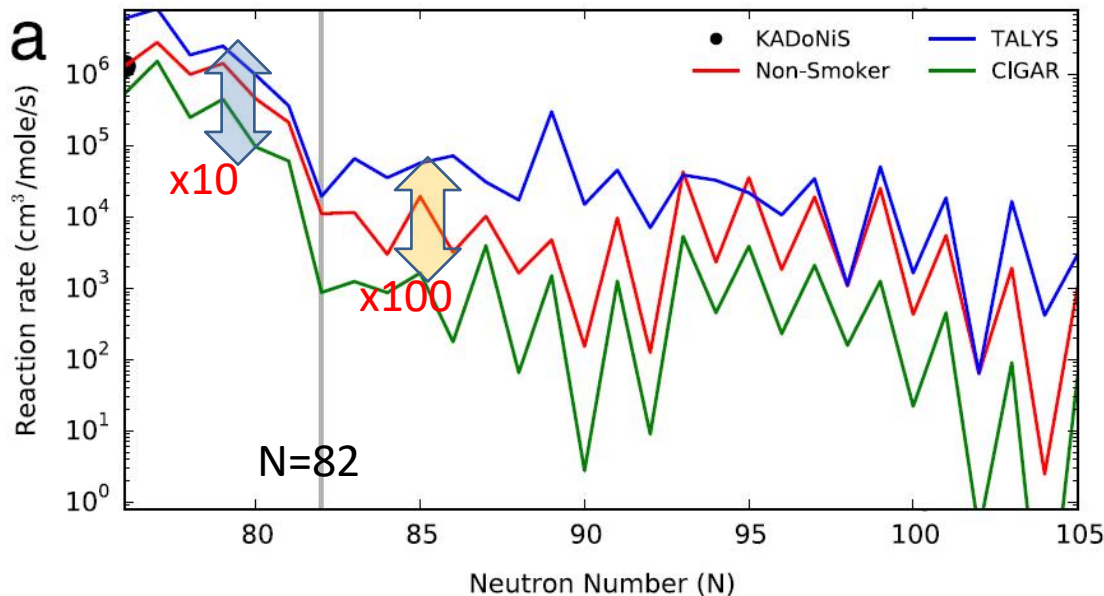


β -decay half-life
 $\times 0.1 \sim \times 10$

$\sigma_{ng} \ 1/10^3 \sim 10^3$

M. Mumpower,
Prog. In Part. and Nucl. Phys. 86
(2016)86-126.

Uncertainties of theoretical $\sigma_{n\gamma}$



M. Mumpower,
Prog. In Part. and Nucl. Phys. 86
(2016)86-126.

Neutron capture cross section
calculation code:

TALYS
NON-Smoker
CIGAR

$^{A}\text{Sn}(n, \gamma) @ T_9 = 1.0$

Only Compound reaction is taken into account.

PRINCIPLE OF NEUTRON CAPTURE REACTION

Direct measurement ?

- Lifetime of neutron ~ 14 min.
- Target nucleus is also short-lived.

eg.) ^{130}Sn $T_{1/2} = 3.7\text{min}$

PHYSICAL REVIEW SPECIAL TOPICS - ACCELERATORS AND BEAMS 17, 014701 (2014)

Measurements of neutron-induced reactions in inverse kinematics

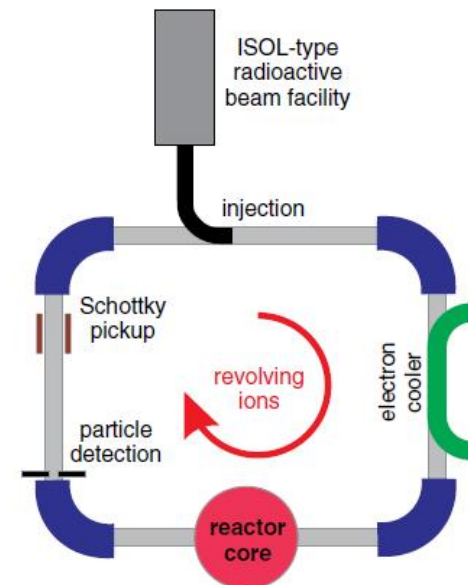
René Reifarth¹ and Yuri A. Litvinov^{2,3}

¹Goethe-Universität Frankfurt am Main, Max-von-Laue-Str.1, 60438 Frankfurt am Main, Germany

²GSI Helmholtzzentrum für Schwerionenforschung, 64291 Darmstadt, Germany

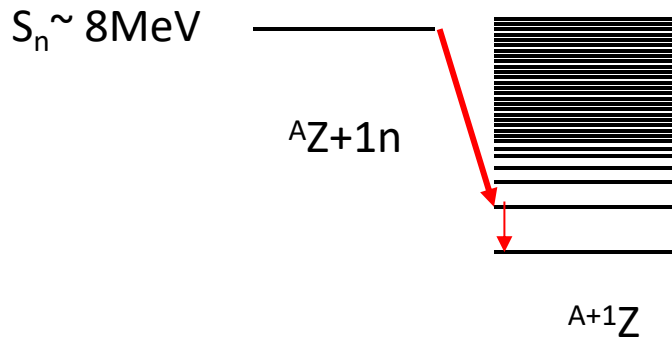
³Max-Planck-Institut für Kernphysik, 69117 Heidelberg, Germany

(Received 17 September 2013; published 10 January 2014)

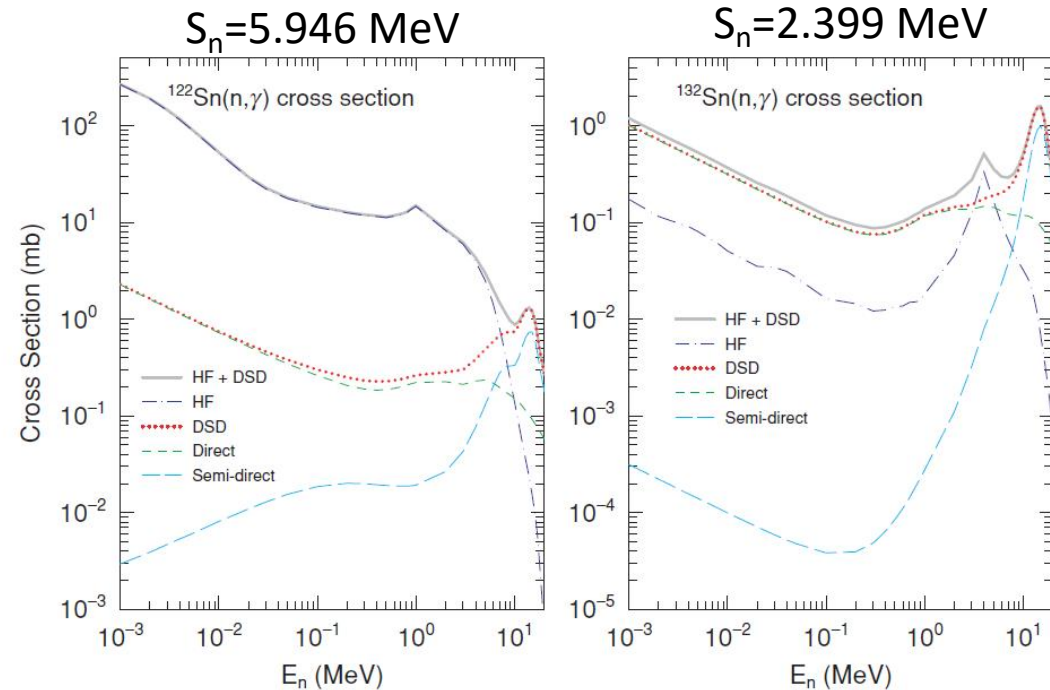
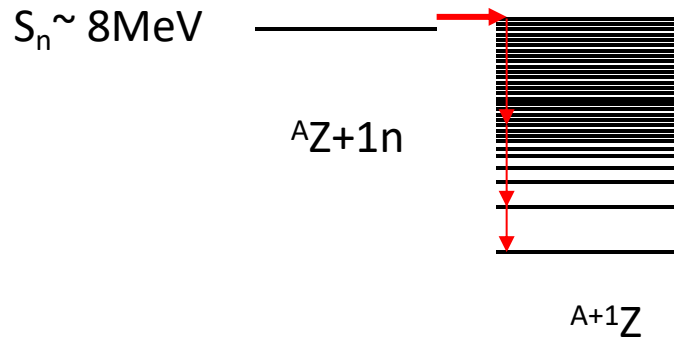


Two reaction mechanisms of (n,γ)

Direct/Semi-direct reaction (DRC)

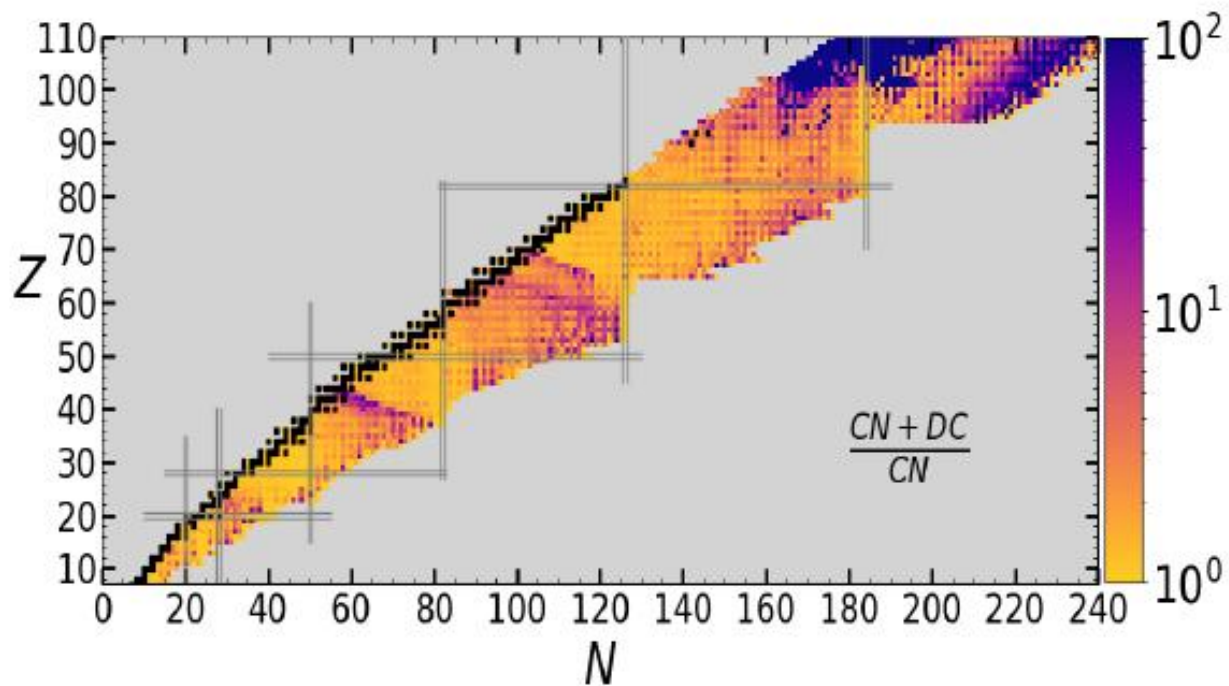


Compound reaction (CN)



S. Chiba et al., PRC77, 015809 ('08)

CN vs DC



I. Kullman, et al., (2023)

Summary 1

- Astrophysical site for r-process element is still mystery even after GW170817.
- Many nuclear physics parameters are needed.
- Neutron capture reaction is one of the missing parameters.
- To evaluate cross sections of short-lived nuclei, we need to use quantum mechanics.

DIRECT RADIATIVE CAPTURE REACTION CHANNEL

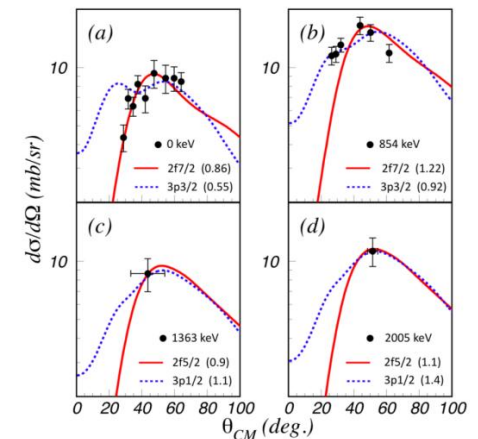
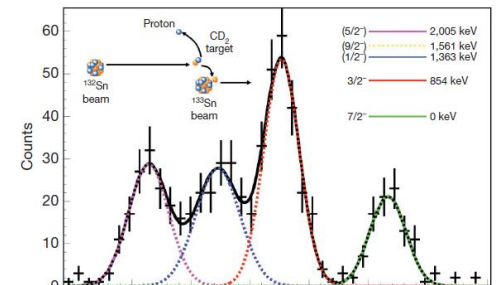
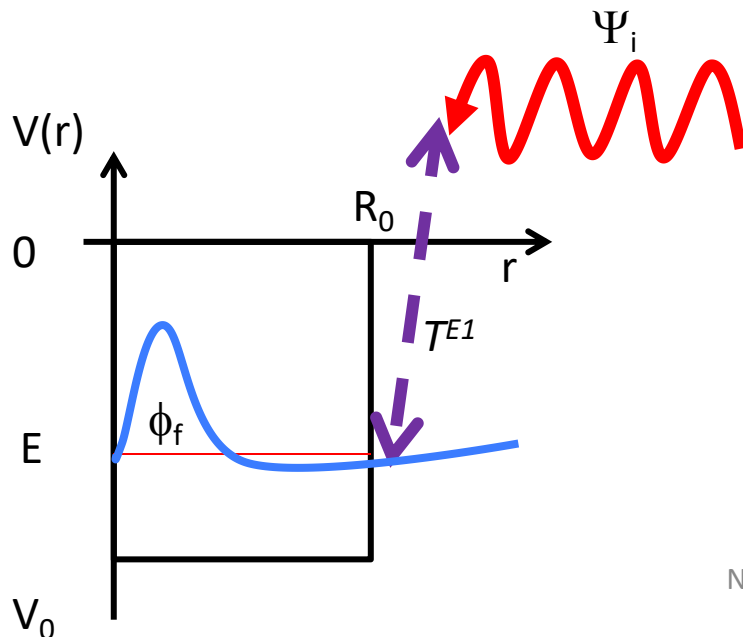
Direct/Semi-Direct reaction

$$\sigma = \frac{16}{9}\pi \frac{\mu k_\gamma^3}{\hbar^2 k} \frac{1}{2I_i + 1} \sum_{MM_i M_f} \left| \langle \Psi_f | \hat{O}_{1M}^*(\mathbf{r}) | \hat{\Psi}_i \rangle + \sum_s \frac{\langle \Psi_f | \hat{O}_{1M}^*(\rho) | \Psi_s \rangle \langle \Psi_s | H' | \hat{\Psi}_i \rangle}{E - (E_s^s + \varepsilon_f) + i\frac{1}{2}\Gamma_s^s} \right|^2, \quad (7)$$

J.P. Boisson and S. Lang, NPA189, 334 (1972)

final bound state wave function; J^π , strength

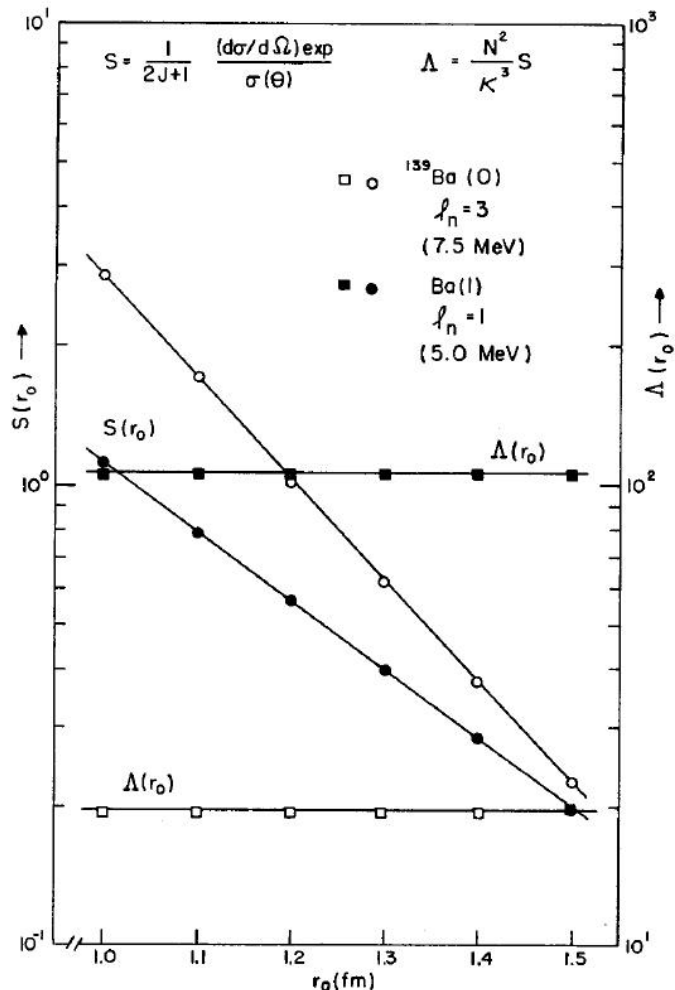
→ (d,p) reactions etc.



$^{132}\text{Sn}(d,p)^{133}\text{Sn}$.

K. Jones et al., Nature 465, 27 (2010)

reduced normalization constant



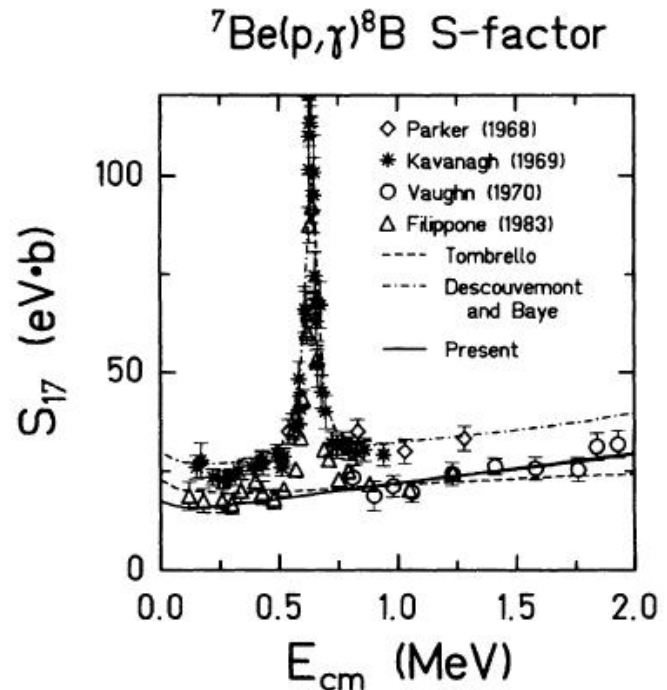
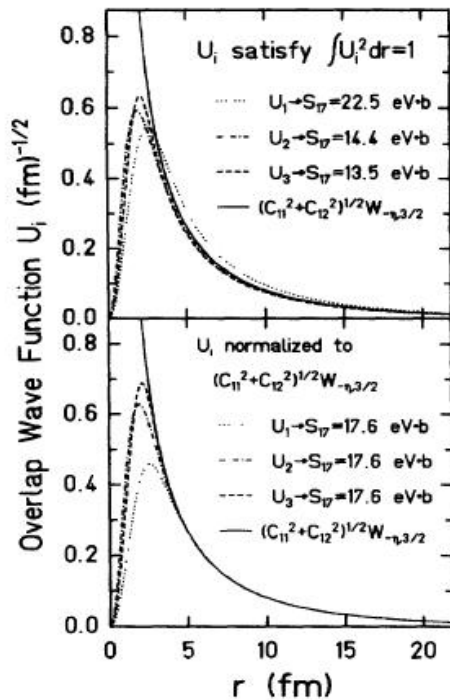
- S from DWBA strongly depends on the form factor.
- Reduced normalization constant $\Delta = N^2/K^3 * S$ was found to be independent.
- “Though introducing reduced normalizations as spectroscopic quantities is somewhat disadvantageous because the single particle fractions of the states in question cannot be recognized directly, ...”

B. Eteinmetz et al., PRC18, 71 ('74).

J. Raraport and A.K. Kerman, NPA119(1968)641.

Asymptotic Normalization Constant

$$\left[-\frac{\hbar^2}{2m} \frac{1}{r} \left(\frac{d}{dr} \right)^2 + \frac{Z_1 Z_2}{r} + \frac{l(l+1)}{2mr^2} - E \right] u_l(r) = 0 \quad u_l(r) \rightarrow \text{Whittaker function}$$



H.M. Xu et al., PRL73,2027 ('94)

σ_{py} was deduced by integrating the Whittaker function normalized with ANC and $r > 5$ fm.

How about the case of n ?

$$\begin{aligned}
 \sigma_{n\gamma} &= \frac{16\pi}{9\hbar} \left(\frac{\varepsilon_\gamma}{\hbar c} \right)^3 \bar{e}^2 \left| \langle \Psi_f | \hat{T}^{E1} | \Psi_i \rangle \right|^2 \\
 &= \frac{16\pi}{9\hbar} \left(\frac{\varepsilon_\gamma}{\hbar c} \right)^3 \bar{e}^2 \left| \sqrt{S} A_{if} \int_0^\infty u_{lf}(r) r w_{li}(r) dr \right|^2
 \end{aligned}$$

S : spectroscopic factor

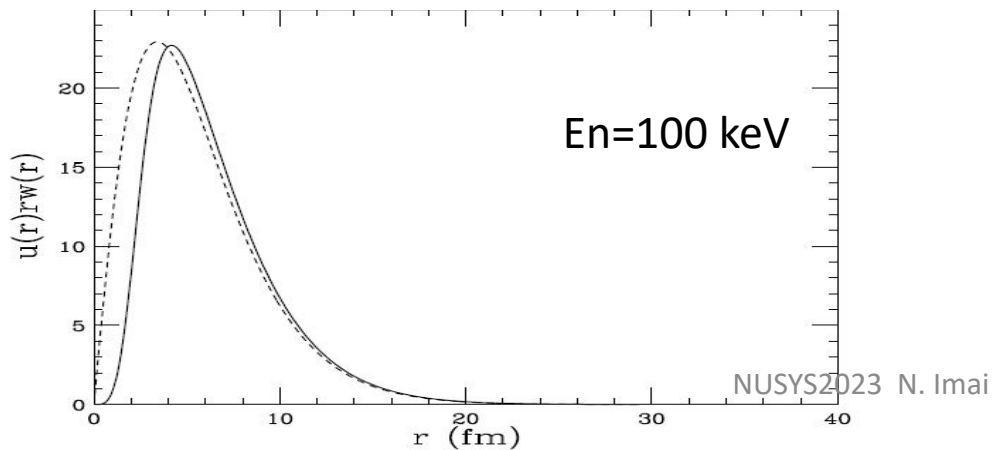
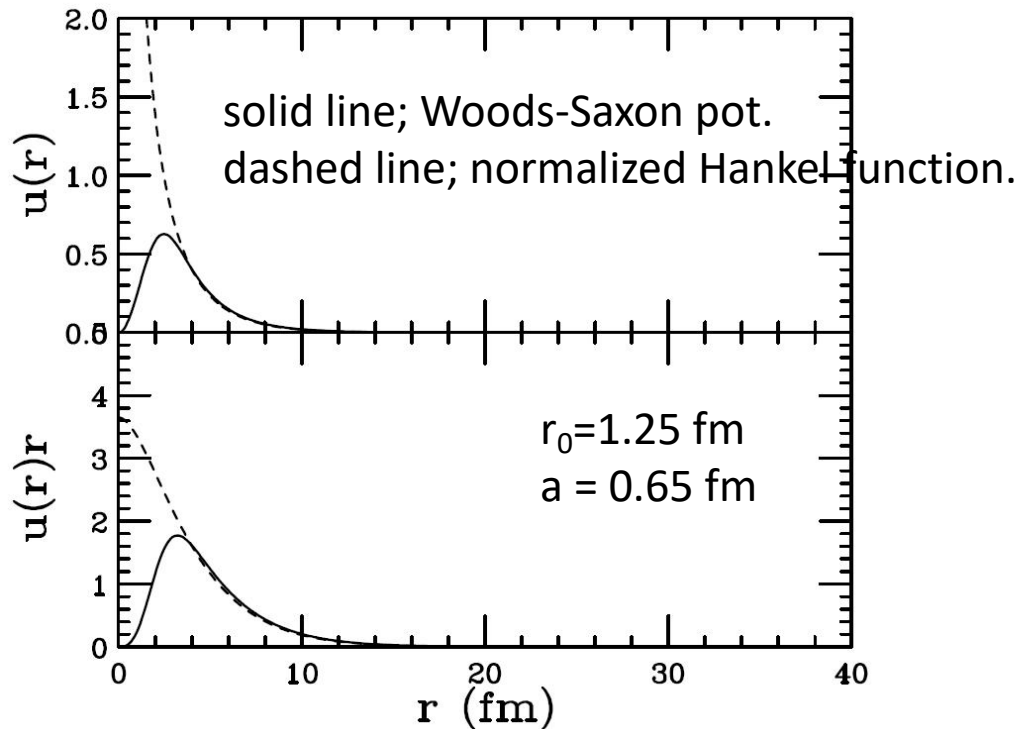
$w_{lj}(r)$; radial part of incoming wave function

$u_{lf}(r)$; radial part of final bound state wave function

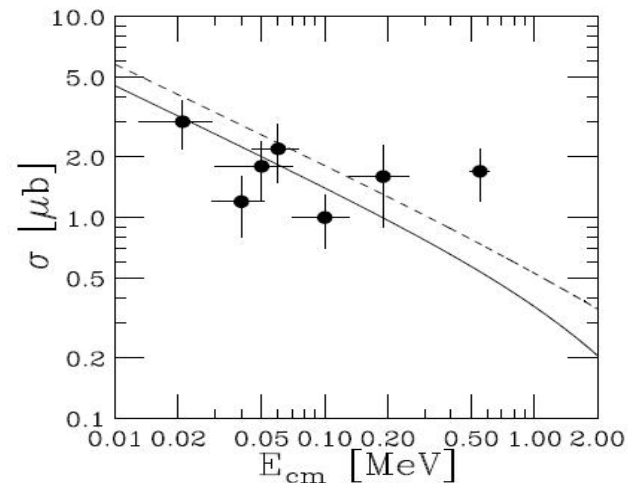
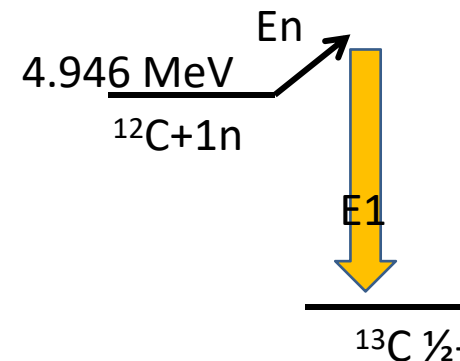
$$T^{E1} = rY^{(1)}(\theta, \varphi)$$

E1 operator magnifies the tail part of the wave function

$^{12}\text{C}(n,\gamma)^{13}\text{C}(1/2^-)$; s-wave n capture



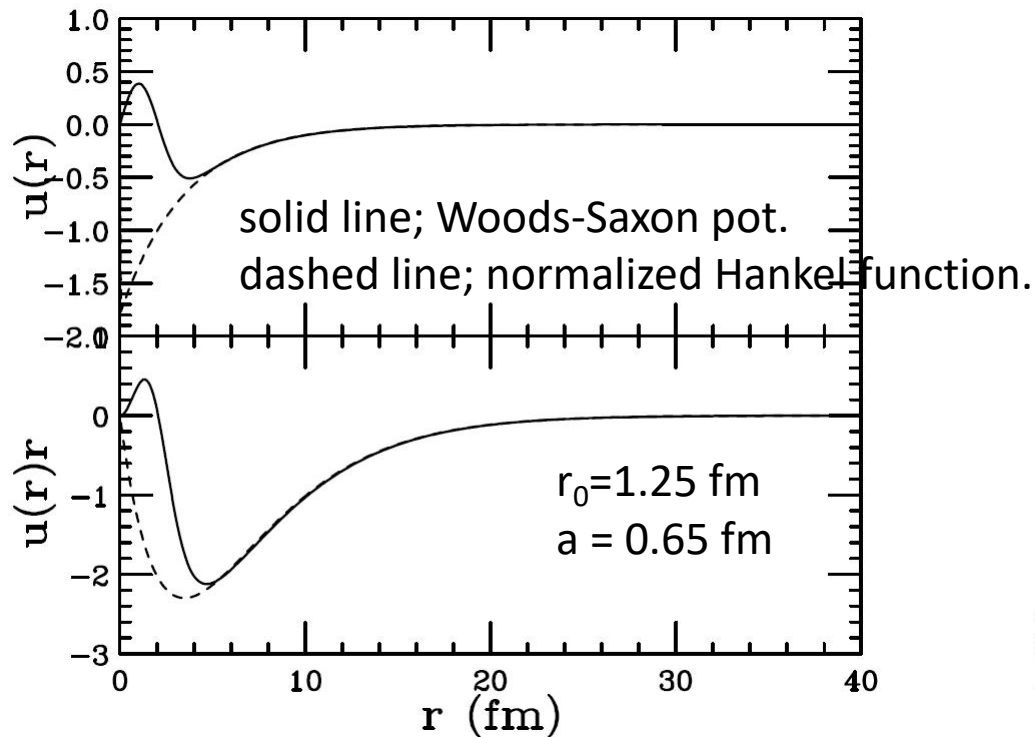
$$0^+ + \frac{1}{2}^+ + \Delta L = E1 + 1/2^-$$



(n, γ)data; APJ 422, 912 (1994)

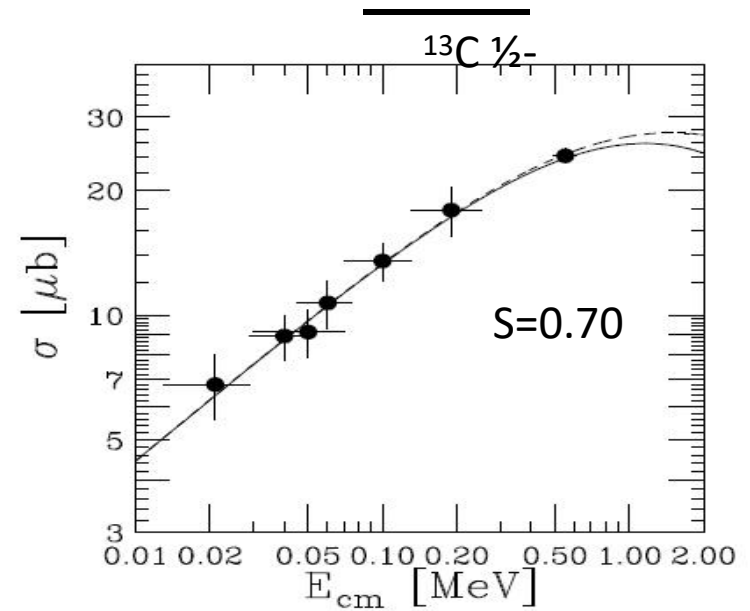
Hankel func. doesn't work well...

$^{12}\text{C}(n,\gamma)^{13}\text{C}(1/2^+)$; p-wave n capture



$$0^+ + \frac{1}{2}^+ + \Delta L = E1 + 1/2^+$$

$^{12}\text{C}+1n$
4.946 MeV E_n
1.853 MeV $E1$
 $1/2^+$



(n, γ)data; APJ 422, 912 (1994)

Hankel func. works well !

Distorted Wave Born Approximation

$$T_{\beta\alpha} \cong \langle \Phi_\beta | V_\beta | \Phi_\alpha \rangle$$

$$\approx D_0 \frac{4\pi}{k_\alpha k_\beta} \frac{m_B}{m_A} \sum_{L_\alpha L_\beta} i^{L_\alpha - L_\beta - m} \quad \text{post form zero range DWBA}$$

$$\times \sqrt{(2L_\alpha + 1)(2l + 1)} \langle L_\beta l 00 | L_\alpha 0 \rangle \langle L_\beta l - m m | L_\alpha 0 \rangle \\ \times Y_{L_\beta}^m(\hat{k}_\beta) \int \frac{u_l(r_\alpha)}{r_\alpha} \chi_{L_\beta}^\beta(k_\beta, \frac{m_A}{m_B} r_\alpha) \chi_{L_\alpha}^\alpha(k_\alpha, r_\alpha) dr_\alpha$$

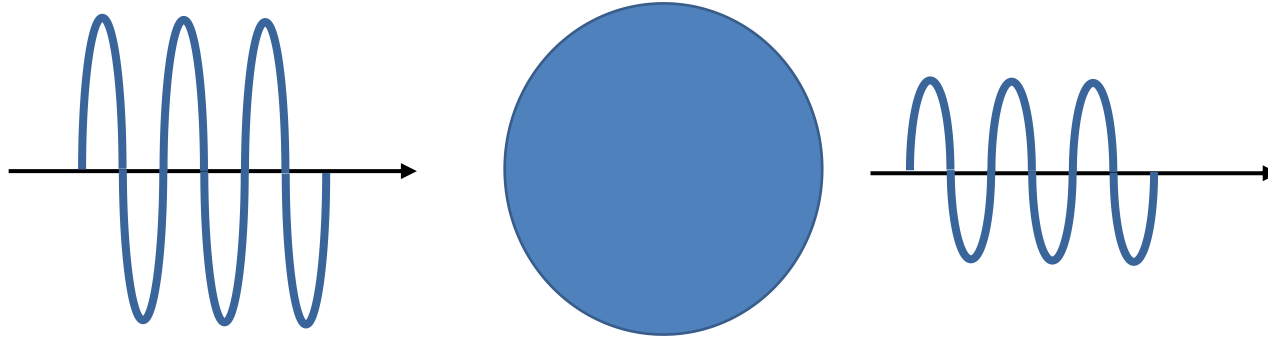
$d\sigma/d\Omega$ of the transfer reaction \rightarrow ANC

if the reaction takes place well outside the target nucleus.

radial distribution of the overlap integral;

$$I_{L_\beta}(r) \equiv \langle L_\beta 1 - m m | L_\alpha 0 \rangle Y_{L_\beta}^m(\hat{k}_\beta) \frac{u_l(r_\alpha)}{r_\alpha} \chi_{L_\beta}^\beta(k_\beta, \frac{m_A}{m_B} r_\alpha) \chi_{L_\alpha}^\alpha(k_\alpha, r_\alpha)$$

Optical model potential



Quantum mechanical wave

Elastic scattering: only direction is changed.

Inelastic scattering: scattering into an exit channel different from the incident one.

Cloudy crystal ball

Elastic scattering: reflection of optical waves

Inelastic scattering: absorption due to the fact that crystal ball is cloudy

Smooth variations of the scattering cross section as a function of incident energy E and target nucleon number A .

Phenomenological OM potential

Optical model potential=

The average interaction between nucleons in the projectile with those in the target

$U_{opt}(\vec{r})$ follows closely the density distribution

$$f(r, r_0, a) = \frac{1}{1 + \exp\{(r - r_0)/a\}}$$

In optical model studies, this is known as the Woods-Saxon form

$$U_{vol}(\vec{r}) = - \{V_0 f(r, r_v, a_v) + iW_0 f(r, r_w, a_w)\}$$

DWBA codes

- DWUCK4,5;
 - <https://github.com/padsley/DWUCK5>
 - <https://github.com/padsley/DWUCK4>
- FRESCO;
 - <https://www.fresco.org.uk/>



Chat GPT?



Can you also let me know the input file for the $^{130}\text{Sn}(d,p)$ reaction at 40 MeV for FRESKO DWBA code?



Certainly! Here is an example input file for the FRESKO DWBA code to calculate the $^{130}\text{Sn}(d,p)$ reaction at 40 MeV. This is a simplified example, and you might need to adjust the parameters according to your specific experiment and requirements:



```
&input
Title = "130Sn(d,p) Reaction at 40 MeV"
Ener = 40.0      ! Incident energy in MeV
React = "130Sn(d,p)131Sn" ! Reaction description
Elab = 45.0      ! Laboratory energy in MeV
ElabStep = 0.5   ! Energy step in MeV
ElabMax = 60.0   ! Maximum laboratory energy in MeV
J_i = 0          ! Spin of the initial state (ground state)
J_f = 1          ! Spin of the final state
/

&channel
Proj = "130Sn"   ! Projectile
Targ = "d"       ! Target
Ex = 0.0         ! Excitation energy of the residual nucleus in MeV
/

&potential
Type = "saxon"   ! Potential type
V0 = -50.0       ! Central potential depth in MeV
R0 = 1.25        ! Central potential radius in fm
a0 = 0.65        ! Central potential diffuseness in fm
/

&output
Dir = "output"   ! Output directory
File = "results" ! Output file name
Plot = true      ! Generate plots
/

&options
Coul = true      ! Include Coulomb interaction
```

```
56Fe(d,p)57Fe @ Ed=12 MeV;
NAMELIST
&FRESKO hcm=0.1 rmatch=20.000
rintp=0.20 hnl=0.100 rnl=4 centre=-0.45 jtmax=15
thmin=1.00 thmax=180.00 thinc=1.00
it0=1 iter=1
chans=1 smats=2 xstabl=1
elab= 12.0 /

&PARTITION name='deu' massp=2.014 zp=1 namet='f56' masst=55.934 zt=26 nex=1 /
&STATES jp=1.0 bandp=1 ep=0.0 cpot=1 jt=1.0 bandt=1 et=0.0000 /

&PARTITION name='pro' massp=1.0078 zp=1 namet='f57' masst=56.935 zt=26 qval=5.421 nex=1 /
&STATES jp=0.5 bandp=1 ep=0.0 cpot=2 jt=0.5 bandt=-1 et=0.0000 /
&partition /

&POT kp=1 itt=F at=56 rc=1.15 /
&POT kp=1 type=1 itt=F p1=90 p2=1.15 p3=0.81 /
&POT kp=1 type=2 itt=F p4=21 p5=1.34 p6=0.68 /

&POT kp=2 itt=F at=57 rc=1.15 /
&POT kp=2 type=1 itt=F p1=47.9 p2=1.25 p3=0.65 /
&POT kp=2 type=2 itt=F p4=11.5 p5=1.25 p6=0.47 /

&POT kp=3 itt=F at=56 rc=1.00 /
&POT kp=3 type=1 itt=F p1=65.0 p2=1.25 p3=0.65 /

&POT kp=4 itt=F ap=1.0000 at=0.0000 rc=1.0000 /
&POT kp=4 type=1 shape=2 itt=F p1=72.1500 p2=0.0000 p3=1.4840 /

&POT kp=5 itt=F at=56 rc=1.15 /
&POT kp=5 type=1 itt=F p1=47.9 p2=1.25 p3=0.65 /
&POT kp=5 type=2 itt=F p4=11.5 p5=1.25 p6=0.47 /
&spot /
```

Sample input of DWUCK4

$^{130}\text{Sn}(d,p)^{131}\text{Sn}^*$ (Ex=3.9 MeV, $J^\pi=3p_{3/2}$)

```

10010000010000000000                                130Sn(d,p)131Sn(Ex=3.9 p3)
 900.000  0.0000  0.1000
 40  1  1  3
  0.1000  0.0000 50.0000  0.0000  0.7000
40.0000  2.0141  1.0000129.914  50.0000  1.3000  0.0000  0.0000  2.0000
  1.000 -91.941  1.150  0.810          -2.348  1.06  0.348
 -2.000  0.000  0.000  0.000  0.000  38.44  1.340  0.680
-0.432  1.0000  1.0000 131.000 50.0000  1.2500  0.0000  0.0000  1.0000
  1.000 -58.419  1.110  0.570
  2.000  0.000  0.000  0.000  0.000 101.618  1.110  0.500
 -4.000 -11.000  1.110  0.570
-1.7920  1.0000  1.0000 129.914 50.0000  1.3000  0.0000  0.0000  1.0000
  1.000 -1.000  1.250  0.600
 -4.000 -6.500  1.250  0.600
  2.0000  1.0000  3.0000  1.0000 36.0000
9999999999
  
```

Incoming wave

outgoing wave

Form factor
(single particle w.f.
Of the final state

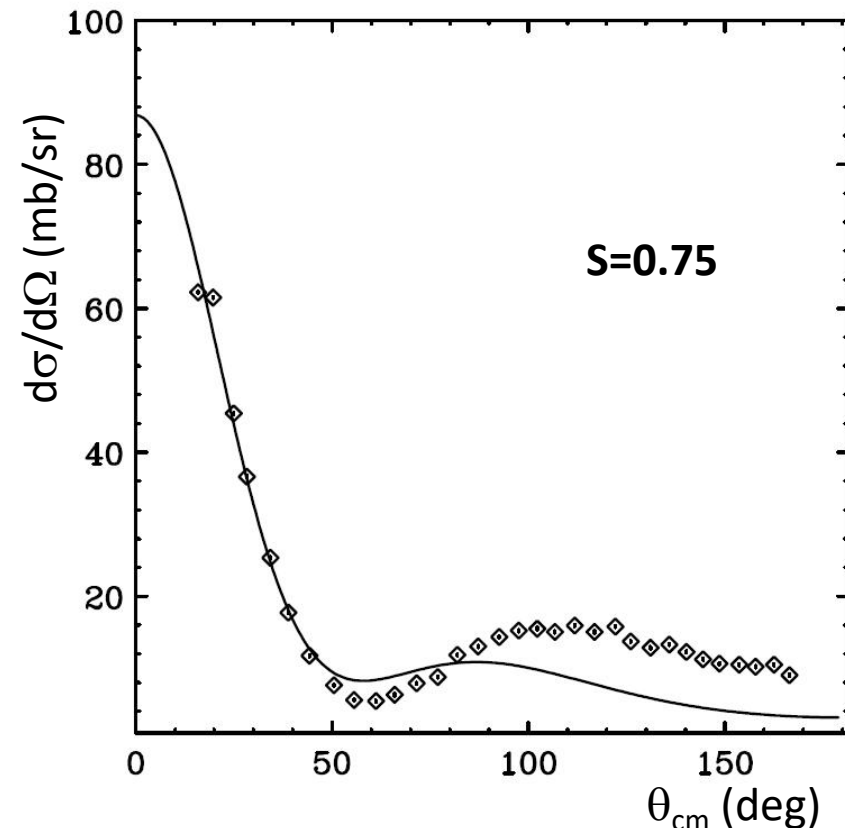
40 2.0141 1.00 129.914 50.0 1.3 0.0 0.0 2.0

^2H ^{130}Sn $2J$

40 1 1 3 transfer to populate $p_{3/2}$
 $2 \times \Delta J$: angular momentum transfer
 Δl : angular momentum transfer
 # of angular momentum transfer

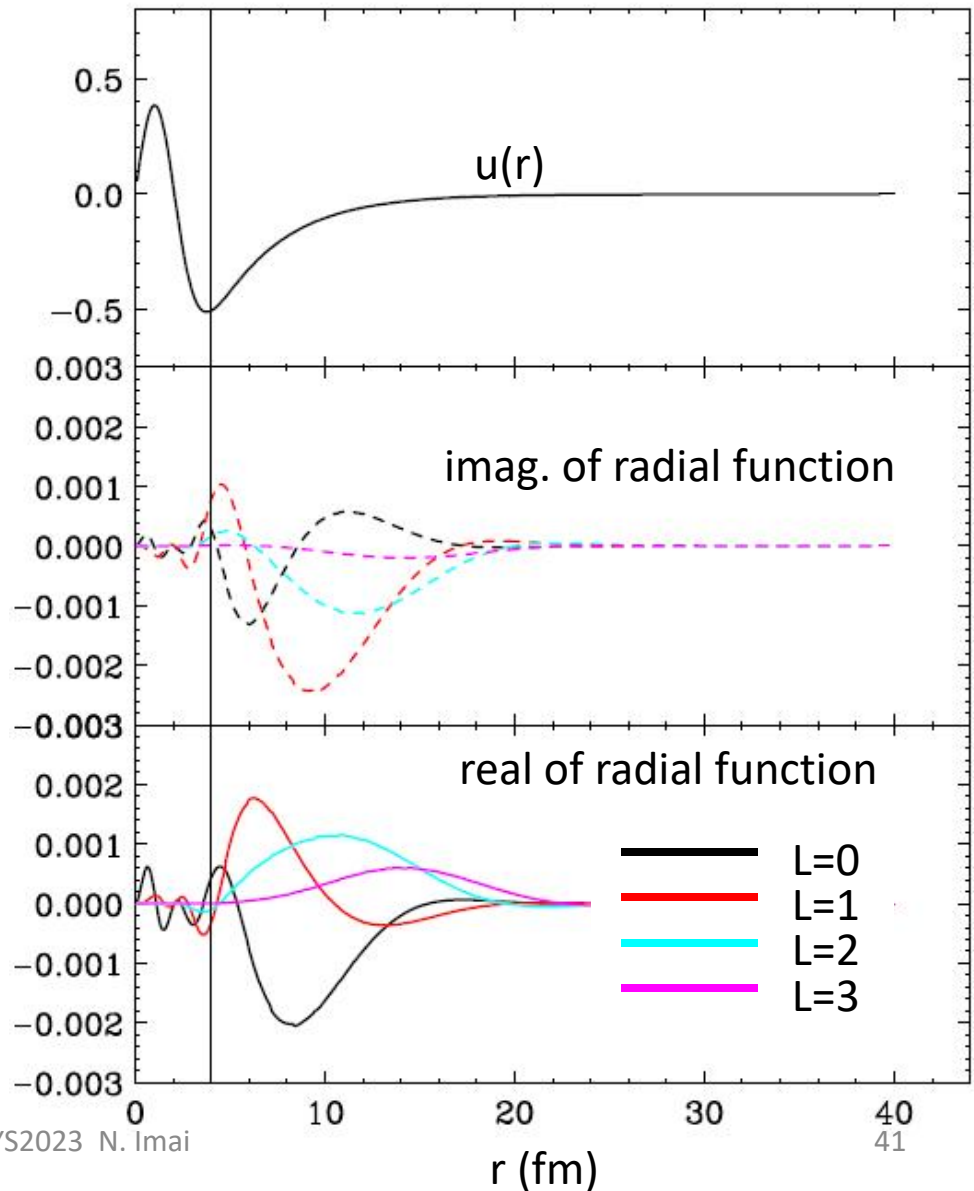
2 1 3 1 36
 $2 \times S$
 $2 \times J$
 L
 # of nodes

$^{12}\text{C}(d,p)^{13}\text{C}^*(1/2^+) @ 2.033 \text{ MeV}$

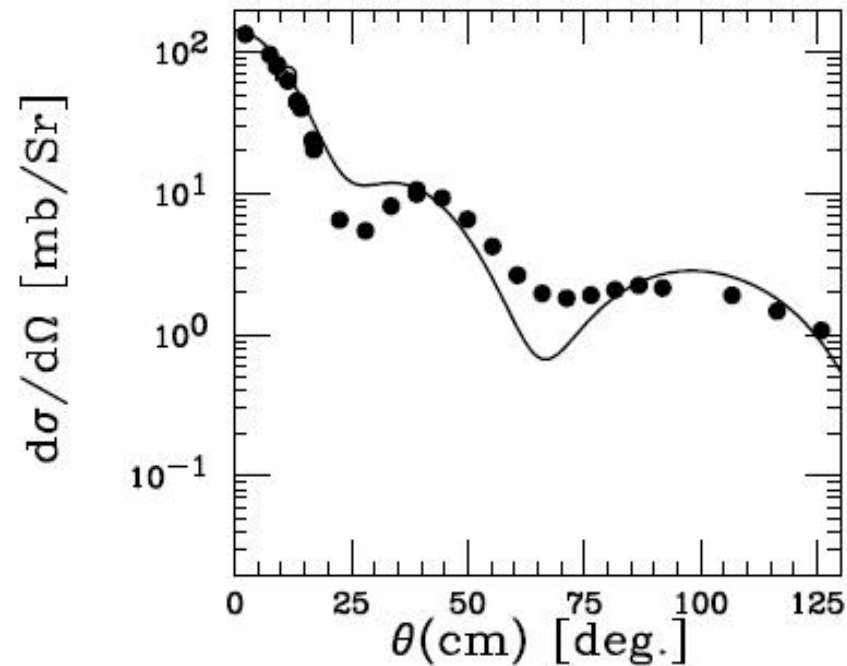


The experimental data and the optical model parameters are taken from NPA92(1967)91-122.

$$\frac{d\sigma/d\Omega_{\text{rcutoff}=0\text{fm}}}{d\sigma/d\Omega_{\text{rcutoff}=4\text{fm}}} = 99\%$$

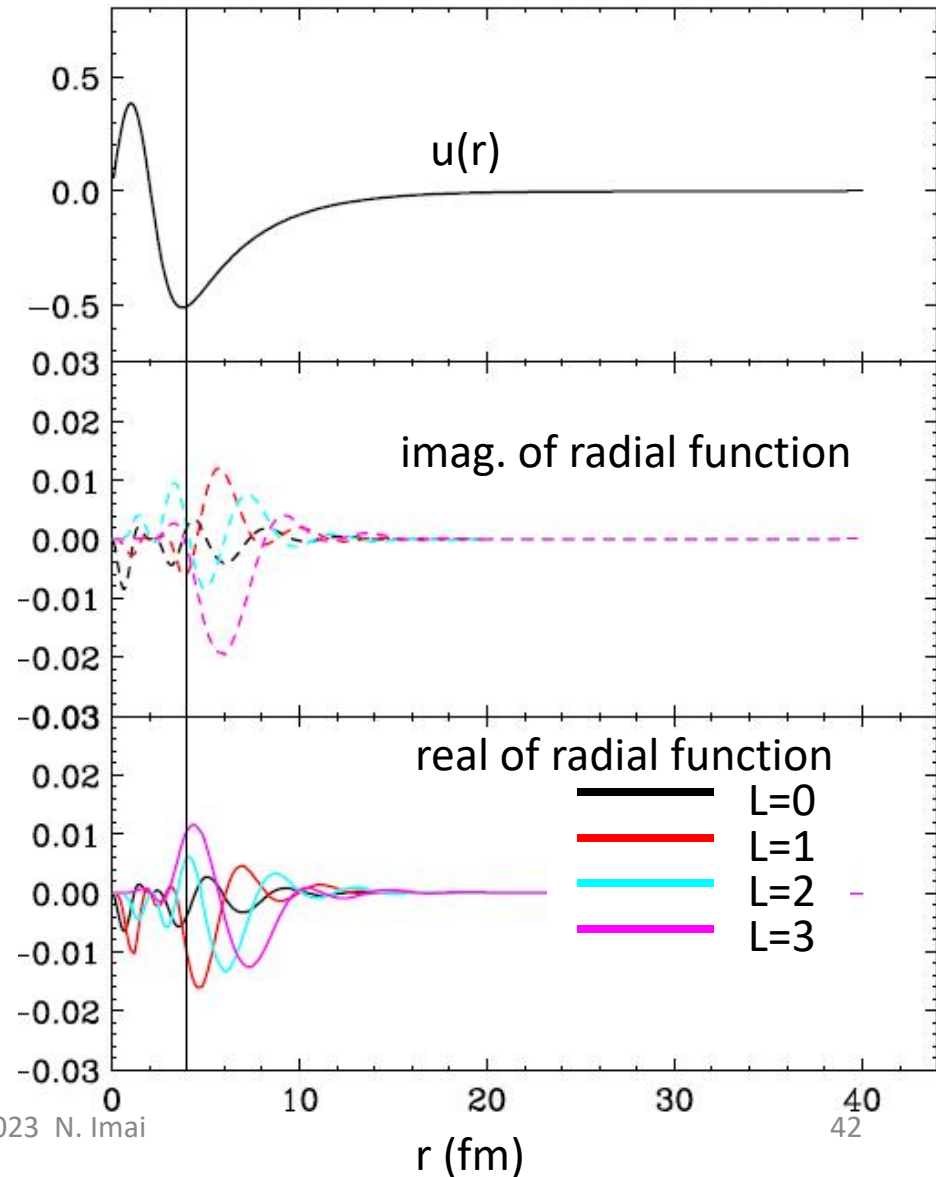


$^{12}\text{C}(d,p)^{13}\text{C}^*(1/2^+)$ at 11.8 MeV

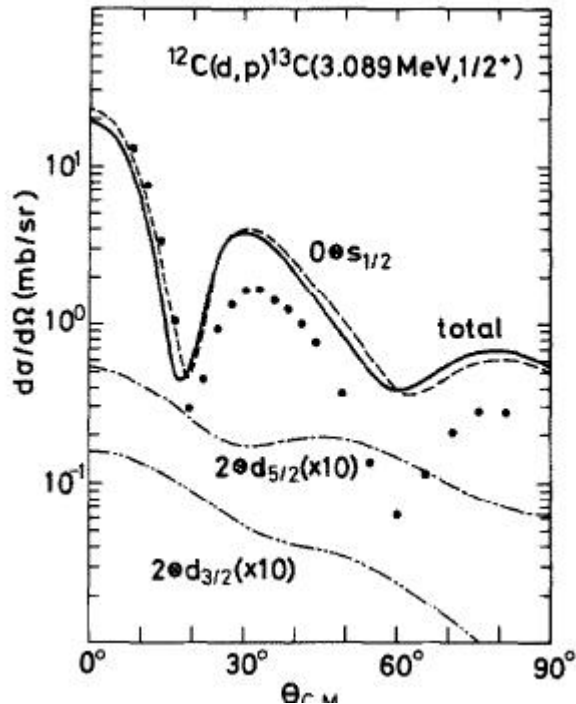


N. Imai et al, NPA 688, 281c (2001)
up to $d\sigma/d\Omega(\theta=2)$ was measured

$$\frac{d\sigma/d\Omega_{\text{rcutoff}=0\text{fm}}}{d\sigma/d\Omega_{\text{rcutoff}=4\text{fm}}} = 79\%$$

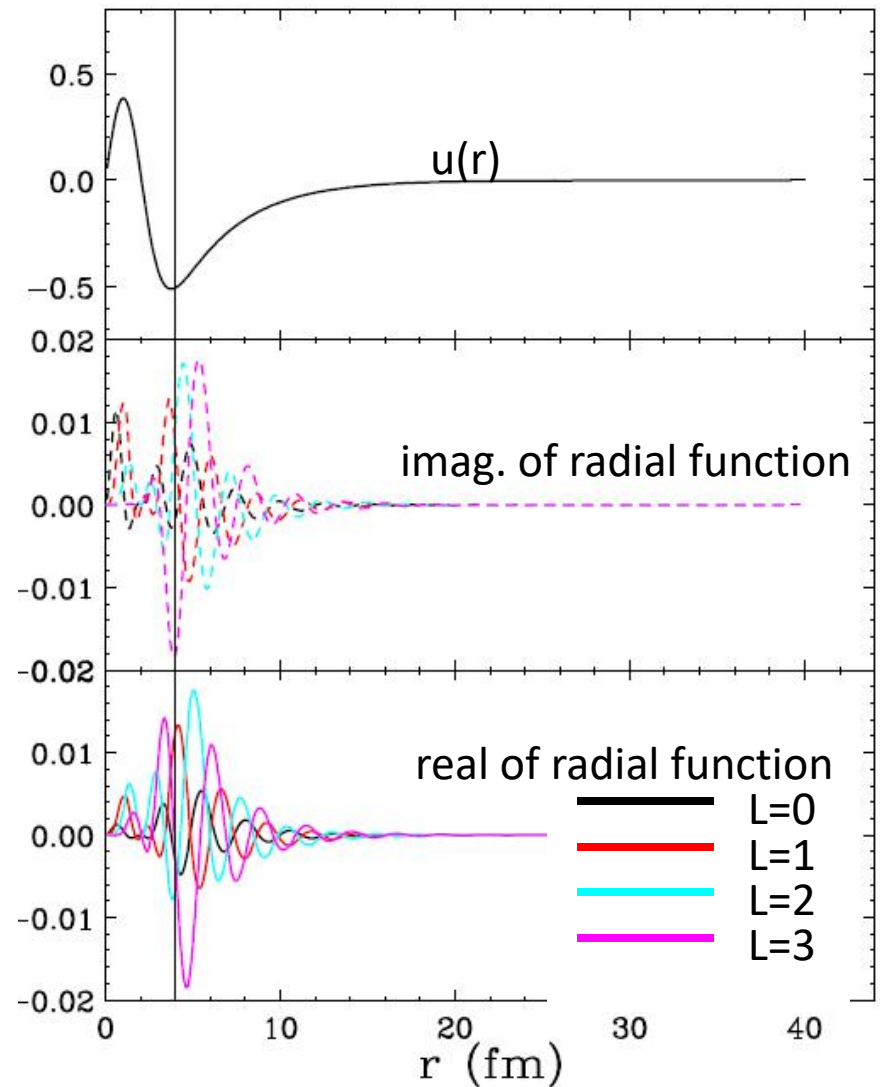


$^{12}\text{C}(d,p)^{13}\text{C}^*(1/2^+)$ at 30 MeV



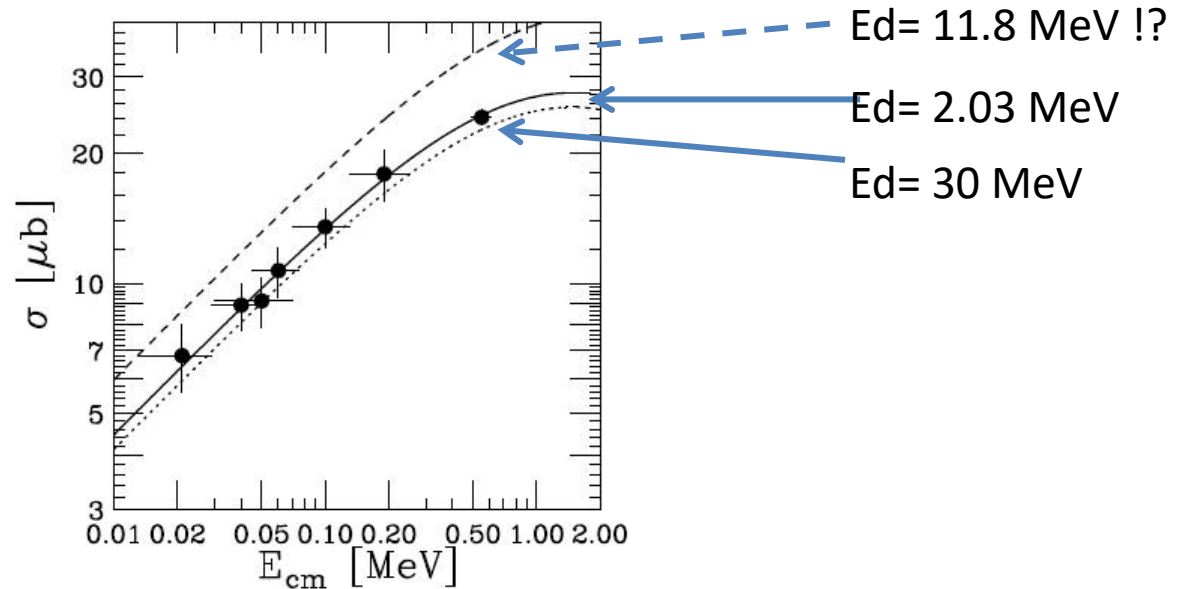
H. Ohnuma et al., NPA 448 ('85)205

$$\frac{d\sigma/d\Omega_{\text{rcutoff}=0\text{fm}}}{d\sigma/d\Omega_{\text{rcutoff}=4\text{fm}}} = 66\%$$

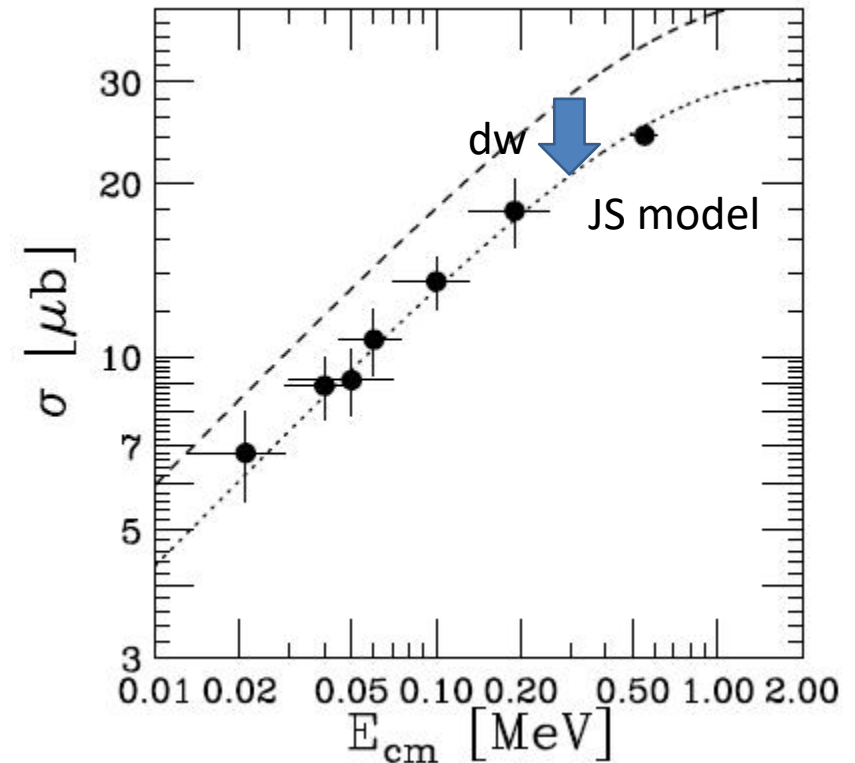
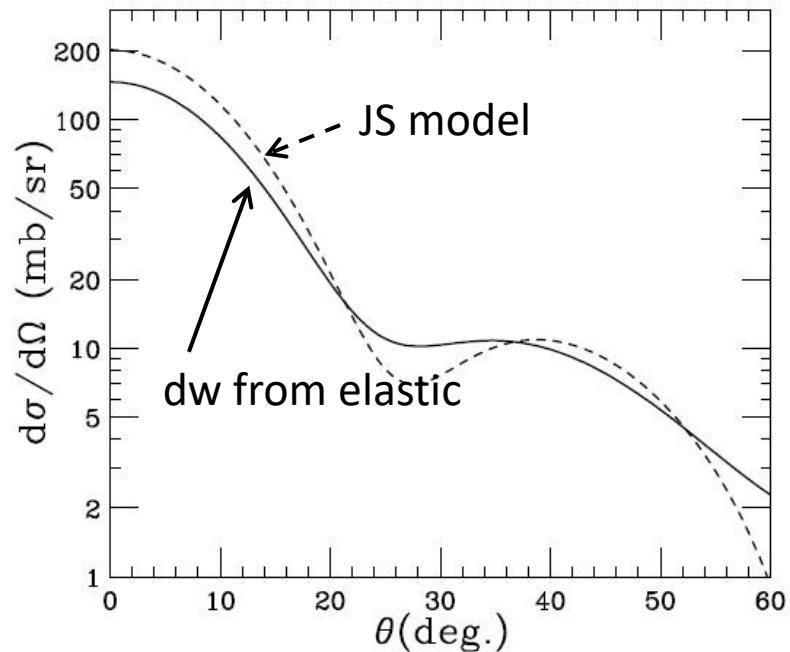


$\sigma(n,\gamma)$ with ANC

	$E_d=2.03$ MeV	$E_d=11.8$ MeV	$E_d=30$ MeV
S	0.75 (11)	0.94 (8)	0.65
ANC (fm^{-1}) ($b^2 \cdot S$)	2.6 (4)	3.6(4)	2.4



d breakup effect; ADBA



Adiabatic breakup model;

R.C. Johnson and P.J.R. Soper, PRC1, 976 ('70)

Prescription;

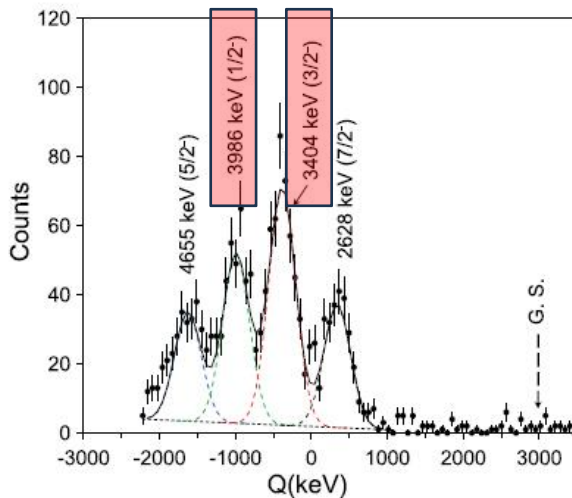
$V_{JS}=V^p+V^n$, $W_{JS}=(W^p+W^n)a/a_{JS}$, $r_{JS}=r$, $a_{JS}=a+0.04$

J.D. Harvey and R.C. Johnson, PRC 3, 636 ('71)

	DW	JS
S	0.94 (8)	0.68 (6)
ANC	3.6(4)	2.6(3)

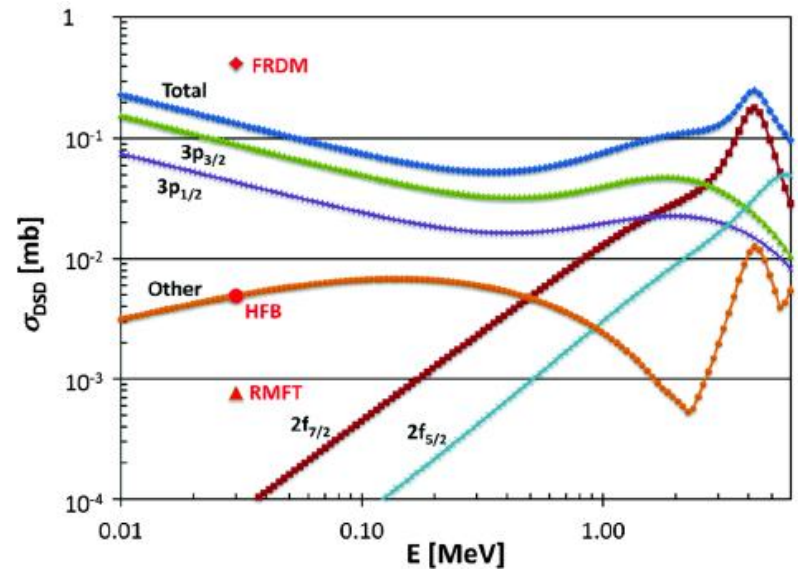
DRC in ^{130}Sn

- low-energy neutron $L \sim 0$
- E1 transition is dominant.
- For the even-odd nuclei, bound states which have $L \sim 1$ are important.



$d(^{130}\text{Sn}, p)$

PRL109 172501 ('12)



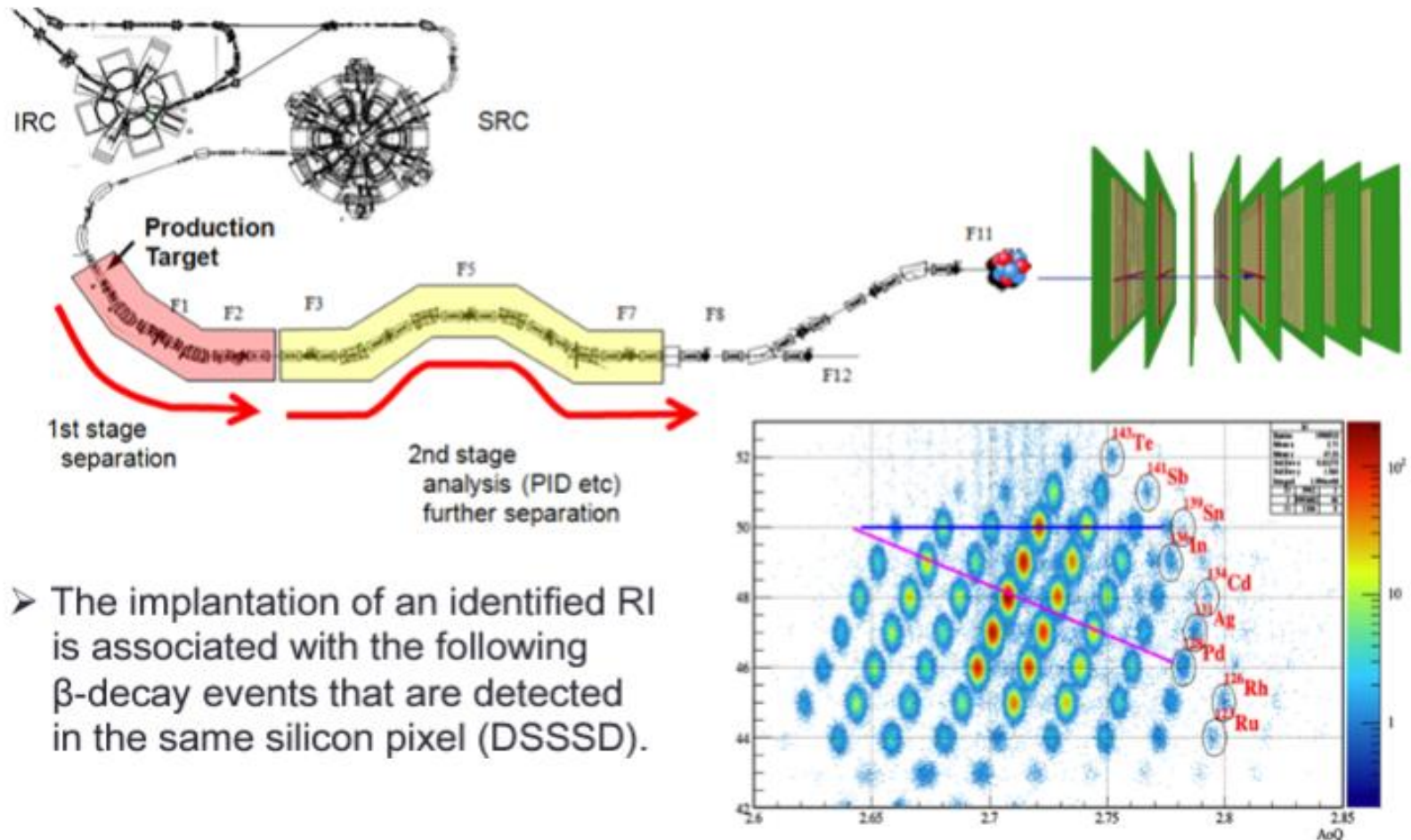
Inverse reactions with RIBs

RIBF; world-leading RIB facility

Any RIB can be produced by the fission of ^{238}U of $\beta=0.7$



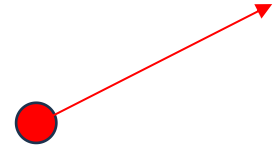
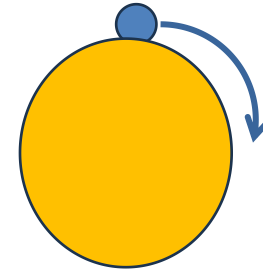
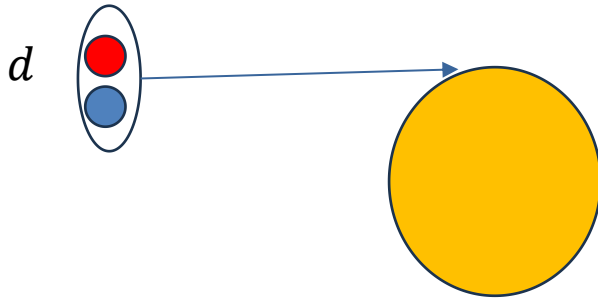
Beam production



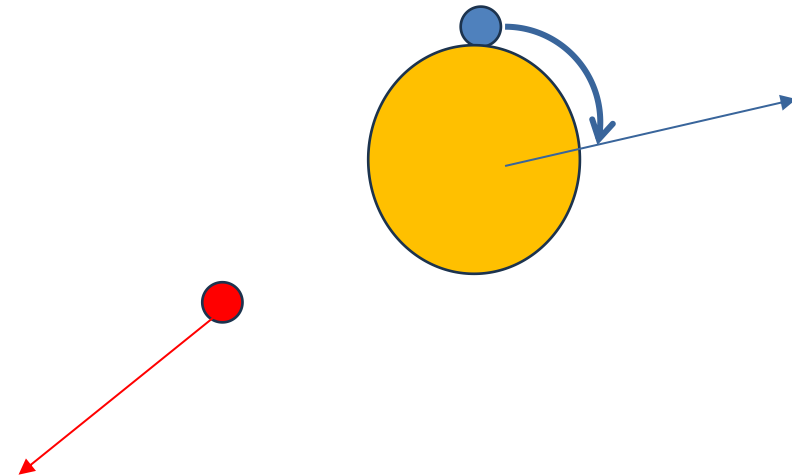
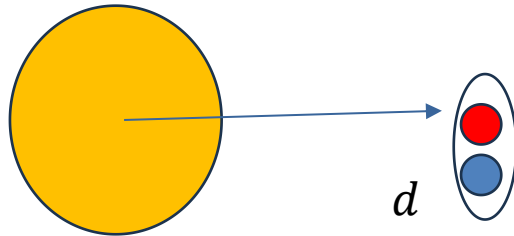
- The implantation of an identified RI is associated with the following β -decay events that are detected in the same silicon pixel (DSSSD).

Reactions with heavy RIB

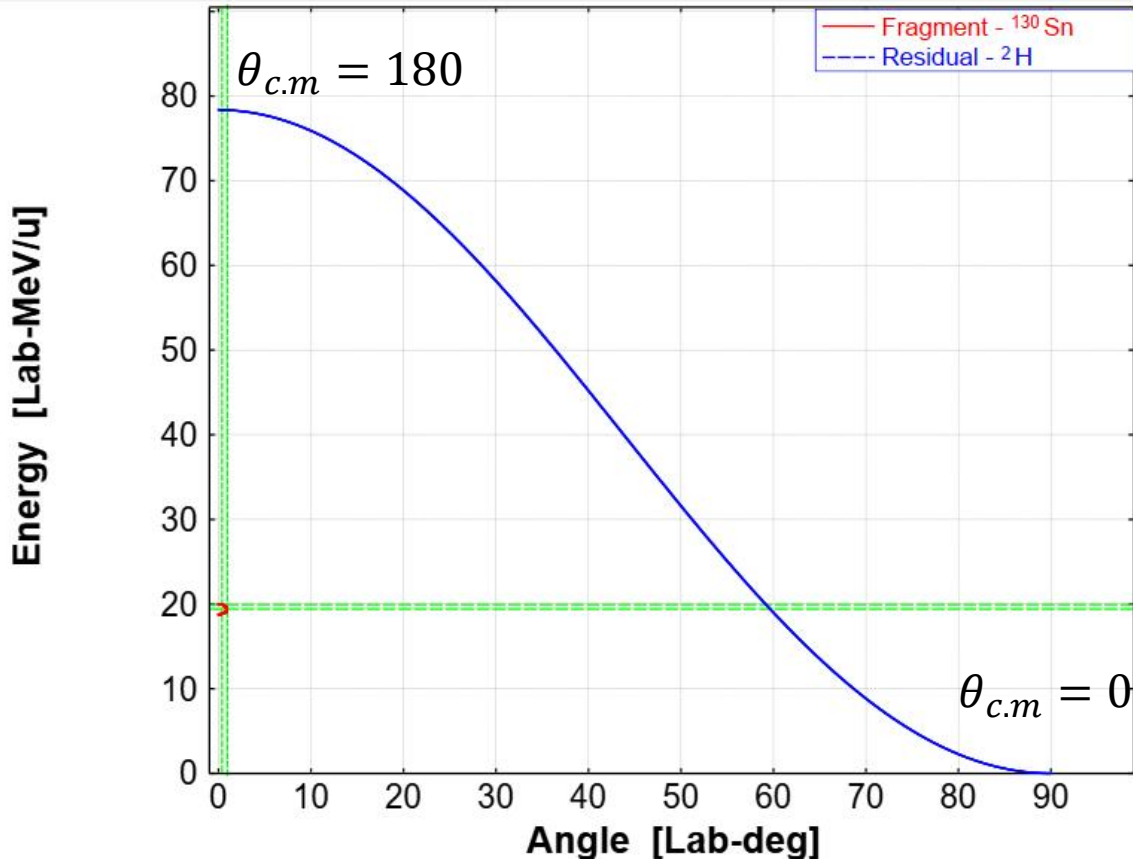
Normal kinematics



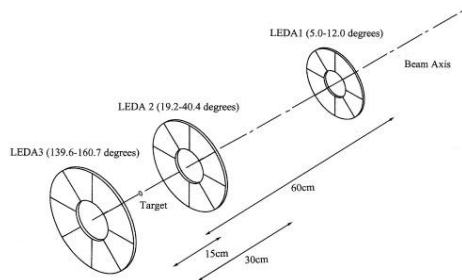
Inverse kinematics



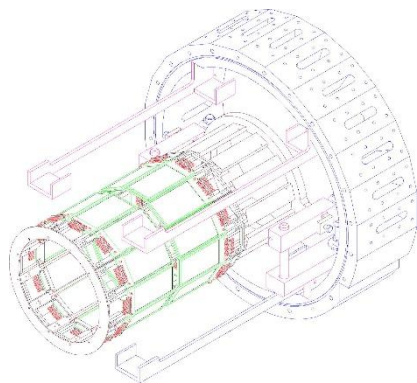
$p(^{130}\text{Sn}, p)@20 \text{ MeV/nucleon}$



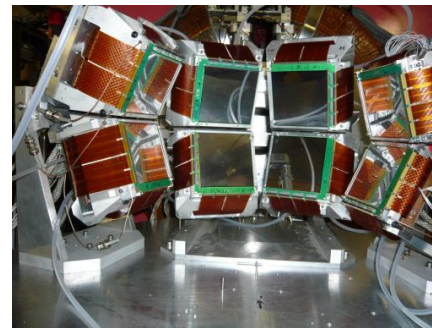
Recoil particle detector array in the world



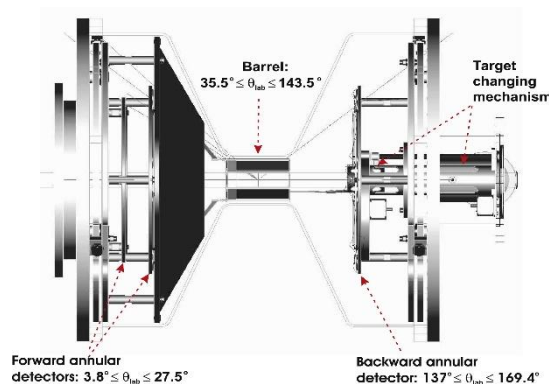
LEDA @ Leuven/Edinburg
T. Davidson, et al., NIMA 454, 350 (2000).



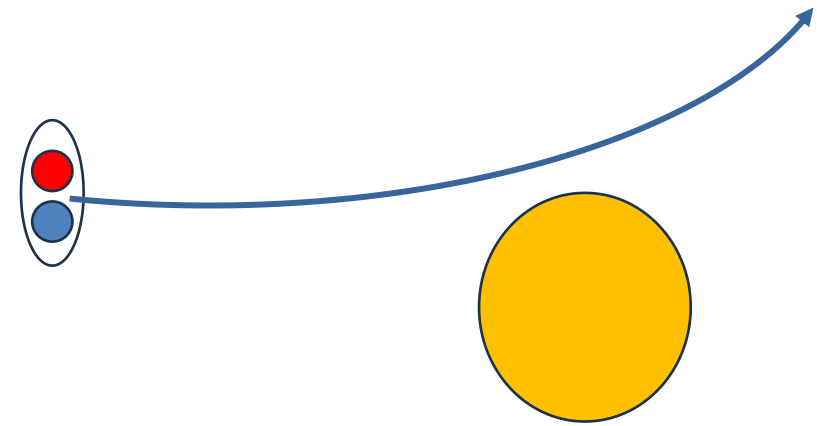
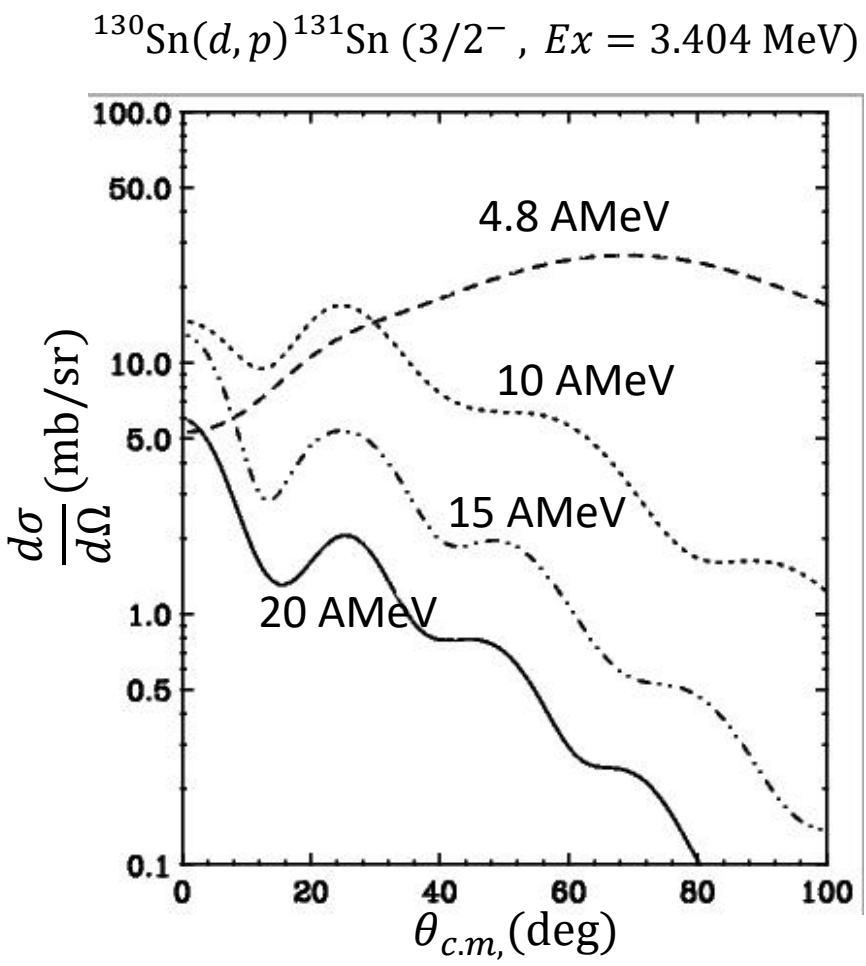
ORRUBA @ Oak Ridge
S.D. Pain, et al., NIMB 261,
1122-1125 (2007)



MUST/MUST2 @ France
Y. Blumenfeld et al., NIMA 421, 471(1999)

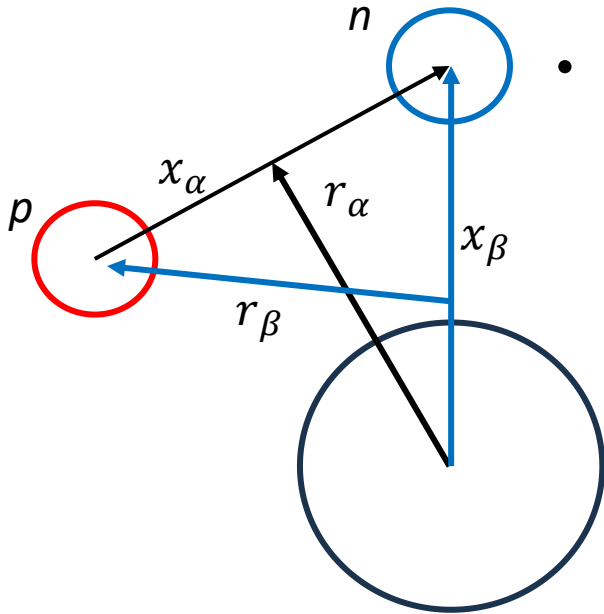


TIARA @ UK
M. Labiche, W.N. Catford, et
al., NIMA 614, 439-448
(2010)



- Coulomb barrier $\sim 6.8 \text{ MeV}$
- $E < V_{\text{Coul}}$; less diffraction

Hamiltonian of (d,p) reaction



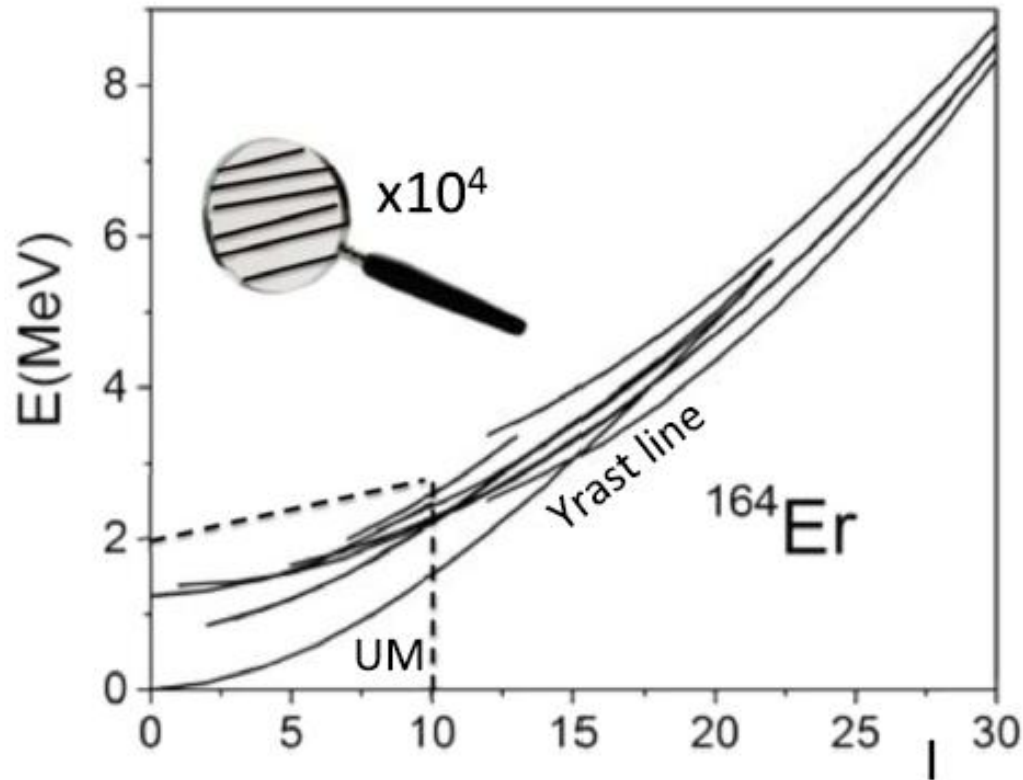
$$\begin{aligned}
 \bullet \quad H &= - \underbrace{\frac{\hbar^2}{2\mu_{dA}} \frac{\partial^2}{\partial \vec{r}_\alpha^2}}_{K_\alpha} - \underbrace{\frac{\hbar^2}{2\mu_{pn}} \frac{\partial^2}{\partial \vec{x}_\alpha^2}}_{H_\alpha} + \underbrace{V_{pn} + V_{nA} + V_{pA}}_{V_\alpha} \\
 &= - \underbrace{\frac{\hbar^2}{2\mu_{pA}} \frac{\partial^2}{\partial \vec{r}_\beta^2}}_{K_\beta} - \underbrace{\frac{\hbar^2}{2\mu_{nA}} \frac{\partial^2}{\partial \vec{x}_\beta^2}}_{H_\beta} + \underbrace{V_{nA} + V_{pA} + V_{pn}}_{V_\beta}
 \end{aligned}$$

Summary (2)

- DRC of neutron can be determined by the final state bound state wave function.
- DWBA can help to determine the ANC.
- ChatGPT still needs trainings.
- Reaction in inverse kinematics, the conversion of the coordinate system looks tricky.

COMPOUND REACTION CHANNEL

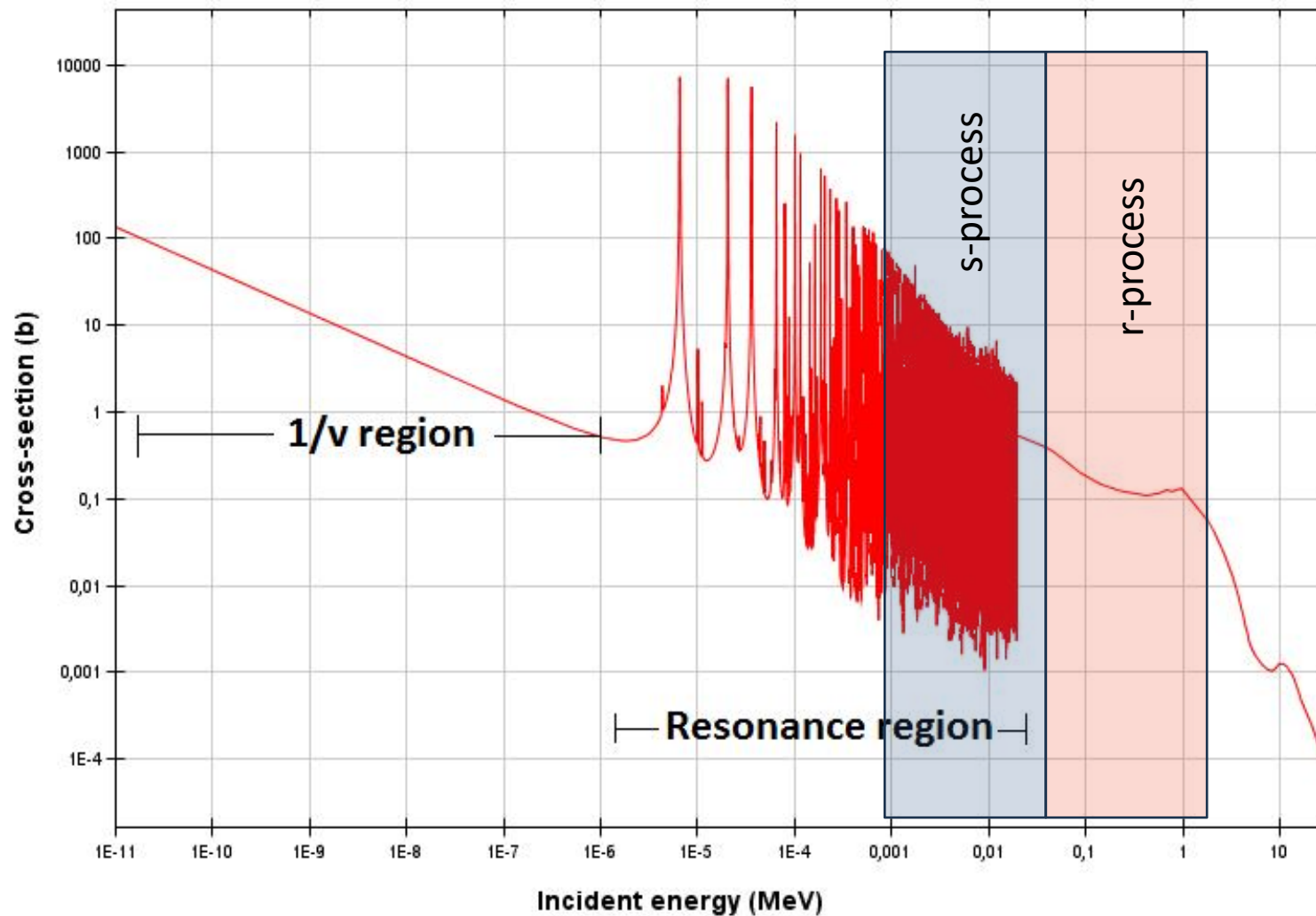
Quantum Chaos above S_n



S. Frauendorf, Phys. Scr. 93 (2018) 043003

Neutron resonance

Incident neutron data / ENDF/B-VII.1 / U238 / MT=102 : (z, γ) / Cross section



NUSTCZ023 IV. IIIId1

Compound reaction

Hauser-Feshbach theory

$$\sigma_{n\gamma}(E) = \frac{\pi}{k^2(2J_i + 1)(2J_n + 1)} \sum_{J^\pi} (2J + 1) \frac{T_n(J^\pi)T_\gamma(J^\pi)}{T_{tot}(J^\pi)}$$

- **T_n : neutron transmission coeff.**

← optical model potential

- **T_γ : photon transmission coeff.**

← level density (cf. @¹³¹Sn $\rho = 40 \text{ MeV}^{-1}$),
gamma strength function (γ SF)

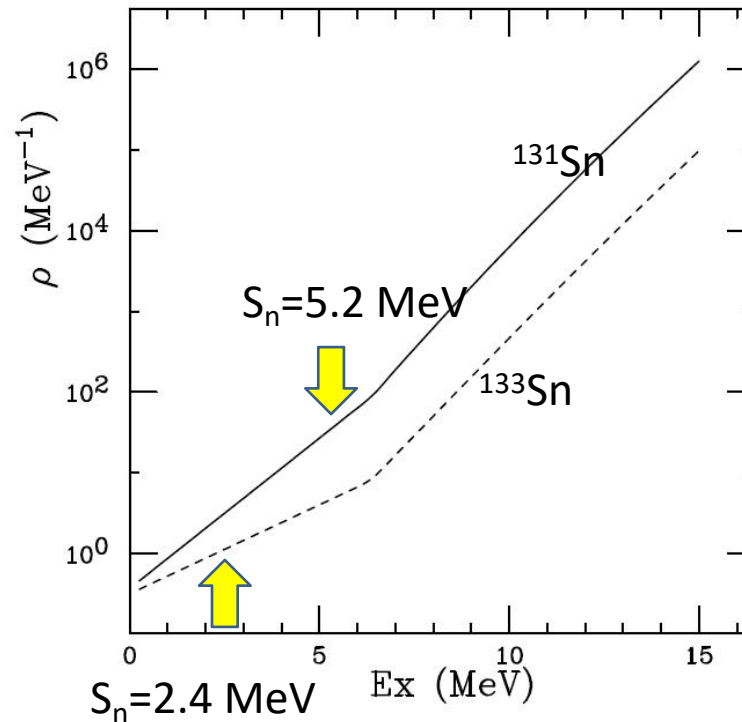
Cf.) Breit-Wigner

$$\sigma_{\beta\alpha} = \frac{\pi}{k^2} \frac{\Gamma_\beta \Gamma_\alpha}{(E - E_c)^2 + \left(\frac{\Gamma}{2}\right)^2}$$

$$(4.186) \quad \Gamma_{\alpha'}(E^{tot}, J, \Pi \longrightarrow E_x, I', \Pi_f) = \frac{1}{2\pi\rho(E^{tot}, J, \Pi)} \sum_{j'=|J-I'|}^{J+I'} \sum_{l'=|j'-s'|}^{j'+s'} \delta_\pi(\alpha') \langle T_{\alpha'l'j'}^J(E_{a'}) \rangle$$

$$T_{(E1)}(E_\gamma) = 2\pi E_\gamma \frac{\sigma_{GDR} \Gamma_{GDR}}{3\pi^2 \hbar^2 c^2} \left[\frac{E_\gamma \Gamma(E_\gamma)}{(E_\gamma^2 - E_{GDR}^2)^2 + E_\gamma^2 \Gamma(E_\gamma)^2} + \frac{0.7 \Gamma_{GDR} 4\pi^2 T^2}{E_{GDR}^5} \right]$$

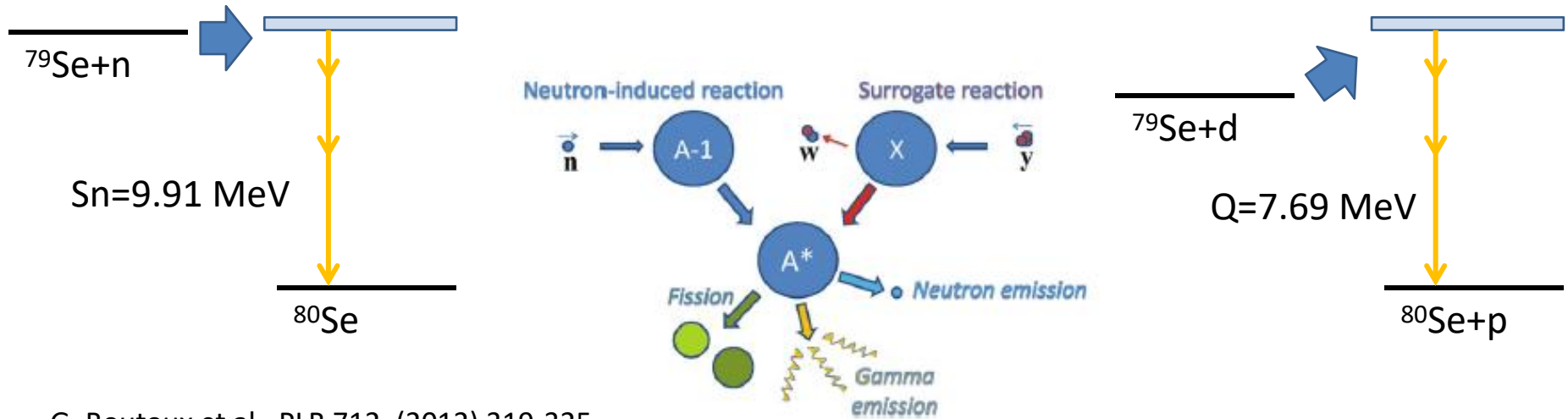
level density around ^{132}Sn



$$\rho_F(E_x, J, \Pi) = \frac{1}{2} \frac{2J+1}{2\sqrt{2\pi}\sigma^3} \exp\left[-\frac{(J+1/2)^2}{2\sigma^2}\right] \frac{\sqrt{\pi} \exp[2\sqrt{a}U]}{12 a^{1/4} U^{5/4}}$$

Fermi-gas model

Surrogate reaction: (n,γ) vs. (d,p)



G. Boutoux et al., PLB 712, (2012) 319-325.

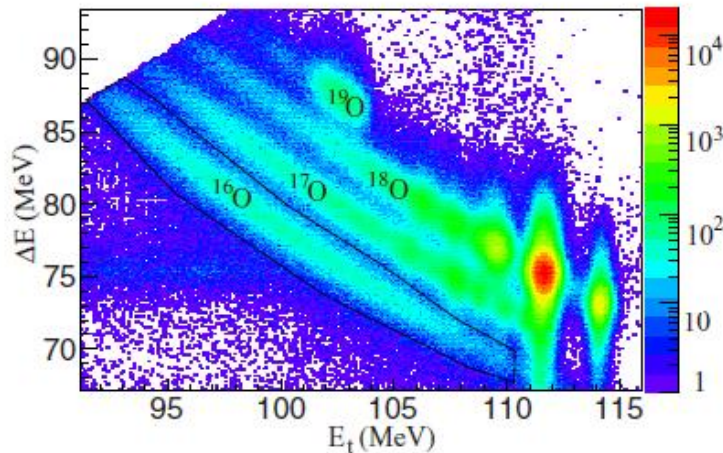
$$\sigma_{^{79}\text{Se}(n,\gamma)^{80}\text{Se}}(E_n) = \sigma_{^{80}\text{Se}}^{CN}(E_n) P_{^{80}\text{Se}^* \rightarrow \gamma + ^{79}\text{Se}}^{decay}(E^*)$$

determined by
the optical model potential

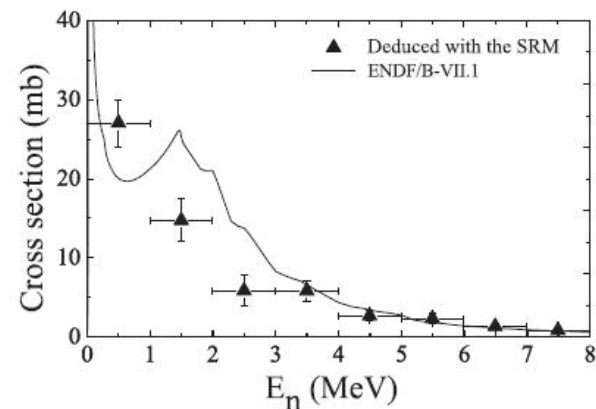
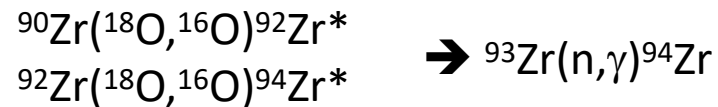
Surrogate ratio method

$$\sigma_{^{79}\text{Se}}^{(n,\gamma)}(E) = \sigma_{^{77}\text{Se}}^{(n,\gamma)}(E) \times \frac{\sigma^{CN}(^{80}\text{Se})}{\sigma^{CN}(^{78}\text{Se})} \times \frac{P_{\gamma}^{^{80}\text{Se}}(E)}{P_{\gamma}^{^{78}\text{Se}}(E)}. \quad (1)$$

Example @JAEA



PRC94.015804('16)

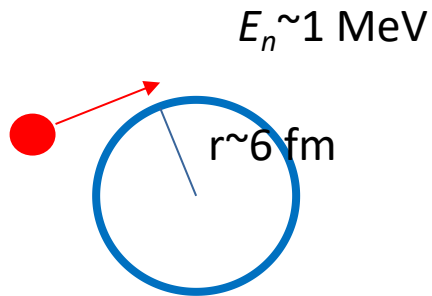




Spin distribution difference ?

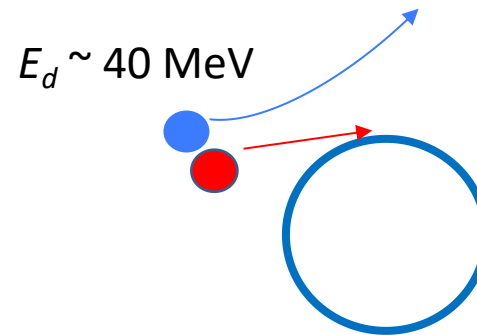
$^{79}\text{Se}(n,\gamma)$ reaction vs $^{79}\text{Se}(d,p)$ reaction

Neutron capture



$$\Delta L = p \times r \sim 1 \hbar$$

Stripping reaction



$$\vartheta = 30 \text{ deg. } E_x = 10 \text{ MeV}$$

$$\Delta p = 364 \text{ MeV}/c$$

$$\Delta L = \Delta p \times r \sim 12 \hbar$$

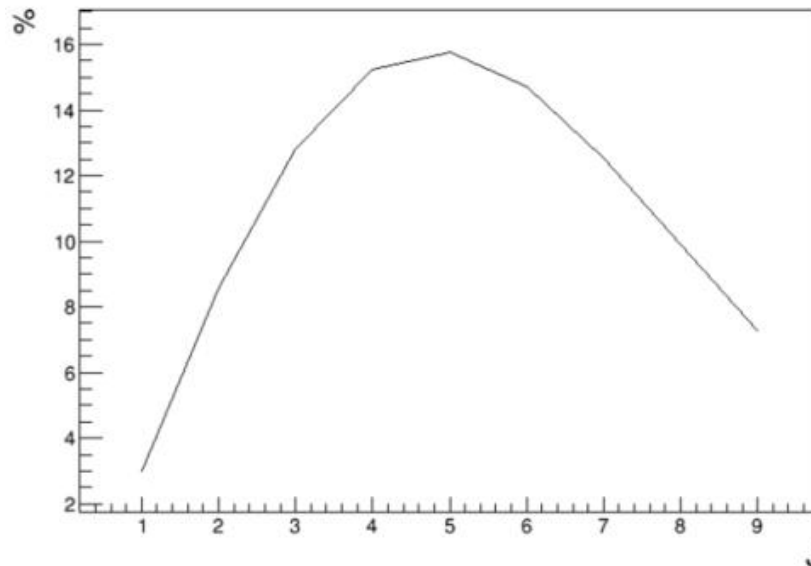
Level density distribution

Fermi-gas model

$$(4.236) \quad \rho_F(E_x, J, \Pi) = \frac{1}{2} \frac{2J+1}{2\sqrt{2\pi}\sigma^3} \exp \left[-\frac{(J + \frac{1}{2})^2}{2\sigma^2} \right] \frac{\sqrt{\pi}}{12} \frac{\exp \left[2\sqrt{aU} \right]}{a^{1/4} U^{5/4}},$$

From TALYS manual

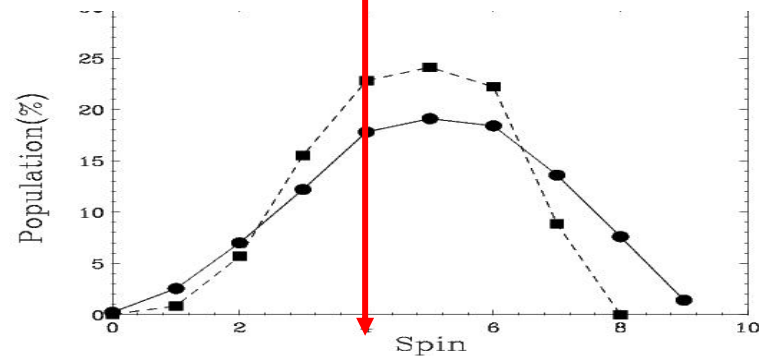
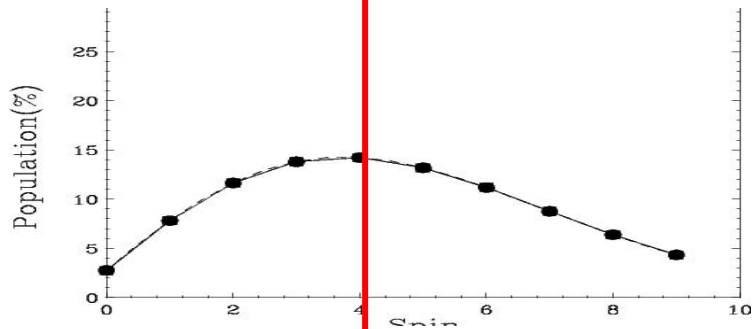
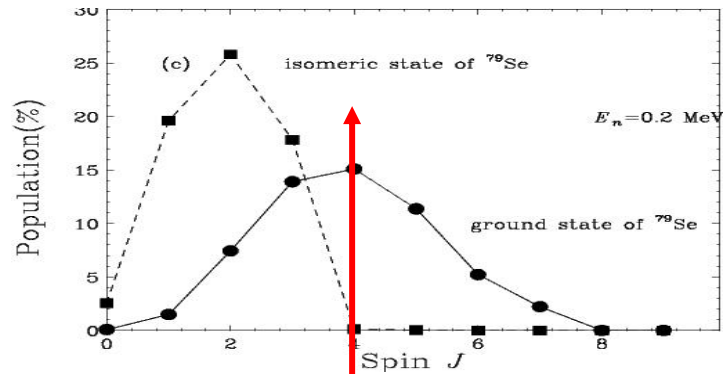
Assumption: The projection of the angular momentum are randomly coupled.



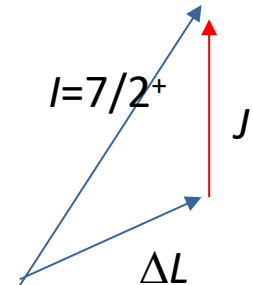
$^{80}\text{Se}^*$ at 10 MeV

$\rho \sim 2 \times 10^5 \text{ MeV}^{-1}$

Calculated spin distribution for ^{79}Se



^{79}Se g.s. $I^\pi = 7/2^+$
iso @96 keV $I^\pi = 1/2^-$



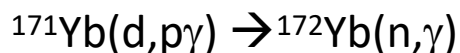
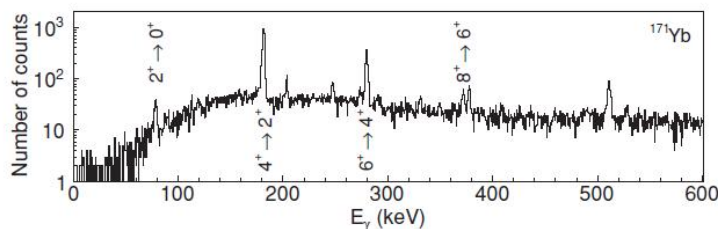
Talys spin distribution at 10 MeV
By $^{79}\text{Se}(d,p)$ reaction @ 40 MeV
(complete compound reaction is assumed.)

DWBA calc. $\Delta J = \frac{1}{2} \sim \frac{13}{2}$, $S=1.0$,
weighted with the level density

Surrogate reaction w/o γ -ray measurement

Typical setup for surrogate reaction exp.

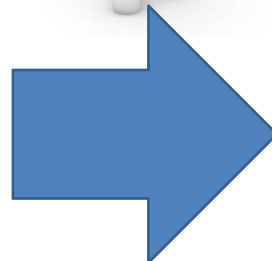
= Recoil particle detectors
+ γ -ray detector array



R. Hatarik et al.,
PRC81, 011602 (R) (2010)

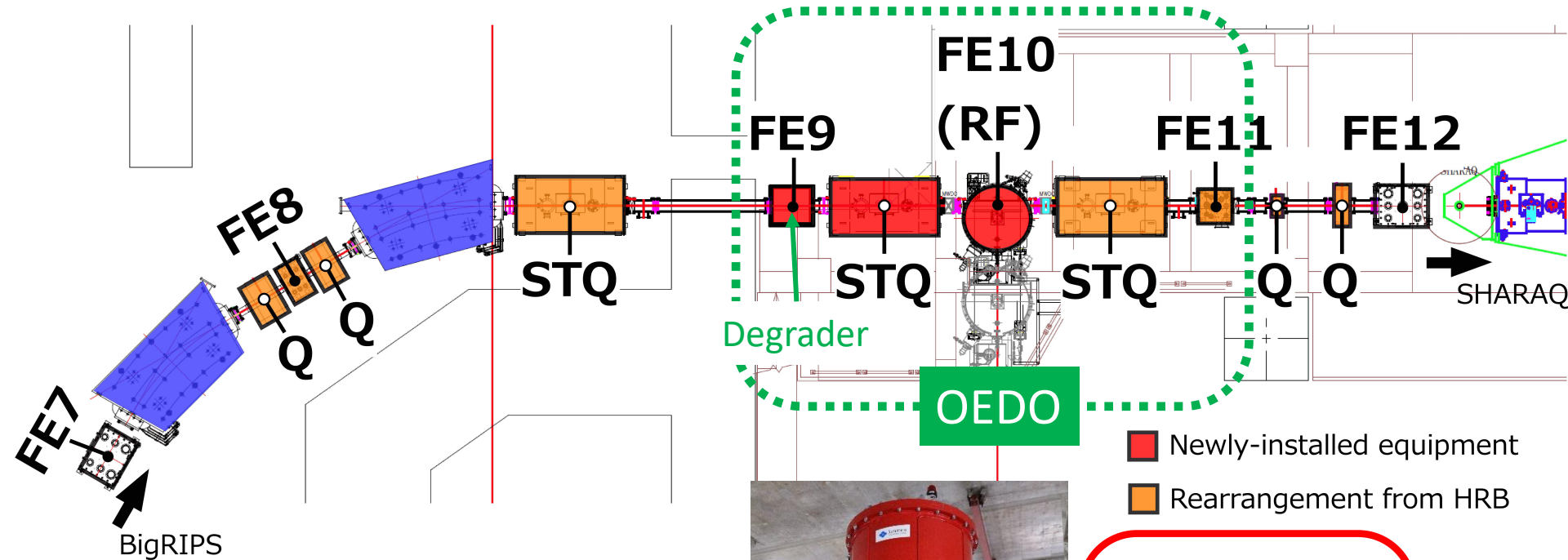


Aha!
Gamma emission means
that the nucleus doesn't
change N and Z number!



**P_γ was determined by identifying
the outgoing residue nucleus.**

Optimized Energy Degrading Optics for RI beams at RIBF



OEDO RFD

$$f_{RF} = 18.25 \text{ MHz}$$

$$V_{max} = 350 \text{ kV}$$

$$\text{Gap(H)} = 200 \text{ mm}$$

$$L(Z) = 1200 \text{ mm}$$

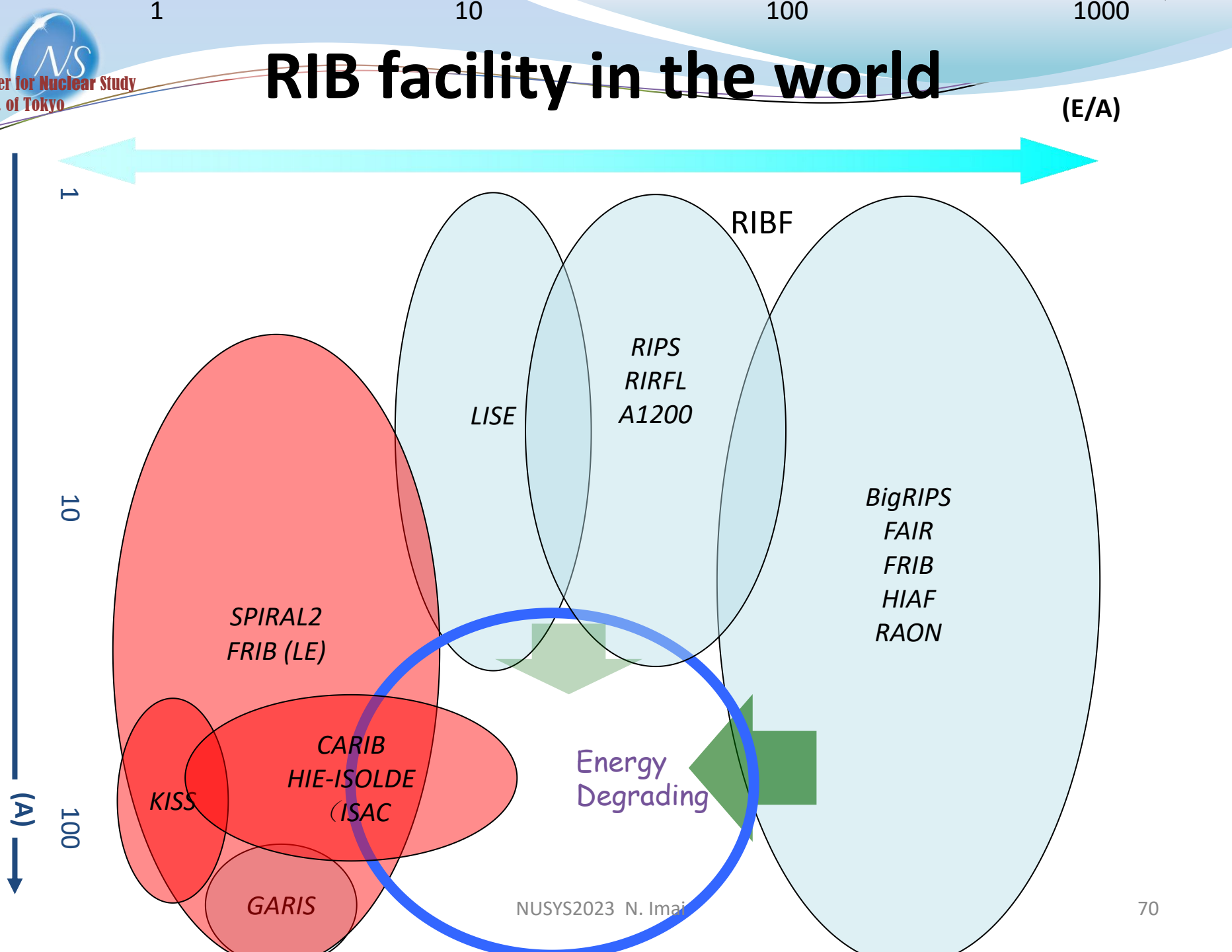
$$W(V) = 400 \text{ mm}$$

Installed in Mar. 2017.

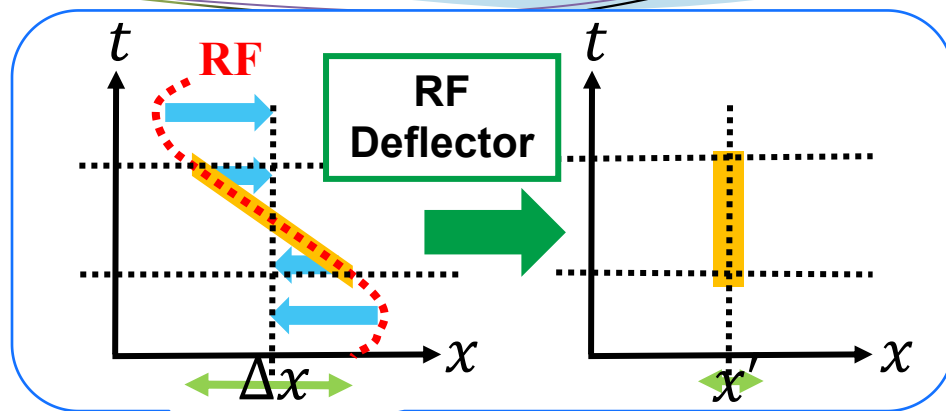
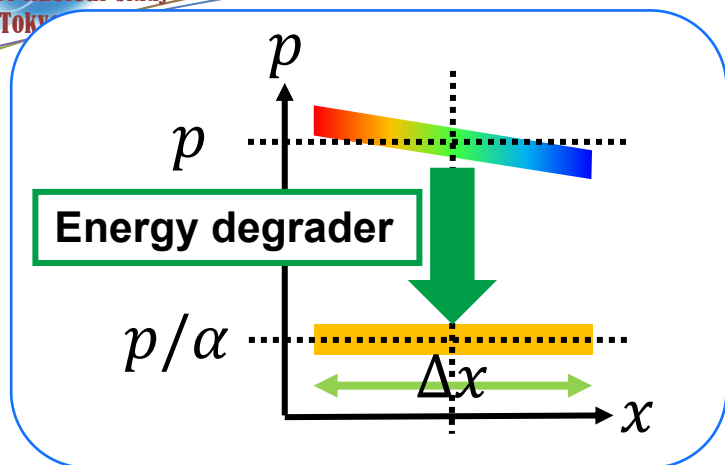
RF deflector



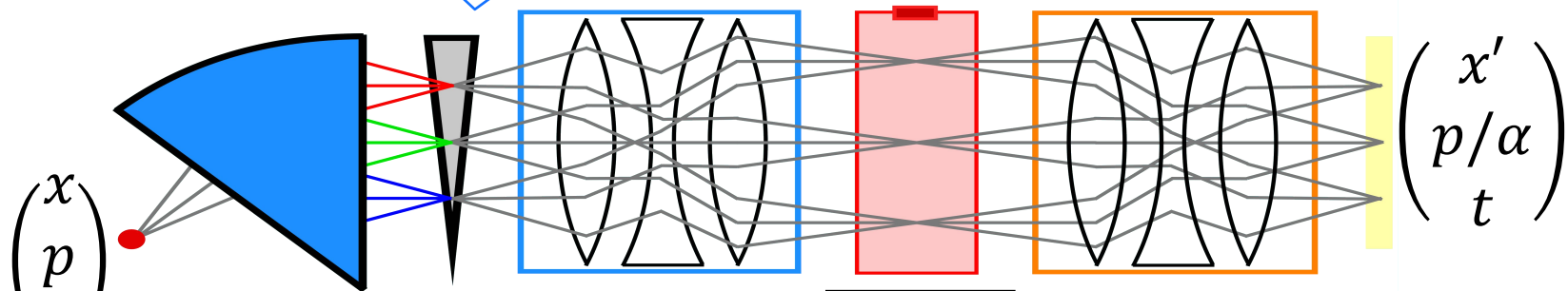
RIB facility in the world



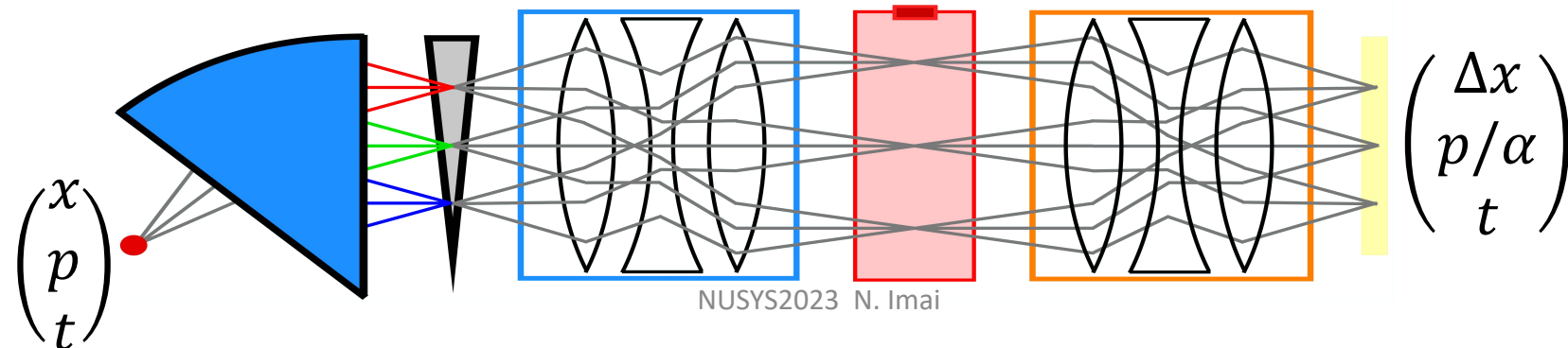
Principle of OEDO



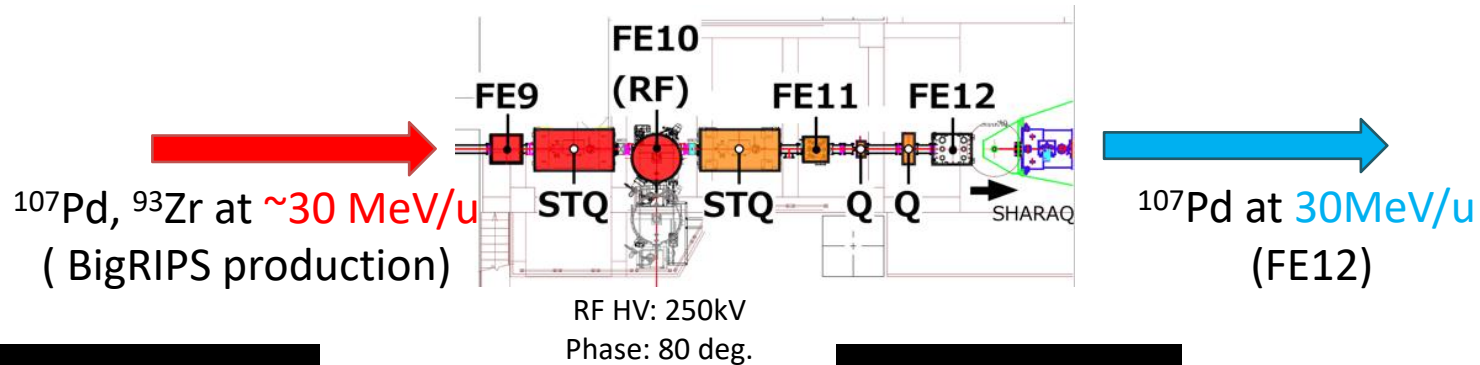
RF on



RF off

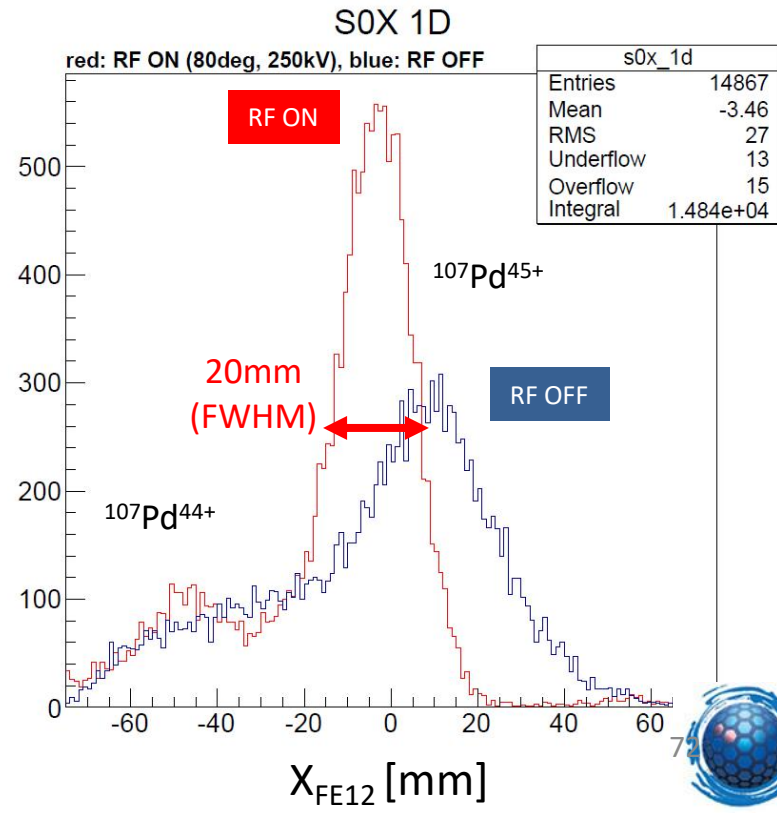
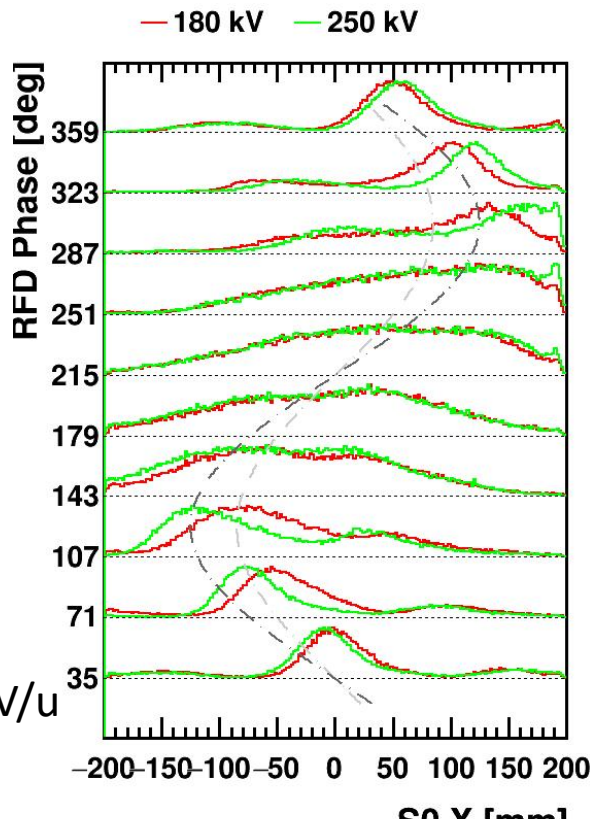


Squeezing the beam spot

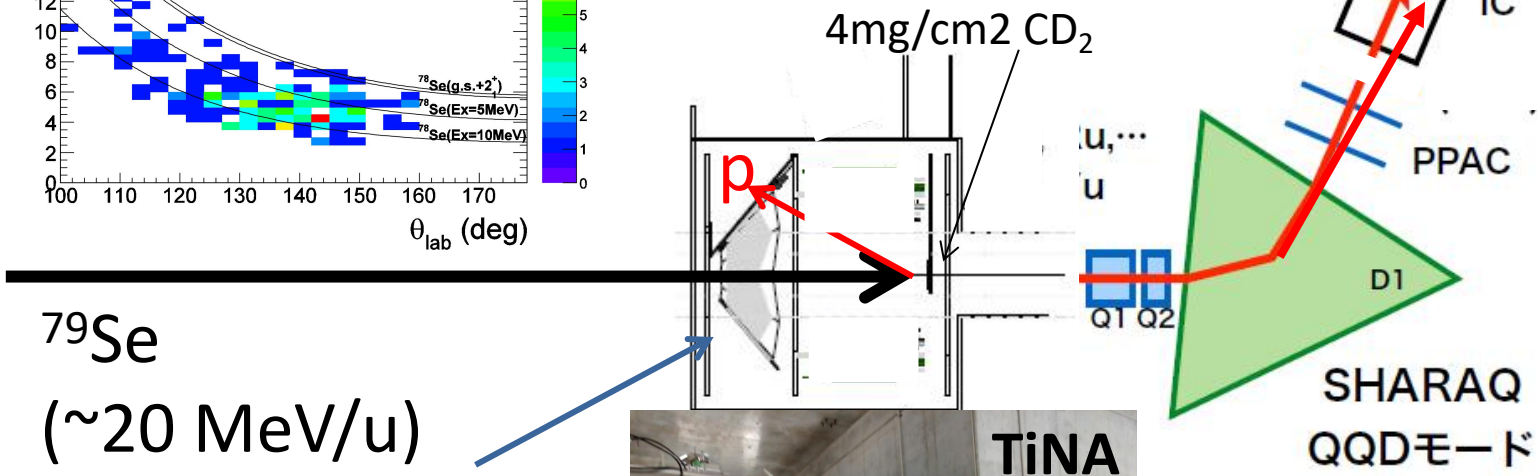
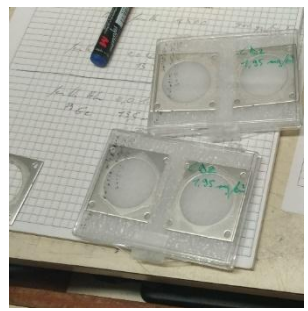
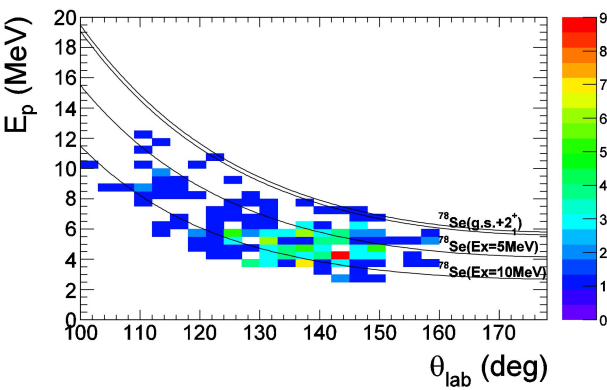


Effects of RF Deflector

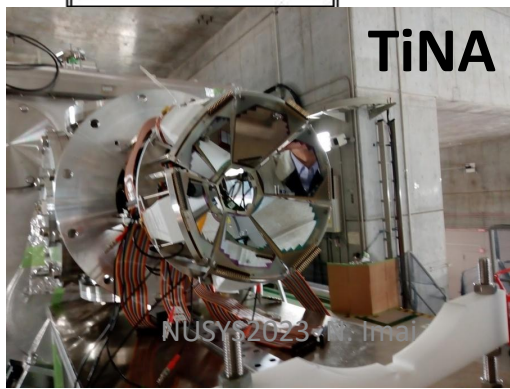
Focusing (FE12)



Recoil particles: TiNA, SSD-CsI (CNS/RCNP/RIKEN)
 reaction products: detectors at final focal plane
 target: CD₂ 4mg/cm²
 Beam int~ 10⁴ pps at on CD₂



^{79}Se
 (~20 MeV/u)
 6x (SSD(YY1 16ch)+ CsI)



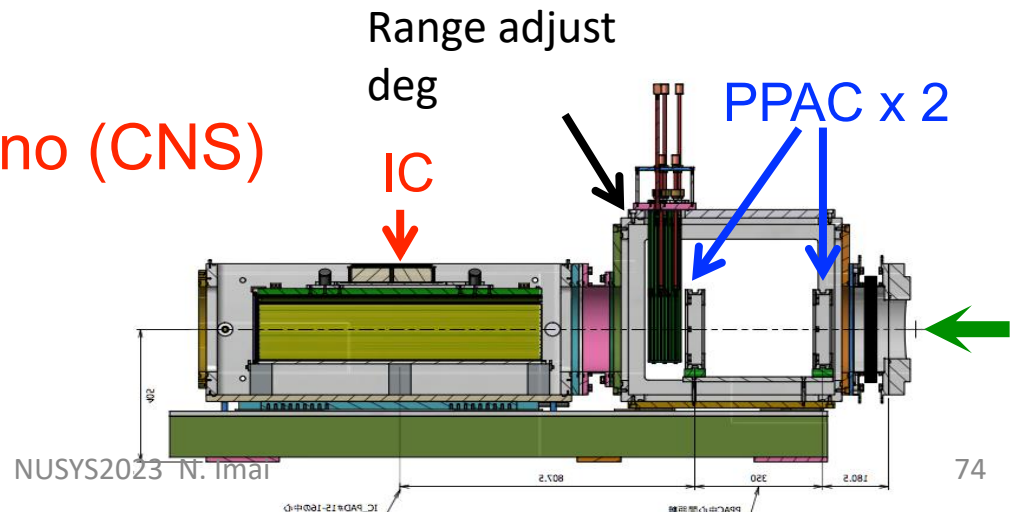
coincidence measurement of
 recoil particles + outgoing particles.

S1 Focal plane detector

- **PPAC** : position, time of flight
 - Single(X-A-Y), Delay-line readout
 - 240 mm^W x 150 mm^H
- **Ionization chamber** : ΔE , Range
 - 30 pads
 - 280 mm^W x 150 mm^H
 - Total depth 757.5 mm
 - CF₄ 110 torr
- **Degrader to tune the range**
- **Kapton foil of 75 μ m**



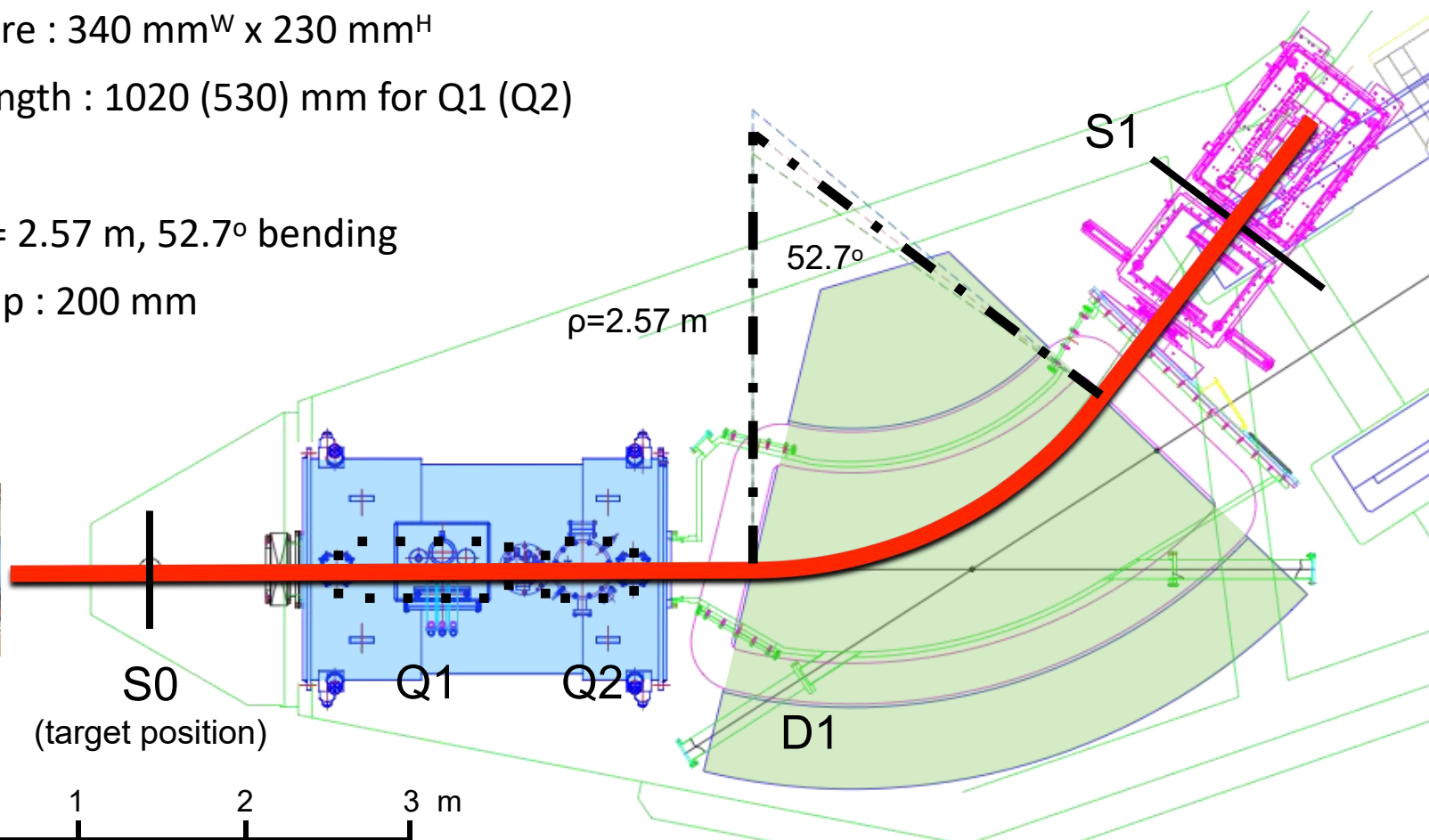
by Chiga(RIBF) and Dozono (CNS)



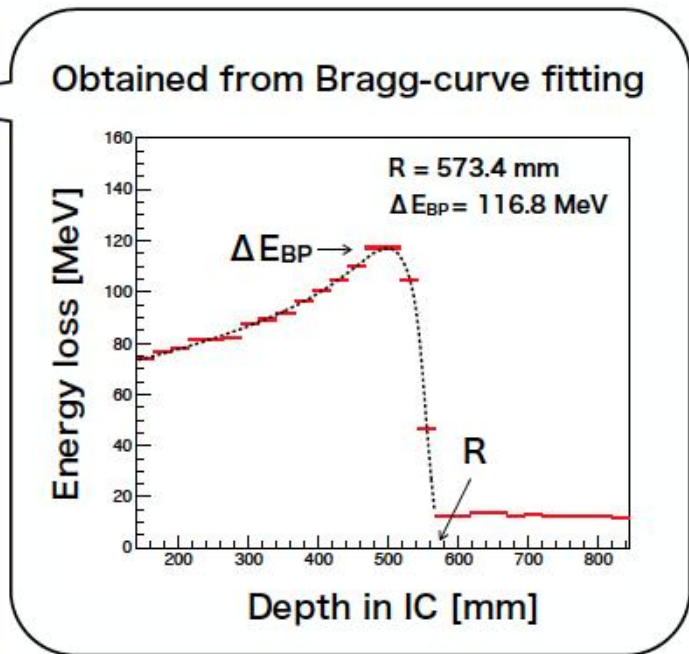
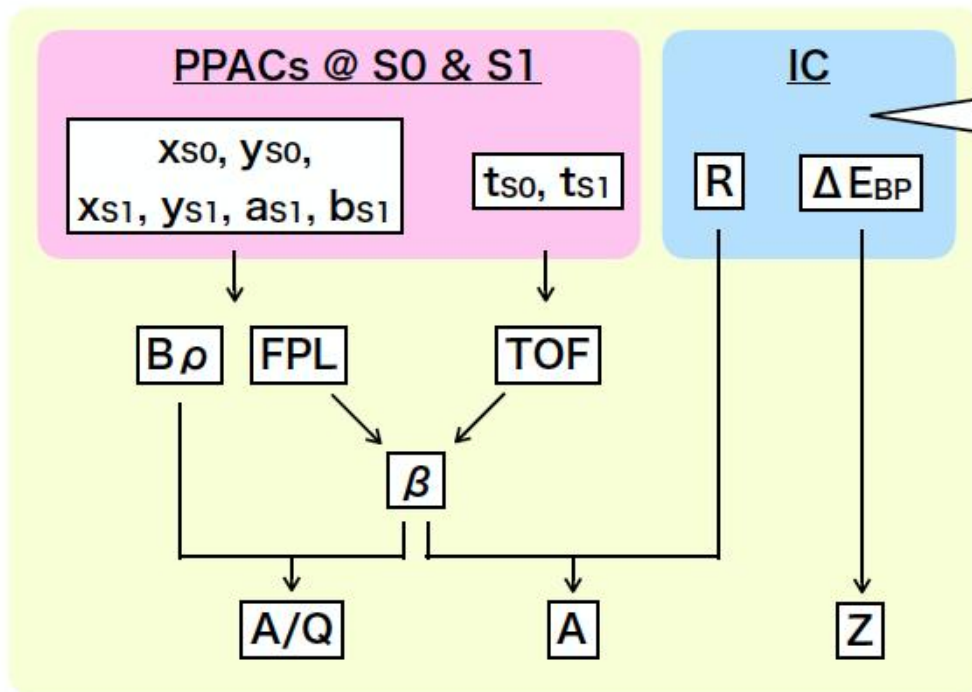
SHARAQ spectrometer

- Q-Q-D magnet configuration (First-half part of SHARAQ spectrometer)
 - Q1, Q2 (Superconducting)
 - Bore : 340 mm^W x 230 mm^H
 - Length : 1020 (530) mm for Q1 (Q2)
 - D1
 - $\rho = 2.57$ m, 52.7° bending
 - Gap : 200 mm

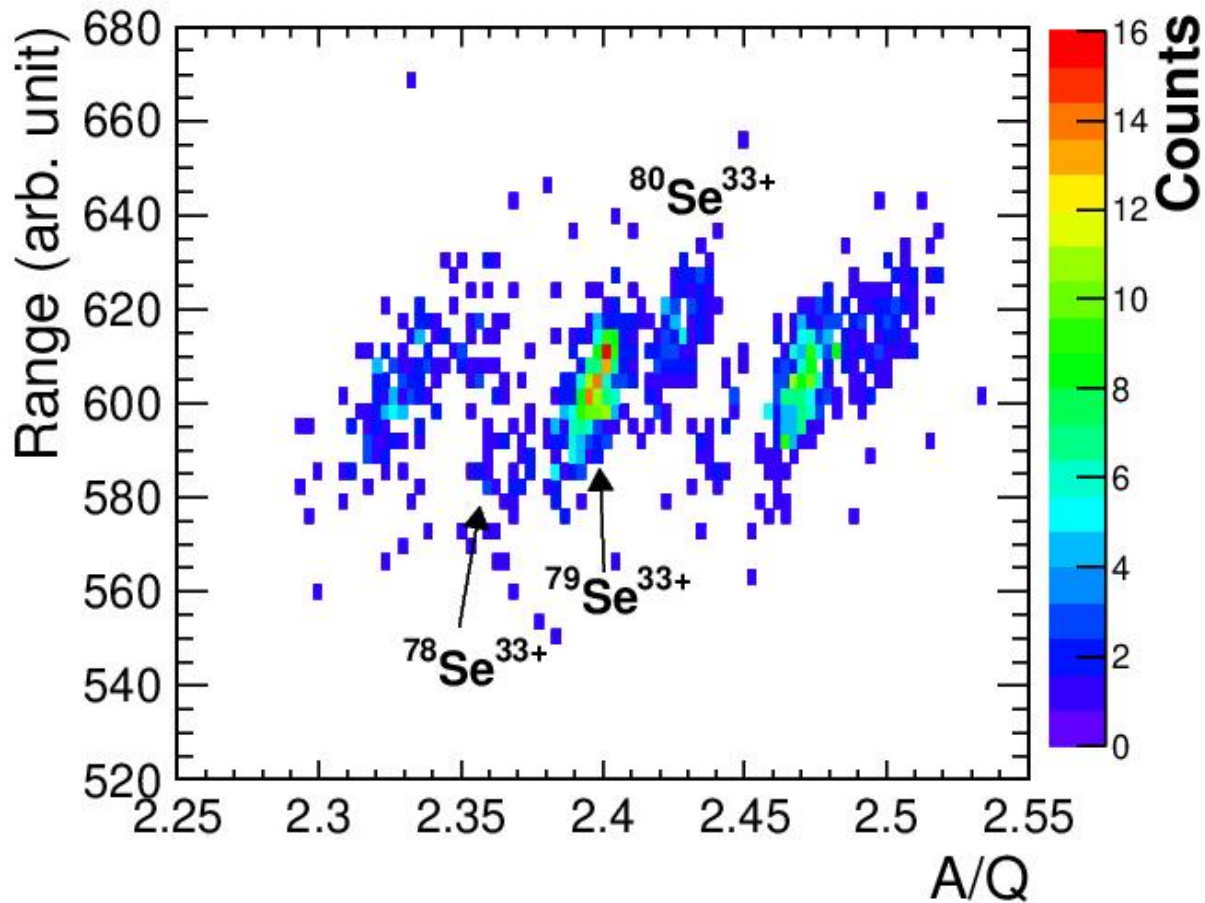
OEDO



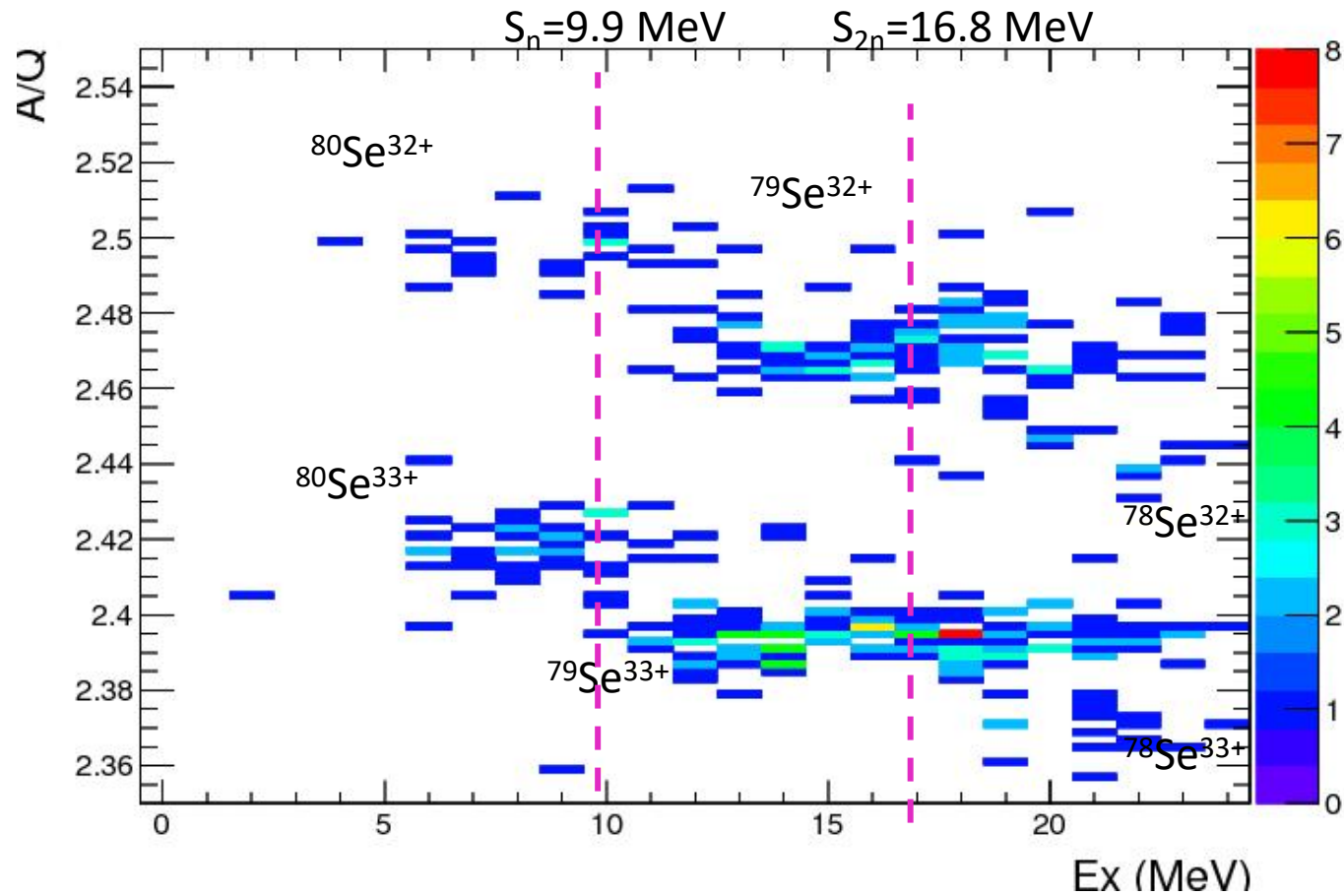
PID of outgoing residue



PID of outgoing residues

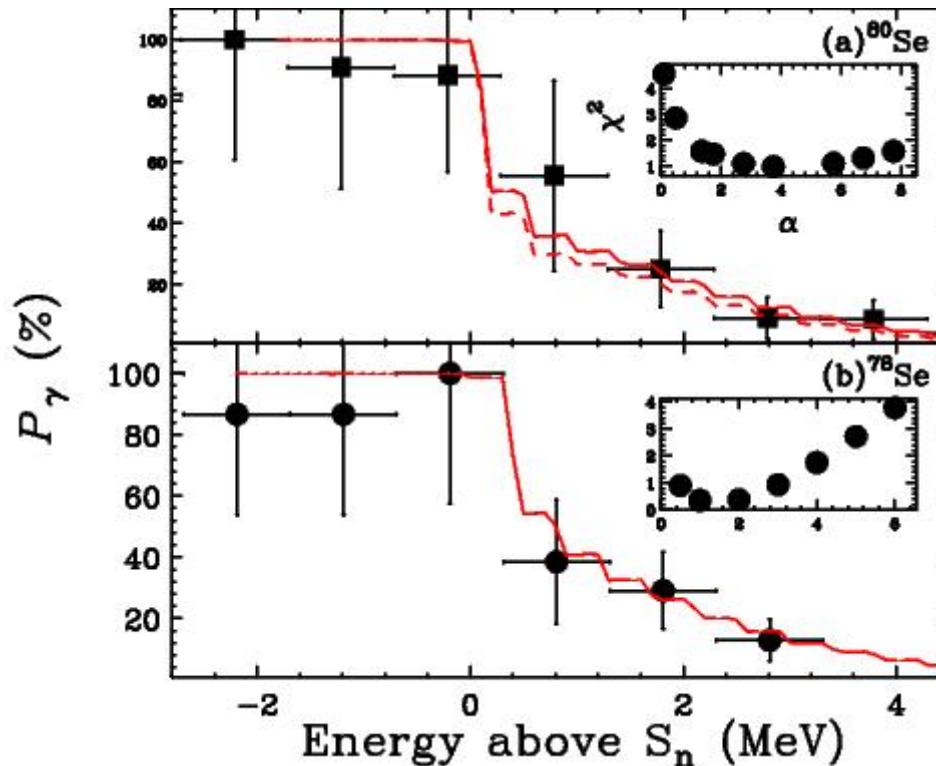


Residual nuclei vs Excitation energy



P_γ in $^{77,79}\text{Se}(d,p)$ reaction

$$P_\gamma(E) = \sum G_{\text{decay}}(J^\pi, E) F^{dp}(J^\pi, E)$$



TENDL2021 recommendation

Normalization $\Gamma_\gamma \equiv \alpha = 1.75$ (dashed)

Best fitting: $\alpha = 3.75$ (solid)

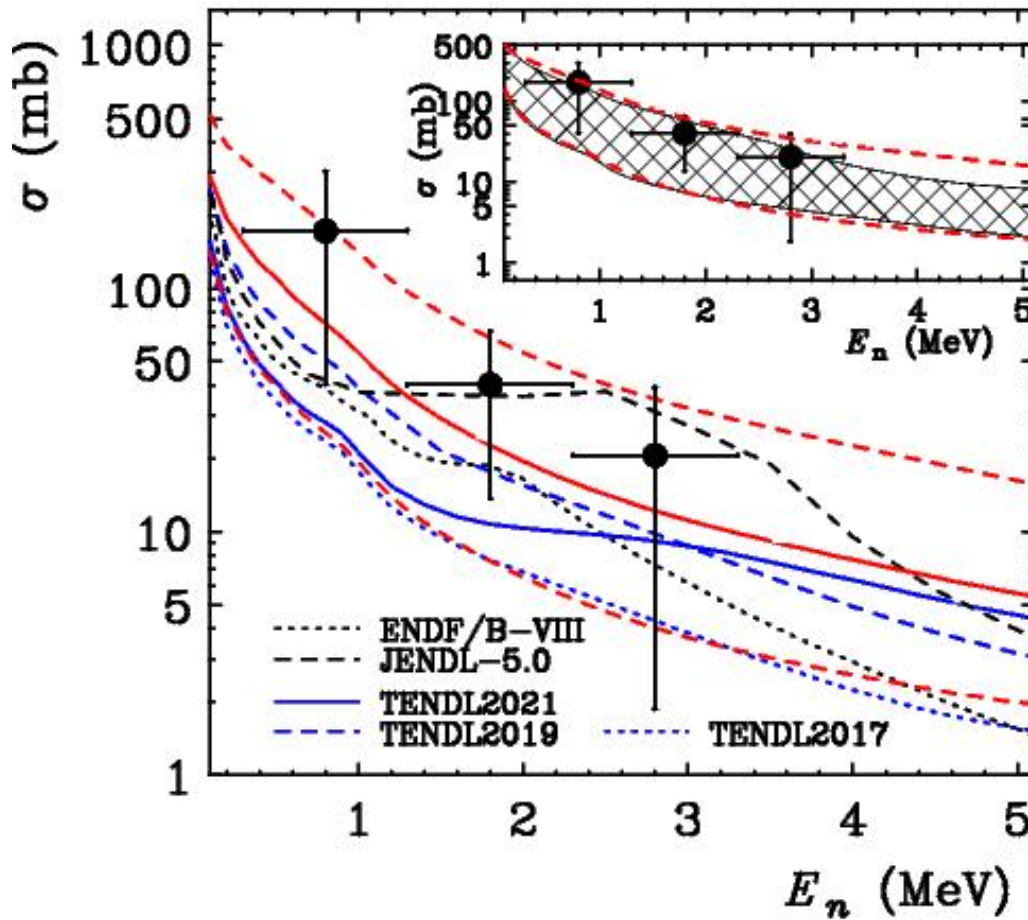
TENDL2021 recommendation

$\alpha = 1.00$

To reproduce Titech data (Igashira et al.,)

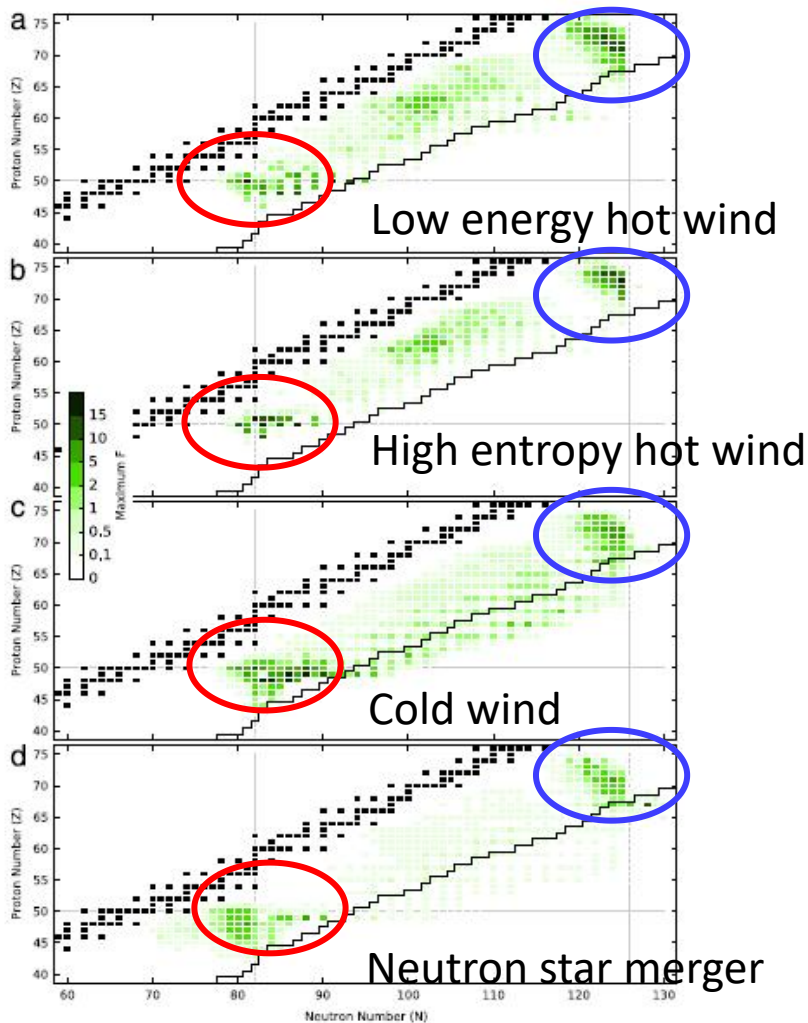
N. Imai et al., submitted to PLB

$^{79}\text{Se}(n,\gamma)$ cross section



EXPERIMENTAL STUDY OF NEUTRON CAPTURE RATE IN R-PROCESS

Which nuclear data are sensitive to the abundance?



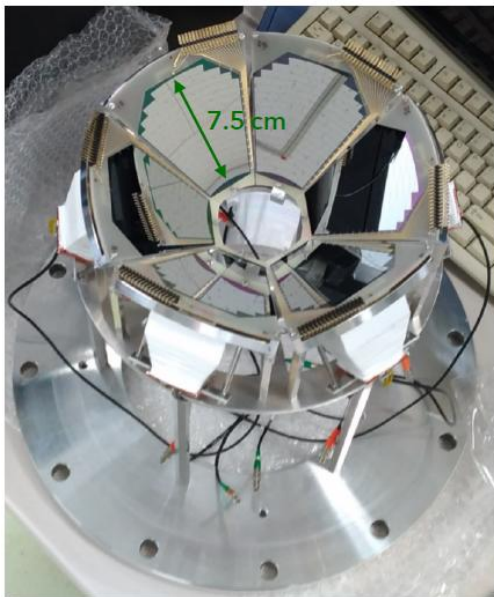
M. Mumpower, Prog. In Part. and Nucl. Phys. 86 (2016)86-126.

σ alters by 100 randomly.

$$F = 100 \sum_A |X(A) - X_b(A)|$$

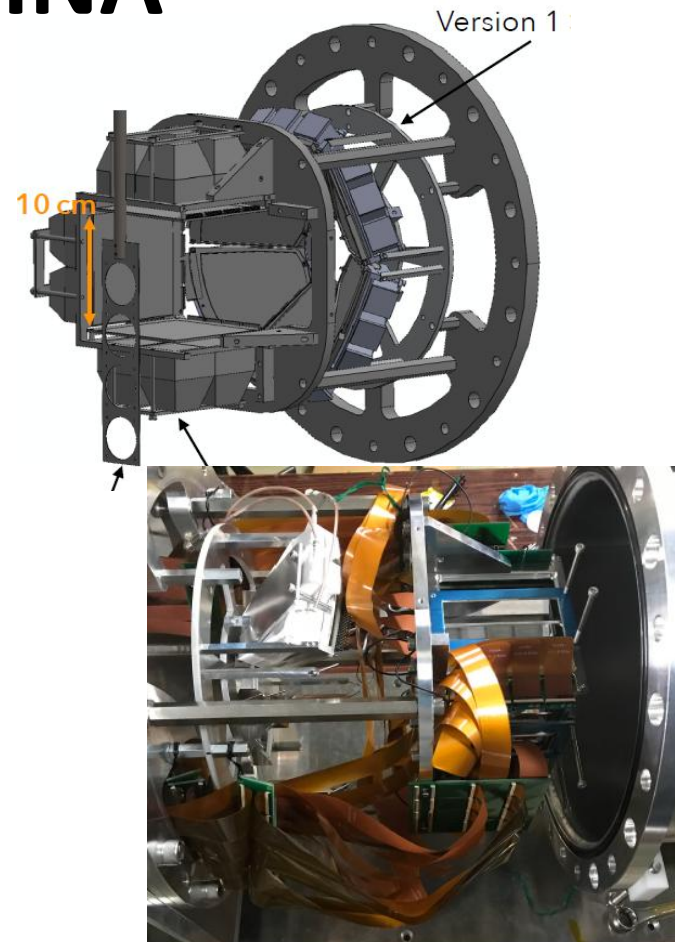
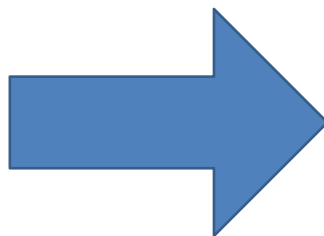
South-west of ^{132}Sn is more sensitive
To abundance

Upgrade of the recoil-particle detector TiNA



Drawbacks:

- Poor angular resolution (0.7° – 2.4°)
- Minimal angle covered $\theta_{\text{lab}} = 21.8^\circ$



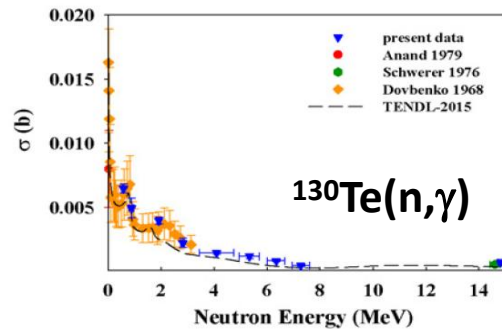
Angular resolution $< 1^\circ$
Angular coverage $\sim 70^\circ$

SAKURA01

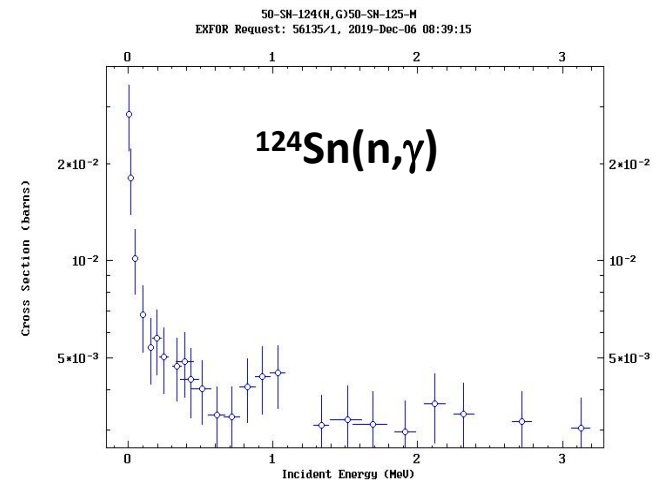
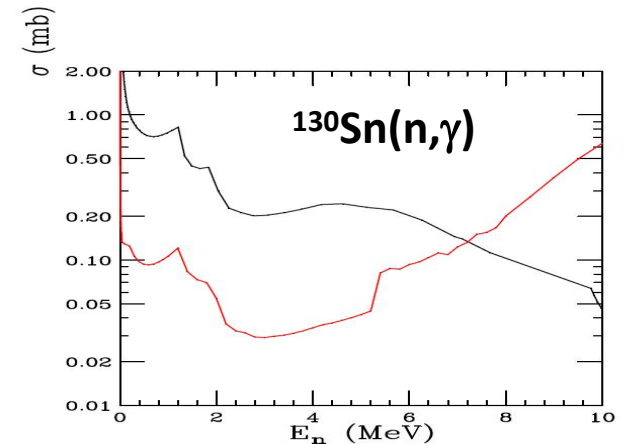
$$^{130}\text{Sn}(d,p)^{131}\text{Sn} \rightarrow P_{\gamma}^1(E)$$

$$^{130}\text{Te}(d,p)^{131}\text{Te} \rightarrow P_{\gamma}^2(E)$$

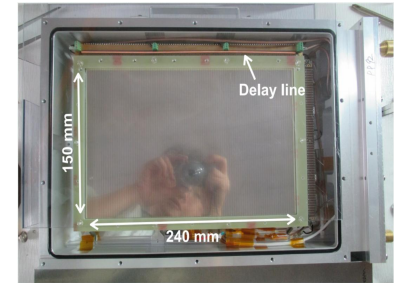
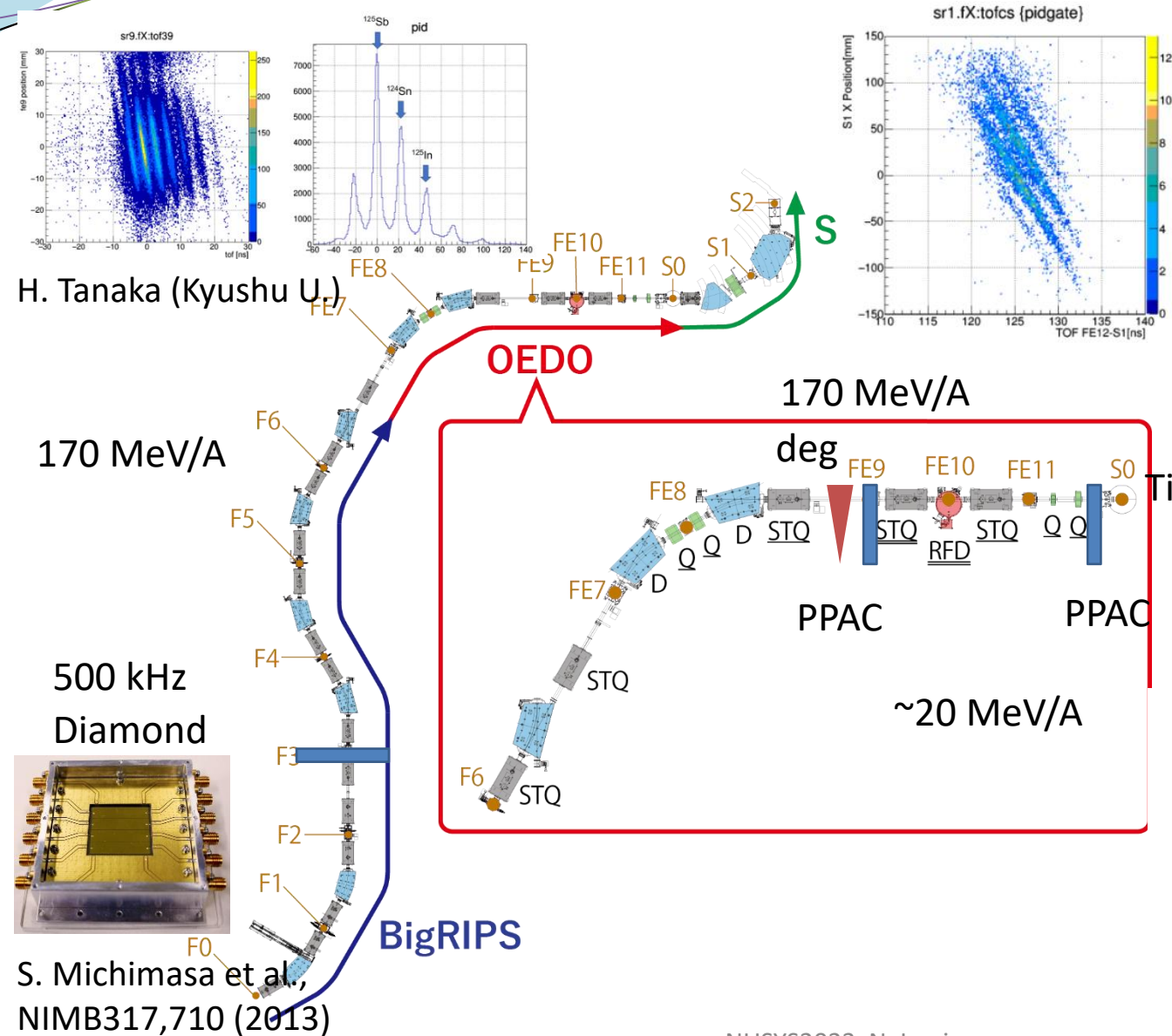
$$^{130}\text{Te}(n,\gamma)^{131}\text{Te}$$



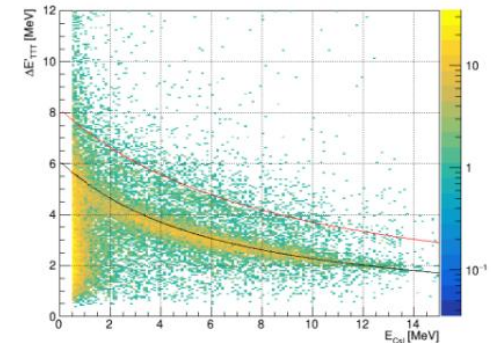
$$^{124}\text{Sn}(d,p)^{125}\text{Sn} \rightarrow P_{\gamma}^3(E)$$



BigRIPS-OEDO beam line

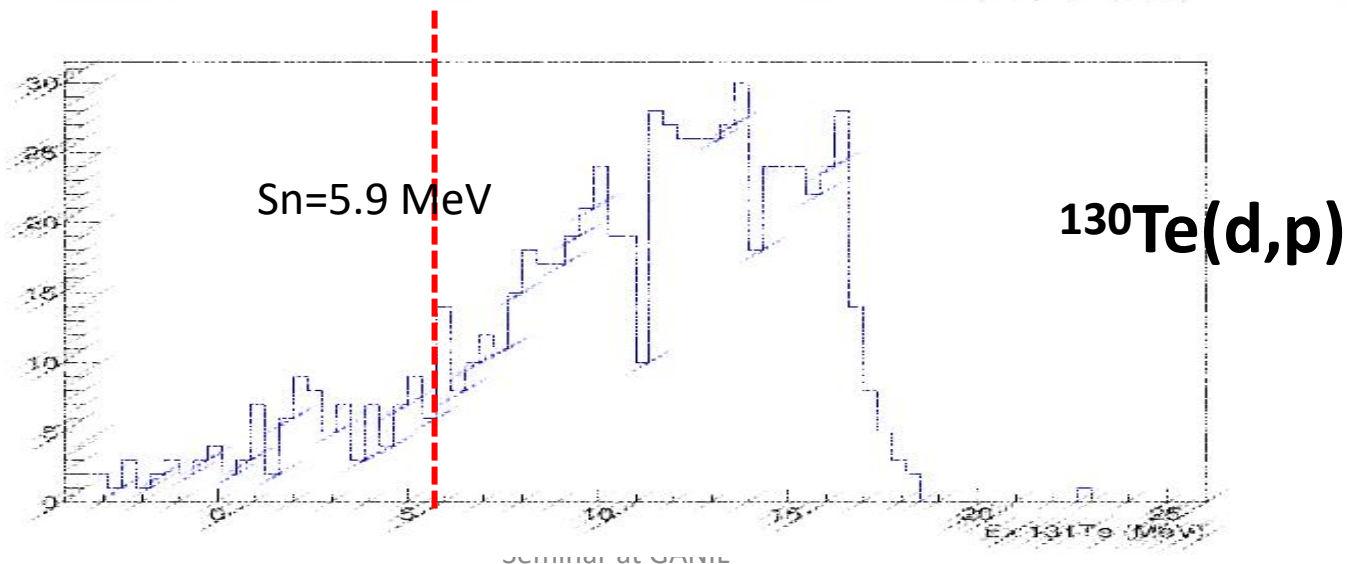
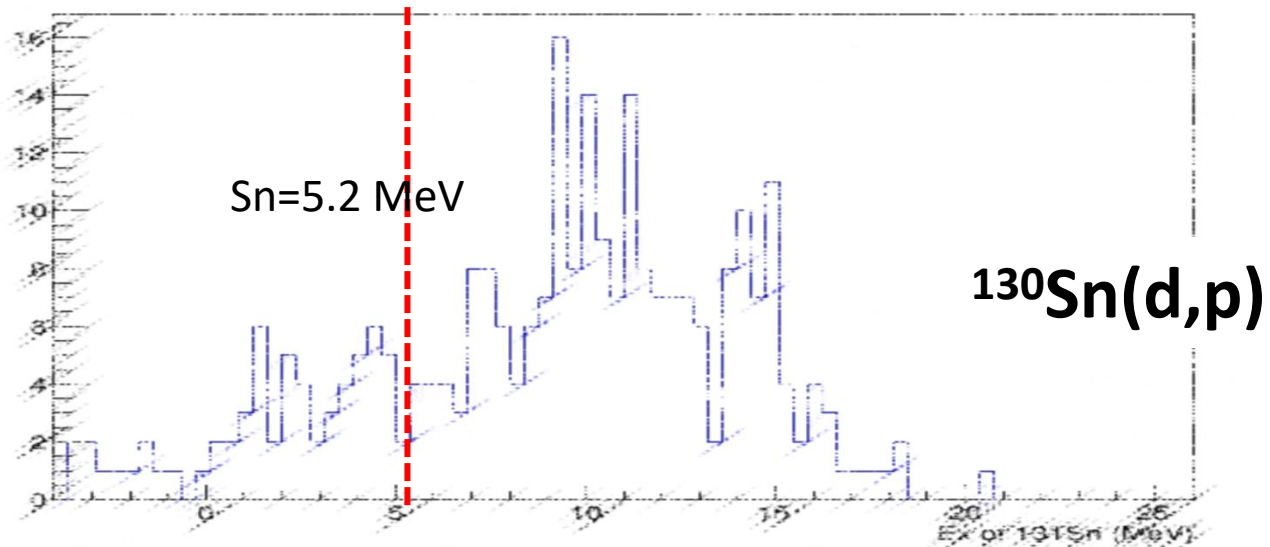


S. Hanai, S. Ota et al.,
NIMB541(2023)194-196.



T. Haginouchi (Tohoku U.)

Mass spectra



Summary

- The astrophysical site of r-process nucleosynthesis is still mystery.
- The kilo-nova after GW170817 boosts the research this field.
- Many RIB facilities are running for the r-process study.
- Neutron capture reaction and the direct nuclear reaction is governed by the quantum physics.
- OEDO/RIBF starts the astrophysical reaction rates with the surrogate idea